

Radiative corrections to the $Zb\bar{b}$ vertex and constraints on extended Higgs sectors

Heather E. Logan

*Santa Cruz Institute for Particle Physics
University of California, Santa Cruz, CA 95064, U.S.A.*

Abstract

We explore the radiative corrections to the process $Z \rightarrow b\bar{b}$ in models with extended Higgs sectors. The observables R_b and A_b are sensitive to these corrections. R_b is the hadronic branching fraction of Z bosons to $b\bar{b}$, $R_b = \Gamma(Z \rightarrow b\bar{b})/\Gamma(Z \rightarrow \text{hadrons})$. A_b is the b quark asymmetry, $A_b = (g_L^2 - g_R^2)/(g_L^2 + g_R^2)$ where g_L and g_R are the left and right handed couplings of Z to b quarks. We find that in models containing only doublets, singlets, or larger multiplets constrained by a custodial $SU(2)_c$ symmetry so that $M_W = M_Z \cos \theta_W$ at tree level, the corrections involving charged Higgs bosons always worsen agreement with experiment. The R_b measurement can be used to set lower bounds on the charged Higgs masses in such models. Corrections involving light neutral Higgs bosons in models with enhanced $H^0 b\bar{b}$ coupling (large $\tan \beta$) can improve agreement with experiment over the Standard Model. We present general formulas for the corrections to R_b and A_b in an arbitrary extended Higgs sector, and derive explicit results for a number of specific models.

*Presented in partial satisfaction of the requirements for the degree of
Doctor of Philosophy in Physics at the University of California, Santa Cruz, June 1999*

Contents

1	Introduction	1
2	Constraints from the data	5
2.1	Extracting the effective $Zb\bar{b}$ couplings from R_b and A_b	5
2.2	Tree-level $Zb\bar{b}$ couplings: The effect of oblique corrections	9
3	Models with extended Higgs sectors	11
3.1	The two Higgs doublet model	14
3.2	A general extended Higgs sector	16
4	Charged Higgs corrections to $Z \rightarrow b\bar{b}$	19
5	Neutral Higgs corrections to $Z \rightarrow b\bar{b}$	26
6	Corrections to $Z \rightarrow b\bar{b}$ in specific models	30
6.1	Models with Higgs doublets and singlets	30
6.1.1	Charged Higgs boson contributions	30
6.1.2	Neutral Higgs boson contributions	35
6.2	Models with Higgs multiplets larger than doublets	47
6.2.1	Models with one Higgs doublet and one triplet	47
6.2.2	Models with two doublets and one triplet	51
6.2.3	Georgi–Machacek model with $SU(2)_c$ symmetry	59
7	Conclusions	66
A	Tree-level $Zq\bar{q}$ couplings in the Standard Model	68

Contents

B	Higgs–Vector boson couplings	69
B.1	Higgs–Vector couplings for complex Higgs representations	71
B.1.1	Higgs–Higgs–Vector couplings	71
B.1.2	Higgs–Higgs–Vector–Vector couplings	72
B.1.3	Higgs–Vector–Vector couplings	74
B.2	Higgs–Vector couplings for real, $Y = 0$ Higgs representations	75
B.2.1	Higgs–Higgs–Vector couplings	75
B.2.2	Higgs–Higgs–Vector–Vector couplings	76
B.2.3	Higgs–Vector–Vector couplings	77
B.2.4	Derivation of ϵ_Q	78
B.3	Higgs–Vector couplings for Higgs mass eigenstates	80
C	The two Higgs doublet model	81
D	Details of the models with two Higgs doublets and one triplet	84
D.1	$Y = 0$ model	84
D.2	$Y = 2$ model	89
E	Custodial $SU(2)$ symmetry and the Georgi–Machacek class of models	96
E.1	Symmetries, notation and conventions	97
E.2	Motivation: the ρ parameter under custodial $SU(2)$ symmetry	99
E.3	The Georgi–Machacek model with Higgs triplets	101
E.4	The generalized Georgi–Machacek models	107
E.4.1	Couplings to fermions	109
E.4.2	Couplings to gauge bosons	114
E.5	Absence of a massless Goldstone boson in the generalized Georgi–Machacek models	117
F	Calculation of one–loop integrals	119
F.1	Notation for one–loop integrals	119
F.2	Calculation of one–loop integrals	121
F.3	Derivatives of two–point integrals	123
F.4	Symmetries of the one–loop integrals under permutaion of their arguments	124
F.5	Approximations for the one–loop integrals in certain limits	126
F.5.1	$(m/M)^2 \equiv R \neq 0, \infty$	127
F.5.2	$m \simeq 0$ ($R \equiv (m/M)^2 \simeq 0$)	128
G	Combining the LEP and SLD measurements of A_b	129
H	SM parameters used in numerical calculations	132

I	Constraints from direct Higgs searches	135
I.1	Charged Higgs searches	135
I.2	Neutral Higgs searches	136
I.2.1	SM Higgs search	136
I.2.2	2HDM Higgs search	139
	Bibliography	143

Chapter 1

Introduction

The Standard Model (SM) of electroweak interactions [1,2,3] has been tested and confirmed to unprecedented precision in the past several years at the e^+e^- colliders LEP at CERN and SLC at SLAC (for recent data, see [4]). Precision measurements of many electroweak observables have confirmed that the electroweak interactions are well described by a spontaneously broken $SU(2) \times U(1)$ gauge symmetry. However, these measurements have not allowed us to determine the dynamics of the symmetry breaking.

The couplings of quarks and leptons to the Z boson and the mass of the Z and W have been measured. At tree level, the couplings of quarks and leptons to the Z are entirely determined by the gauge structure of the theory. These couplings depend only on the $SU(2) \times U(1)$ quantum numbers of the quarks and leptons, and the electric charge and weak mixing angle $\sin^2 \theta_W$.

The measurement of the Z and W masses provides us with one more piece of information about electroweak symmetry breaking (EWSB). In the SM, the Z and W masses M_Z and M_W are related at tree-level by

$$M_W = M_Z \cos \theta_W. \quad (1.1)$$

This relation is satisfied experimentally to better than 1% [5]. In the SM this relation is a consequence of the presence of an unbroken global $SU(2)$ symmetry of the EWSB sector, often called “custodial $SU(2)$ symmetry” [6]. The three Goldstone bosons and the three $SU(2)$ gauge currents transform as triplets under the custodial symmetry. (For a pedagogical discussion see [7].)

At the one-loop level the situation is different. The electroweak measurements are precise enough to begin to probe the effects of one-loop corrections in the couplings

of quarks and leptons to the Z and the W and Z masses. By measuring the one-loop corrections we can gain more information about the EWSB sector.

In the SM, the electroweak symmetry is broken by the Higgs mechanism [8,9,10]. A set of scalar (Higgs) fields are introduced, with a potential which is symmetric under $SU(2) \times U(1)$. The potential has a continuous set of degenerate minima at nonzero field values; the symmetry is spontaneously broken by the ground state choosing one of the degenerate minima.

The minimal SM Higgs sector consists of one complex $SU(2)$ doublet of scalar fields. After EWSB, three of the degrees of freedom are “eaten” by the W and Z bosons, giving them mass, and leaving one CP-even neutral Higgs boson H^0 in the physical spectrum. (For a review of the properties of the SM Higgs boson, see [11].)

Since the couplings of Higgs bosons to fermions and gauge bosons are proportional to the fermion or gauge boson mass, one-loop corrections involving Higgs bosons coupled to W , Z or third-generation quarks can be significant. In the SM, loop corrections involving H^0 coupling to gauge bosons depend logarithmically on the H^0 mass. A fit to the electroweak data gives an upper bound on the SM Higgs mass of $M_H < 220$ GeV at the 95% confidence level [4]. In the SM the Higgs couplings to third-generation quarks do not give us additional information about the Higgs sector. Such corrections would contribute to the decay $Z \rightarrow b\bar{b}$; the decays $Z \rightarrow t\bar{t}$ and $W^+ \rightarrow t\bar{b}$ and its complex conjugate are kinematically forbidden for on-shell W and Z . The coupling of H^0 to b quarks is too small to make an observable contribution to $Z \rightarrow b\bar{b}$. The coupling of the charged Goldstone bosons G^\pm to $t\bar{b}$ is large enough to make an observable contribution to $Z \rightarrow b\bar{b}$, but the contribution is fixed by electroweak symmetry; it depends only on the W and t -quark masses, the electric charge and $\sin^2 \theta_W$ [12,13,14,15,16].

Many extensions to the minimal SM Higgs sector are possible. (For a review and references see [11].) As in the SM, extended models typically must contain at least one $SU(2)$ doublet in order to give mass to the fermions. They can also contain additional $SU(2)$ doublets, singlets, and/or larger multiplets. In general, extended Higgs sectors will yield charged Higgs bosons and additional neutral Higgs bosons in the physical spectrum. Extended Higgs sectors contribute to the radiative corrections to the process $Z \rightarrow b\bar{b}$ through the charged Higgs couplings to $t\bar{b}$ and the neutral Higgs couplings to $b\bar{b}$.

The process $Z \rightarrow b\bar{b}$ yields two observable quantities, R_b and A_b . R_b is the hadronic branching ratio of Z to b quarks,

$$R_b \equiv \frac{\Gamma(Z \rightarrow b\bar{b})}{\Gamma(Z \rightarrow \text{hadrons})} \quad (1.2)$$

and A_b is the b asymmetry,

$$A_b = \frac{\sigma(e_L^- \rightarrow b_F) - \sigma(e_L^- \rightarrow b_B) + \sigma(e_R^- \rightarrow b_B) - \sigma(e_R^- \rightarrow b_F)}{\sigma(e_L^- \rightarrow b_F) + \sigma(e_L^- \rightarrow b_B) + \sigma(e_R^- \rightarrow b_B) + \sigma(e_R^- \rightarrow b_F)}, \quad (1.3)$$

where $e_{L,R}^-$ are left and right handed initial-state electrons and $b_{F,B}$ are final-state b quarks moving in the forward and backward directions. The forward direction is defined as the direction of the initial-state electrons. In terms of the b quark couplings to Z ,

$$A_b = \frac{(g_{Zb\bar{b}}^L)^2 - (g_{Zb\bar{b}}^R)^2}{(g_{Zb\bar{b}}^L)^2 + (g_{Zb\bar{b}}^R)^2}. \quad (1.4)$$

Until 1996 the R_b measurement was significantly higher than the SM prediction [17], and a number of models were introduced to bring the prediction into better agreement with experiment [18]. These include models with a modified tree-level $Zb\bar{b}$ coupling [19], a significantly lower value for the top mass [20], or extra particles which contribute to R_b through loop corrections [21,22,23,24,25]. The last two approaches take advantage of the fact that the discrepancy in R_b was the same size as the top-mass-dependent loop corrections to $Z \rightarrow b\bar{b}$, which arise from the exchange of longitudinally polarized W^\pm bosons (*i.e.*, the SM Goldstone bosons G^\pm). Since 1996 the R_b measurement has come closer to the SM prediction but is still slightly high. It is best used to constrain models that would predict a lower R_b than the SM.

In this thesis we introduce a parameterization for a general extended Higgs sector and calculate the contribution to $Z \rightarrow b\bar{b}$ from one-loop radiative corrections involving singly charged and neutral Higgs bosons. We obtain general expressions for the corrections to the left- and right-handed $Zb\bar{b}$ couplings, and then use the measurements of R_b and A_b to constrain specific models. This approach has the advantage of yielding general formulas for the corrections in terms of the couplings and masses of the Higgs bosons. The formulas can then be specialized to any extended Higgs model by inserting the appropriate couplings. Kundu and Mukhopadhyaya [26] have taken the same approach and calculated the charged Higgs boson contributions to $Z \rightarrow b\bar{b}$ in a general extended Higgs sector. However, the neutral Higgs boson contributions in a general extended Higgs sector do not appear in the literature. Previously, the corrections to $Z \rightarrow b\bar{b}$ in extended Higgs sectors had only been computed for the two Higgs doublet model (2HDM) [27,28,29,21].

This thesis does not take into account corrections to $Z \rightarrow b\bar{b}$ coming from loops involving supersymmetric particles. However, in the limit of large superpartner masses, the supersymmetric contributions decouple [30,31,32]. In this limit, our formulas are relevant in supersymmetric models with extended Higgs sectors.

The method of parameterizing a general extended Higgs sector developed in this thesis can also be used to calculate Higgs boson corrections to other processes, such as $b \rightarrow s\gamma$ and $b \rightarrow c\tau^-\bar{\nu}_\tau$.

This thesis is organized as follows. In chapter 2 we discuss the measurements of R_b and A_b and the constraints that they put on the $Zb\bar{b}$ couplings. In chapter 3 we introduce the two Higgs doublet model and then generalize to an arbitrary extended Higgs sector, as well as describing some of the features that such models contain. In chapters 4

and 5 we calculate the radiative corrections to the $Zb\bar{b}$ coupling. In chapter 4 we consider the loops involving charged Higgs bosons while in chapter 5 we consider the loops involving neutral Higgs bosons. In chapter 6 we apply the general formulas for loop corrections to a number of specific models and exhibit constraints on the charged Higgs sector. We first consider extended Higgs sectors containing only doublets and singlets, and then extend the analysis to Higgs sectors containing larger multiplets as well. We summarize our conclusions in chapter 7.

In the appendices we summarize a number of extended Higgs models, and list formulas which we have used in our analysis. In appendix A we list the tree-level Z couplings to quarks in the SM. In appendix B we list the Higgs couplings to vector bosons for an arbitrary extended Higgs sector. In appendices C, D, and E we describe the details of some of the extended Higgs models which are considered in our analysis. In appendix C we list the couplings in the two Higgs doublet model. In appendix D we describe the models containing two Higgs doublets and one triplet. In appendix E we describe a class of models in which the Higgs sector preserves a “custodial” $SU(2)$ symmetry. In appendix F we give details of the calculation of one-loop integrals. Finally, in appendices G, H, and I, we describe the experimental data used in this thesis. In appendix G we describe how the A_b measurement was extracted from the data. In appendix H we list the SM parameters used in our numerical calculations. Lastly, in appendix I, we describe the lower bounds on Higgs masses from direct searches.

Chapter 2

Constraints from the data

The radiative corrections to $Z \rightarrow b\bar{b}$ modify the $Zb\bar{b}$ couplings from their tree-level values. In this section we show how the experimental constraints on R_b and A_b constrain the possible values of the effective $Zb\bar{b}$ couplings. These constraints will provide limits on the radiative corrections. The effective couplings are

$$\bar{g}_b^{L,R} = g_{Zb\bar{b}}^{L,R} + \delta g^{L,R} \quad (2.1)$$

where $\bar{g}_b^{L,R}$ are the radiatively-corrected effective couplings, $g_{Zb\bar{b}}^{L,R}$ are the tree-level couplings, and $\delta g^{L,R}$ contain the radiative corrections. Our notation and the tree-level couplings are listed in appendix A.

The effective couplings $\bar{g}_b^{L,R}$ are extracted from the measured values of R_b and A_b in the next section. In order to use these to constrain new physics, the SM prediction for $\bar{g}_b^{L,R}$ must be known precisely. This requires an accurate value of $\sin^2 \theta_{eff}^{lept}$, which can be affected by oblique corrections from new physics. This issue is addressed in section 2.2.

2.1 Extracting the effective $Zb\bar{b}$ couplings from R_b and A_b

Following the discussion by Field [19] and using his notation, the effective couplings $\bar{g}_b^{L,R}$ are related to R_b and A_b as follows.

$$R_b = \left[1 + \frac{S_b}{\bar{s}_b C_b^{QCD} C_b^{QED}} \right]^{-1} \quad (2.2)$$

$$A_b = \frac{2\bar{r}_b(1 - 4\mu_b)^{1/2}}{1 - 4\mu_b + (1 + 2\mu_b)\bar{r}_b^2} \quad (2.3)$$

where

$$\bar{r}_b = \frac{\bar{v}_b}{\bar{a}_b} \quad (2.4)$$

$$\bar{s}_b = (\bar{a}_b)^2(1 - 6\mu_b) + (\bar{v}_b)^2 \quad (2.5)$$

$$\bar{v}_b = \bar{g}_b^L + \bar{g}_b^R \quad (2.6)$$

$$\bar{a}_b = \bar{g}_b^L - \bar{g}_b^R \quad (2.7)$$

$$S_b = \sum_{q \neq b} (\bar{a}_q)^2 + (\bar{v}_q)^2. \quad (2.8)$$

μ_b is a correction factor coming from the nonzero mass of the b quark. Using the running b quark mass in the $\overline{\text{MS}}$ scheme evaluated at M_Z , $\bar{m}_b(M_Z) = 3.0$ GeV [33], this correction factor is $\mu_b = (\bar{m}_b(M_Z)/M_Z)^2 \simeq 1.0 \times 10^{-3}$.

C_b^{QED} and C_b^{QCD} are QED and QCD correction factors,

$$C_b^{QED} = 1 + \delta_b^{QED} - \langle \delta_{q \neq b}^{QED} \rangle \quad (2.9)$$

$$C_b^{QCD} = 1 + \delta_b^{QCD} - \delta_{q \neq b}^{QCD}, \quad (2.10)$$

where $\langle \delta_{q \neq b}^{QED} \rangle$ denotes the average of $\delta_{q \neq b}^{QED}$ over u , d , c , and s quarks, and,

$$\delta_q^{QED} = \frac{3(e_q)^2}{4\pi} \alpha(M_Z) \quad (2.11)$$

$$\delta_{q \neq b}^{QCD} = 1.00 \left(\frac{\alpha_s(M_Z)}{\pi} \right) + 1.42 \left(\frac{\alpha_s(M_Z)}{\pi} \right)^2 \quad (2.12)$$

$$\delta_b^{QCD} = 0.99 \left(\frac{\alpha_s(M_Z)}{\pi} \right) - 1.55 \left(\frac{\alpha_s(M_Z)}{\pi} \right)^2, \quad (2.13)$$

where e_q is the quark electric charge in units of the positron charge. Numerically, with $\alpha_s(M_Z) = 0.12$ and $\alpha^{-1}(M_Z) = 128.9$,

$$C_b^{QED} = 0.99975 \quad (2.14)$$

$$C_b^{QCD} = 0.9953. \quad (2.15)$$

The non- b quark couplings are written as,

$$\bar{a}_q = \sqrt{\rho_q} T_3^q \quad (2.16)$$

$$\bar{v}_q = \sqrt{\rho_q} (T_3^q - 2e_q(\bar{s}_W^q)^2) \quad (2.17)$$

where, assuming non- b quark universality, for all $q \neq b$,

$$\sqrt{\rho_q} = \sqrt{\rho_l} = 2|\bar{a}_l| \quad (2.18)$$

$$(\bar{s}_W^q)^2 = \frac{1}{4}(1 - \bar{r}_l), \quad (2.19)$$

2.1 Extracting the effective $Zb\bar{b}$ couplings from R_b and A_b

and T_3^q is the third component of weak isospin of quark q . The SM prediction for the effective couplings is then [19],

$$\bar{g}_b^L = -0.4208 \quad (2.20)$$

$$\bar{g}_b^R = 0.0774. \quad (2.21)$$

Together with the SM predictions for the leptonic couplings,

$$\bar{a}_l = -0.50124 \quad (2.22)$$

$$\bar{r}_l = 0.07332, \quad (2.23)$$

these yield the SM predictions for R_b and A_b ,

$$R_b^{SM} = 0.21587 \quad (2.24)$$

$$A_b^{SM} = 0.935. \quad (2.25)$$

These are the SM predictions quoted in [4]. (For a discussion of how R_b^{SM} was obtained, see appendix H.)

The measured values are [4],

$$R_b = 0.21680 \pm 0.00073 \quad (2.26)$$

$$A_b = 0.895 \pm 0.016 \quad (2.27)$$

R_b is measured directly at LEP and SLD. A_b is measured directly at SLD from the left-right forward-backward asymmetry, and indirectly at LEP from the measured value of A_e and the forward-backward asymmetry $A_{FB}^{0,b} = \frac{3}{4}A_e A_b$. Details of the calculation of A_b , and the inputs used, are listed in appendix G. The R_b measurement is 1.3σ above the SM prediction, and the A_b measurement is 2.5σ below the SM prediction.

Defining

$$(\bar{g}_b^{L,R})_{\text{expt}} = (\bar{g}_b^{L,R})_{SM} + \delta g_{\text{new}}^{L,R} \quad (2.28)$$

we plot the experimental constraints from R_b and A_b on $\delta g_{\text{new}}^{L,R}$ in figure 2.1. The central value is at $\delta g^L = 0.0032$ and $\delta g^R = 0.0210$. Comparing these to the SM predictions, we see that δg^L is a 1% correction while δg^R is close to a 30% correction. This is in approximate agreement with the results of Field, [19] who found that a model independent fit of the Z pole data yielded a right-handed b quark coupling 42% above the SM prediction.

It is also useful to expand R_b and A_b about their SM values, to first order in $\delta g_{\text{new}}^{R,L}$. Using the SM parameters given above, we find

$$\delta R_b = -0.7788\delta g_{\text{new}}^L + 0.1410\delta g_{\text{new}}^R \quad (2.29)$$

$$\delta A_b = -0.2984\delta g_{\text{new}}^L - 1.623\delta g_{\text{new}}^R. \quad (2.30)$$

Note that a positive δg_{new}^L decreases both R_b and A_b , while a positive δg_{new}^R increases R_b and decreases A_b .

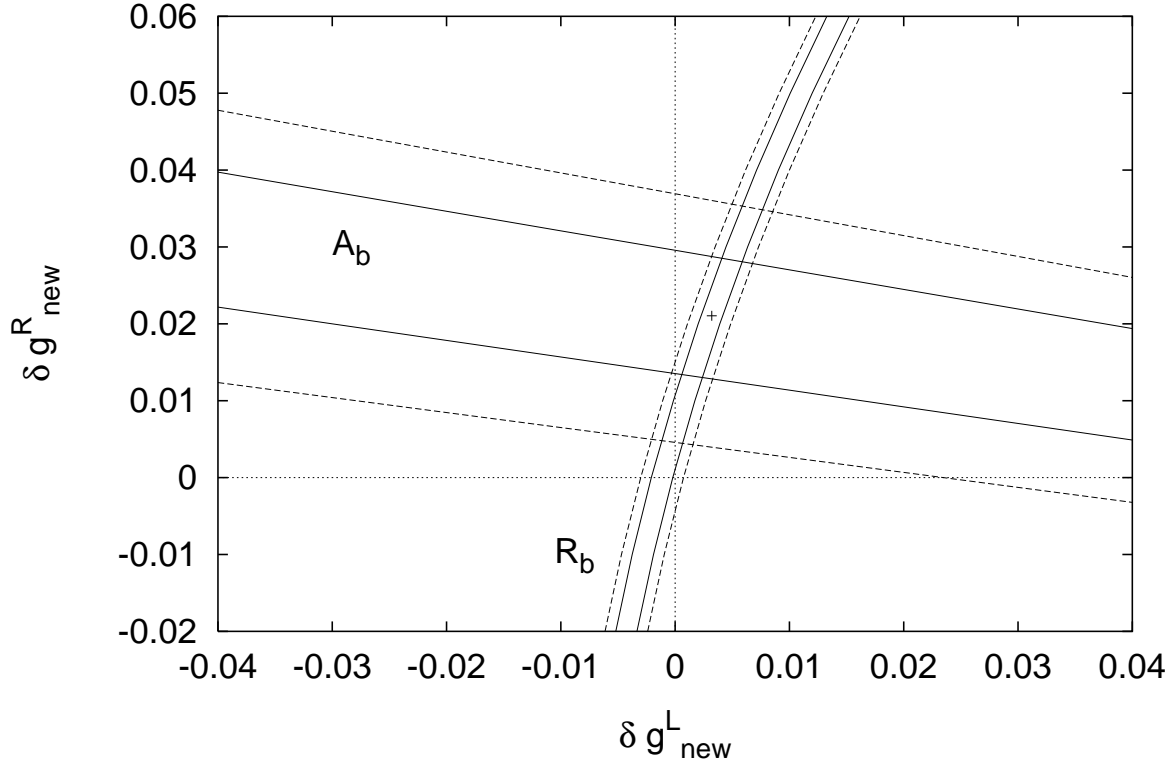


Figure 2.1: The constraints from R_b and A_b on the right- and left-handed $Zb\bar{b}$ couplings. Plotted are the allowed deviations $\delta g_{\text{new}}^{R,L}$ of the couplings from their SM values. The 1σ errors are shown as solid lines and the 2σ errors as dashed lines. The central value, at $\delta g_{\text{new}}^L = 0.0032$ and $\delta g_{\text{new}}^R = 0.0210$, is marked by the cross.

2.2 Tree-level $Zb\bar{b}$ couplings: The effect of oblique corrections

2.2 Tree-level $Zb\bar{b}$ couplings: The effect of oblique corrections

In the SM, all electroweak observables are fixed by the measurement of three quantities, commonly chosen to be the electromagnetic fine structure constant α , the muon decay constant G_μ , and the Z mass. In particular, by measuring these quantities, one can predict the value of $\sin^2 \theta_{eff}^{lept}$. In practice, many more electroweak observables are measured and a fit is made to the SM parameters (see e.g., [34]).

However, the dependence of $\sin^2 \theta_{eff}^{lept}$ on other electroweak observables can be modified in models with new physics that contributes to oblique corrections. These modifications are parameterized by the Peskin–Takeuchi parameters S , T , and U [35]. In particular [36],

$$\sin^2 \theta_{eff}^{lept} - [\sin^2 \theta_{eff}^{lept}]_{SM} \equiv \delta s_W^2 = \frac{\alpha}{c_W^2 - s_W^2} \left[\frac{1}{4} S - s_W^2 c_W^2 T \right]. \quad (2.31)$$

Nonzero values of the S and T parameters therefore modify the prediction for the tree-level $Zb\bar{b}$ couplings $g_{Zb\bar{b}}^{L,R}$.

The S , T , and U parameters are defined relative to a reference SM, with a fixed SM Higgs mass. In the reference SM they are all zero. For $M_H^{SM} = M_Z$, a fit of the electroweak data gives [37]

$$S = -0.16 \pm 0.14 \quad (2.32)$$

$$T = -0.21 \pm 0.16 \quad (2.33)$$

$$U = 0.25 \pm 0.24. \quad (2.34)$$

In order to understand the significance of oblique corrections of this size, we compute the corrections to the SM predictions for R_b and A_b due to S , T , and U . To first order in δs_W^2 ,

$$\delta R_b = \frac{R_b}{\bar{s}_b} \left[4\bar{v}_b g_b^R (1 - R_b) + \frac{32R_b \bar{a}_l^2}{C_b^{QCD} C_b^{QED}} \left(\frac{1}{2s_W^2} - \frac{10}{9} \right) \right] \frac{\delta s_W^2}{s_W^2} \quad (2.35)$$

$$= 0.0373 \delta s_W^2 = 1.35 \times 10^{-4} S - 9.62 \times 10^{-5} T \quad (2.36)$$

$$\delta A_b = \left[A_b \left(1 - A_b \frac{(1 + 2\mu_b)}{\sqrt{1 - 4\mu_b}} \bar{r}_b \right) \frac{2g_b^R}{\bar{v}_b} \right] \frac{\delta s_W^2}{s_W^2} \quad (2.37)$$

$$= -0.642 \delta s_W^2 = -2.32 \times 10^{-3} S + 1.66 \times 10^{-3} T \quad (2.38)$$

where we have used the SM values all parameters as given in section 2.1 and $[\sin^2 \theta_{eff}^{lept}]_{SM} \equiv (s_W^2)_{SM} = 0.23157$. The oblique corrections to the SM predictions for R_b and A_b do not depend on U .

Inserting the measured central values of S and T , we find

$$\delta R_b = -1.4 \times 10^{-6} \tag{2.39}$$

$$\delta A_b = 2.3 \times 10^{-5}. \tag{2.40}$$

Comparing these corrections to the measured values in equations 2.26 and 2.27, we see that the correction due to nonzero values of S and T is less than 1% of the experimental error on both R_b and A_b . We can safely neglect these corrections.

Chapter 3

Models with extended Higgs sectors

A wide variety of extensions to the minimal SM Higgs sector are possible. (For a review and references see [11].) In this section we discuss some of the interesting features of models with extended Higgs sectors. We also list some important formulas for the couplings and Goldstone bosons in the two Higgs doublet model and a general extended Higgs sector. These formulas will be used later in the corrections to the process $Z \rightarrow b\bar{b}$.

The ρ parameter in an extended Higgs sector

In an extended Higgs sector which contains one or more multiplets larger than doublets, there is the possibility of having $\rho \neq 1$ at tree level. It is well known that $\rho = 1$ at tree-level in a Higgs sector containing only doublets and singlets [38,39]. In a general Higgs sector, however, the tree-level ρ parameter is given by [11,40]

$$\rho \equiv \frac{m_W^2}{m_Z^2 c_W^2} = \frac{\sum_k 2(T_k(T_k + 1) - Y_k^2/4)v_k^2 + \sum_i 2T_i(T_i + 1)v_i^2}{\sum_k Y_k^2 v_k^2}, \quad (3.1)$$

where k runs over the complex multiplets and i runs over the real multiplets in the Higgs sector, and $c_W = \cos \theta_W$. The Higgs vacuum expectation values (vevs) v_k and v_i for each multiplet are defined as,

$$\langle \phi_k^0 \rangle = v_k / \sqrt{2} \quad (3.2)$$

for complex representations, and

$$\langle \eta_i^0 \rangle = v_i \quad (3.3)$$

for real representations.

Experimentally, ρ has been shown to be very close to one; in particular, $\Delta\rho \equiv \rho - 1 = (3.9 \pm 1.2) \times 10^{-3}$ ([5], in which $\Delta\rho = \epsilon_1$). Certain multiplets automatically satisfy $\rho = 1$. These are multiplets for which [11],

$$(2T + 1)^2 - 3Y^2 = 1. \quad (3.4)$$

This equation is satisfied by the singlet $(T, Y) = (0, 0)$, the familiar doublet $(\frac{1}{2}, 1)$, and a series of complicated larger multiplets, $(3, 4)$, $(\frac{25}{2}, 15)$, etc. Higgs sectors that contain only multiplets of this type yield $\rho = 1$ without any fine-tuning of the parameters of the Higgs potential.

However, problems arise when one attempts to construct a Higgs sector in which the only multiplets larger than doublets satisfy equation 3.4. First, the Higgs sector must contain at least one doublet in order to give mass to the fermions. Then the Higgs potential will be forced by $SU(2)_L \times U(1)_Y$ -invariance to have an accidental continuous global symmetry (e.g., a separate $U(1)$ rotation of each of the multiplets larger than doublets). The global symmetry is spontaneously broken when the larger multiplets get vevs, resulting in massless Goldstone bosons in the physical spectrum. As described in reference [41], the physical spectrum must also contain a light CP-even Higgs boson H^0 with mass on the order of the vev of the larger multiplet. This is required because the mass splitting between the massless Goldstone boson and H^0 is on the order of the vev that breaks the accidental global symmetry. Such a massless Goldstone boson is then ruled out by the experimental limits on $Z \rightarrow a^0 H^0$, where a^0 is the massless Goldstone boson [41].

The accidental global symmetries can be eliminated by introducing a set of new Higgs multiplets to couple the $U(1)$ rotations of the larger multiplets to those of the doublet, so that the model has only one $U(1)$ symmetry, that of hypercharge. However, these new multiplets will in general spoil $\rho = 1$. There are two ways that $\rho \approx 1$ can be maintained. First, we can require that the vevs of the new multiplets must be small enough to satisfy the experimental constraints on ρ . This requires an unnatural fine-tuning. A completely general Higgs sector can be made to agree with $\rho \approx 1$ by fine-tuning the parameters of the model so that the multiplets that would contribute to $\rho \neq 1$ have very small vevs. Second, we can introduce a set of new Higgs multiplets such that the entire Higgs sector preserves a custodial $SU(2)_c$ symmetry. This can be done for each of the multiplets that satisfy equation 3.4. The new multiplets eliminate the accidental $U(1)$ symmetry, while at the same time the $SU(2)_c$ symmetry ensures that $\rho = 1$ by ensuring that equal masses are given to the W^\pm and W^3 gauge bosons. Models with $SU(2)_c$ symmetry are discussed in detail in appendix E.

In general, the $SU(2)_c$ symmetry is preserved through a conspiracy of the vevs and electroweak quantum numbers of the Higgs multiplets in the model. This conspiracy can be made exact to all orders in the Higgs self-couplings by requiring that the Higgs potential be

invariant under the custodial $SU(2)_c$ symmetry. This is only possible when the Higgs sector consists of certain sets of multiplets, which transform together under an $SU(2)_L \times SU(2)_R$ symmetry. Such a model involving triplet Higgs fields has been constructed by Georgi and Machacek [42]. It was considered in greater depth by Chanowitz and Golden [43], who showed that a Higgs potential for the model could be constructed that was invariant under the full $SU(2)_L \times SU(2)_R$. This ensured that radiative corrections from Higgs self-interactions preserved $SU(2)_c$. A more detailed study of the phenomenology of the model [44] and naturalness problems from one-loop effects [45] was made by Gunion, Vega, and Wudka. The fields in this model consist of one $Y = 1$ complex doublet, one real ($Y = 0$) triplet, and one $Y = 2$ complex triplet. The $SU(2)_c$ symmetry ensures that the vevs of the neutral members of the two triplets are equal, yielding $\rho = 1$. This model must be fine tuned because $SU(2)_c$ -breaking terms arise in the Higgs potential at the one-loop level [45] from corrections involving the hypercharge interactions. For more details, see appendix E.

Higgs couplings in an extended Higgs sector

An extended Higgs sector that contains multiplets larger than doublets can have Higgs couplings which differ from the analogous couplings in the SM and in models containing only doublets and singlets. Some couplings can be enhanced relative to their values in models containing only doublets and singlets, and other couplings exist that are not present in simpler models. For simplicity, we assume that the Higgs sector is CP-conserving. We denote the CP-even neutral Higgs bosons by H_i^0 , the CP-odd neutral Higgs bosons by A_i^0 , and the charged Higgs bosons by H_i^+ , H_i^{++} , etc.

The Higgs couplings to Z and W^\pm are affected because of their dependence on the isospin of the electroweak eigenstates involved. For example [see equations 3.26 – 3.29], the couplings $g_{ZH_i^0 A_j^0}$, $g_{ZH_i^+ H_i^-}$, $g_{W^+ W^- H_i^0}$, and $g_{ZZ H_i^0}$ can be enhanced in a model containing multiplets larger than doublets. This can lead to an enhancement of the production cross section for certain Higgs bosons through the processes $Z^* \rightarrow H_i^0 A_j^0$, $Z^* \rightarrow H_i^+ H_i^-$, $W^* \rightarrow W H_i^0$, and $Z^* \rightarrow Z H_i^0$, as well as enhancement of the loop correction to $Z \rightarrow b\bar{b}$ from the diagram of figure 4.3(a).

Certain couplings exist in models with multiplets larger than doublets that are zero in models containing only doublets and singlets. For example, off-diagonal charged Higgs couplings to Z (equation 3.27), and the $H_i^\pm W^\mp Z$ vertex, described in [11] and references therein, are generally nonzero in Higgs sectors that include multiplets larger than doublets. The off-diagonal charged Higgs couplings to Z can lead to loop corrections to $Z \rightarrow b\bar{b}$ involving two charged Higgs bosons of different mass in the loop. The Feynman diagram for this process is given in figure 4.3(a).

3.1 The two Higgs doublet model

In this section we briefly review some properties of the two Higgs doublet model (2HDM). A working knowledge of this model will be useful when we consider a general extended Higgs sector in the next section. For a more complete treatment see reference [11,21]. The discussion below follows [21]. The complete Higgs couplings to fermions and the Z –Higgs–Higgs couplings in this model are listed in appendix C.

The 2HDM is the usual $SU(2)_L \times U(1)_Y$ SM with an extended Higgs sector consisting of two complex doublets of scalar fields, Φ_1 and Φ_2 , with hypercharge $Y = 1$. Note that any model that contains a complex Higgs multiplet Φ with hypercharge Y can be rewritten in terms of the conjugate multiplet $i\sigma_2\Phi^*$ with hypercharge $-Y$. The electroweak gauge symmetry $SU(2)_L \times U(1)_Y$ is broken down to electromagnetic $U(1)_{EM}$ by choosing a Higgs potential such that the two real neutral Higgs fields acquire the vevs v_1 and v_2 . The Goldstone bosons are then

$$G^0 = \cos \beta \phi_1^{0,i} + \sin \beta \phi_2^{0,i} \quad (3.5)$$

$$G^+ = \cos \beta \phi_1^+ + \sin \beta \phi_2^+ \quad (3.6)$$

where the Higgs doublets are $\Phi_k = (\phi_k^+, \phi_k^0)$, the neutral component is $\phi_k^0 = \frac{1}{\sqrt{2}}(v_k + \phi_k^{0,r} + i\phi_k^{0,i})$, and the ratio of the vevs is parameterized by $\tan \beta = v_2/v_1$. The W^\pm and Z bosons acquire mass through the Higgs mechanism and the fermions acquire mass through their Yukawa couplings to the Higgs bosons. The vevs of the two Higgs doublets are constrained by the W mass, $M_W^2 = g^2(v_1^2 + v_2^2)/4 = g^2 v_{SM}^2/4$, where $v_{SM} = 246$ GeV.

In addition to the Goldstone bosons, the 2HDM contains one charged Higgs boson H^\pm , one CP–odd neutral Higgs boson A^0 , and two CP–even neutral Higgs bosons h^0 and H^0 . The Higgs mass eigenstates are

$$H^\pm = -\sin \beta \phi_1^\pm + \cos \beta \phi_2^\pm \quad (3.7)$$

$$A^0 = -\sin \beta \phi_1^{0,i} + \cos \beta \phi_2^{0,i} \quad (3.8)$$

$$h^0 = -\sin \alpha \phi_1^{0,r} + \cos \alpha \phi_2^{0,r} \quad (3.9)$$

$$H^0 = \cos \alpha \phi_1^{0,r} + \sin \alpha \phi_2^{0,r}. \quad (3.10)$$

The two CP–even neutral states are defined so that h^0 is lighter than H^0 . α is a mixing angle determined by the Higgs potential.

In the SM, the diagonalization of the quark mass matrix automatically diagonalizes the Yukawa couplings of the neutral Higgs boson to quarks. Thus in the SM, there are no tree–level flavor–changing neutral Higgs interactions. In the 2HDM with the most general Higgs Yukawa couplings, however, flavor–changing neutral Higgs interactions can arise.

3.1 The two Higgs doublet model

These interactions are severely constrained by the measurements of $K^0 - \bar{K}^0$ and $B^0 - \bar{B}^0$ mixing, which arise at the one-loop level in the SM. Because the constraints on flavor-changing neutral Higgs couplings involving first-generation quarks are the strongest, it has been suggested that the flavor-changing couplings should be proportional to the masses of the quarks involved in the coupling, so that the couplings are of order $\sqrt{m_i m_j}/v_{SM}$, where $v_{SM} = 246$ GeV is the SM Higgs vev. Even with the Yukawa couplings suppressed by first-generation quark masses, however, the measurements of $K^0 - \bar{K}^0$ and $B^0 - \bar{B}^0$ mixing require that M_{A^0} is above 2 TeV [46]. The constraint on M_{A^0} from flavor-changing neutral Higgs interactions is significantly stronger than the constraints on Higgs masses from R_b that we will present.

The severe constraints on flavor-changing neutral Higgs interactions led Glashow and Weinberg [47] and Paschos [48] to introduce a discrete symmetry in order to forbid tree-level flavor-changing neutral Higgs interactions in models with more than one doublet. They showed that a sufficient condition to eliminate flavor-changing neutral Higgs interactions in a model containing more than one Higgs doublet is that the fermions of each charge receive their mass from couplings to exactly one neutral Higgs field. (Note that mass terms for quarks that conserve baryon number and are $SU(2)_L \times U(1)_Y$ -invariant can only arise from couplings to Higgs doublets with hypercharge $Y = \pm 1$.)

With the discrete symmetry of references [47,48], there are two possible configurations for the quark Yukawa couplings in the 2HDM, referred to as the Type I and Type II models. In the Type I model, all the quarks couple to Φ_1 , and not to Φ_2 . In the Type II model, the down-type quarks couple to Φ_1 and the up-type quarks couple to Φ_2 . The Higgs sector in the minimal supersymmetric model is a Type II 2HDM.

In a Type I model, one Higgs doublet Φ_1 gives mass to both t and b quarks. The Yukawa couplings are,

$$\lambda_t = \frac{\sqrt{2}m_t}{v_1} \quad (3.11)$$

$$\lambda_b = \frac{\sqrt{2}m_b}{v_1}. \quad (3.12)$$

Note that in a Type I model, $\lambda_b/\lambda_t = m_b/m_t$, so $\lambda_b \ll \lambda_t$ for all values of v_1 .

In a Type II model, Φ_1 couples to b quarks and Φ_2 couples to t quarks. The quark Yukawa couplings are then,

$$\lambda_t = \frac{\sqrt{2}m_t}{v_2} \quad (3.13)$$

$$\lambda_b = \frac{\sqrt{2}m_b}{v_1} \quad (3.14)$$

Note that in a Type II model, $\lambda_b/\lambda_t = (m_b/m_t) \tan \beta$, so λ_b can be enhanced relative to λ_t by choosing v_1 much less than v_2 (i.e., choosing $\tan \beta$ to be large). The Yukawa couplings

for the 2HDM Higgs mass eigenstates are listed in appendix C.

3.2 A general extended Higgs sector

In this thesis we consider the effects of a general extended Higgs sector on the $Z \rightarrow b\bar{b}$ decay rate. We remind the reader that an extended Higgs sector consists of a number of scalars organized into multiplets according to their transformation properties under $SU(2)_L \times U(1)_Y$. The Higgs sector must contain at least one $SU(2)_L$ doublet to give mass to the SM fermions. The Higgs sector is divided into complex representations, denoted by ϕ_k , and real representations, denoted by η_i . We define a real representation as consisting of a real multiplet of fields with integer weak isospin and hypercharge $Y = 0$, as in reference [11]. We also assume that the Higgs sector is CP-conserving, so that the neutral Higgs mass eigenstates are either CP-even or CP-odd. We will denote a CP-even state by H_i^0 and a CP-odd state by A_j^0 . A Higgs potential is chosen to break $SU(2)_L \times U(1)_Y$ down to $U(1)_{EM}$ such that the neutral member of each of the Higgs multiplets acquires a vev. We denote the vevs of complex representations by v_k and the vevs of real representations by v_i . The vevs are normalized as in equations 3.2 and 3.3. These vevs are constrained by the W mass, which for a general extended Higgs sector is given by,

$$M_W^2 = \frac{g^2}{4} \left\{ \sum_k 2v_k^2(T_k(T_k + 1) - \frac{Y_k^2}{4}) + \sum_i 2v_i^2 T_i(T_i + 1) \right\} = \frac{g^2}{4} v_{SM}^2, \quad (3.15)$$

where $v_{SM} = 246$ GeV. The Goldstone bosons are given by,

$$G^0 = \frac{\sum_k Y_k v_k \phi_k^{0,i}}{\sqrt{\sum_k Y_k^2 v_k^2}} \quad (3.16)$$

$$\begin{aligned} G^+ &= \left\{ \sum_k \left[[T_k(T_k + 1) - Y_k(Y_k - 2)/4]^{1/2} v_k \phi_k^+ \right. \right. \\ &\quad \left. \left. - [T_k(T_k + 1) - Y_k(Y_k + 2)/4]^{1/2} v_k (\phi_k^-)^* \right] + \sum_i [2T_i(T_i + 1)]^{1/2} v_i \eta_i^+ \right\} \\ &\quad \times \left\{ \sum_k 2v_k^2(T_k(T_k + 1) - Y_k^2/4) + \sum_i 2v_i^2 T_i(T_i + 1) \right\}^{-1/2}, \end{aligned} \quad (3.17)$$

and we use the phase convention,

$$G^- = -(G^+)^*. \quad (3.18)$$

3.2 A general extended Higgs sector

Note that for a Higgs boson in a complex representation, $(\phi^Q)^*$ is a state with charge $-Q$ but is not the same as ϕ^{-Q} . For a Higgs boson in a real representation, we use the phase convention $(\eta^+)^* = -\eta^-$.

In a Higgs sector that contains only multiplets for which $\rho = 1$ automatically (see equation 3.4), the W mass and the formula for G^+ simplify to,

$$M_W^2 = \frac{g^2}{4} \sum_k Y_k^2 v_k^2 \quad (3.19)$$

$$G^+ = \frac{\sum_k \left[[(Y_k^2 + Y_k)/2]^{1/2} v_k \phi_k^+ - [(Y_k^2 - Y_k)/2]^{1/2} v_k (\phi_k^-)^* \right]}{\sqrt{\sum_k Y_k^2 v_k^2}}. \quad (3.20)$$

The Yukawa couplings of a general extended Higgs sector take the form of either a Type I or Type II model, and are defined in the same way as in the 2HDM. If the extended model contains only one Higgs doublet, Φ_1 , it is necessarily a Type I model, with the Yukawa couplings given in equations 3.11 and 3.12. If the extended model contains two or more Higgs doublets, then it can be either a Type I model or a Type II model. If all the quarks couple only to one Higgs doublet Φ_1 , the model is Type I, with the Yukawa couplings given in equations 3.11 and 3.12. Alternatively, if the down-type quarks couple to one Higgs doublet Φ_1 and the up-type quarks couple to a different Higgs doublet Φ_2 , then the model is Type II, with the Yukawa couplings given in equations 3.13 and 3.14.

When the Higgs mass-squared matrix is diagonalized, the electroweak eigenstates mix to form mass eigenstates. Recall that we have assumed that the Higgs sector is CP-conserving. We denote the CP-even neutral Higgs bosons by H_i^0 and the CP-odd neutral Higgs bosons by A_i^0 . The couplings of the Higgs mass eigenstates to quarks take the form,

$$i(g_{H\bar{q}q}^L P_L + g_{H\bar{q}q}^R P_R) = i(g_{H\bar{q}q}^V + g_{H\bar{q}q}^A \gamma_5). \quad (3.21)$$

The individual couplings to $b\bar{b}$ and $b\bar{t}$ in a Type II model are given by,

$$g_{H_i^0 b\bar{b}}^V = -\frac{1}{\sqrt{2}} \lambda_b \langle H_i^0 | \phi_1^{0,r} \rangle \quad (3.22)$$

$$g_{A_i^0 b\bar{b}}^A = -\frac{i}{\sqrt{2}} \lambda_b \langle A_i^0 | \phi_1^{0,i} \rangle \quad (3.23)$$

$$g_{H_i^+ t\bar{b}}^R = -\lambda_b \langle H_i^+ | \phi_1^+ \rangle \quad (3.24)$$

$$g_{H_i^+ t\bar{b}}^L = +\lambda_t \langle H_i^+ | \phi_2^+ \rangle. \quad (3.25)$$

The couplings for a Type I model are obtained by replacing ϕ_2^+ with ϕ_1^+ in equation 3.25; the other couplings remain the same.

The Z –Higgs–Higgs couplings take the form given in equation B.4. The Z –Higgs–Higgs couplings involving neutral and singly–charged Higgs bosons are,

$$g_{ZH_i^0 A_j^0} = \frac{ie}{s_W c_W} \sum_{k=1}^N \langle H_i^0 | \phi_k^{0,r} \rangle \langle A_j^0 | \phi_k^{0,i} \rangle T_{\phi_k^0}^3 \quad (3.26)$$

$$g_{ZH_i^+ H_j^-} = -\frac{e}{s_W c_W} \left\{ \sum_{k=1}^N \langle H_i^+ | \phi_k^+ \rangle \langle H_j^- | \phi_k^+ \rangle T_{\phi_k^+}^3 - s_W^2 \delta_{ij} \right\}. \quad (3.27)$$

For completeness, we also give the $W^+ W^- H_i^0$ and $ZZ H_i^0$ couplings. The V –Higgs–Higgs ($V = W, Z$) take the form given in equation B.6. The $W^+ W^- H_i^0$ coupling is,

$$g_{W^+ W^- H_i^0} = g^2 \sum_k \langle H_i^0 | \phi_k^{0,r} \rangle v_k \left(T_k(T_k + 1) - \frac{Y_k^2}{4} \right), \quad (3.28)$$

and the $ZZ H_i^0$ coupling is,

$$g_{ZZ H_i^0} = \frac{g^2}{2c_W^2} \sum_k \langle H_i^0 | \phi_k^{0,r} \rangle v_k Y_k^2 \quad (3.29)$$

where $s_W = \sin \theta_W$, $c_W = \cos \theta_W$, and T_ϕ^3 is the third component of the weak isospin of ϕ . The complete Higgs–Vector boson couplings can be found in appendix B.

Although the Z –Higgs–Higgs couplings are diagonal in the electroweak basis, they are not necessarily diagonal in the mass eigenstate basis. In addition, the $ZH^+ H^-$ couplings can differ from the SM $ZG^+ G^-$ coupling. This can happen in a general model if H^+ has some admixture of a multiplet larger than a doublet. In the SM, the $ZG^+ G^-$ coupling is,

$$g_{ZG^+ G^-} = -\frac{e}{s_W c_W} \left(\frac{1}{2} - s_W^2 \right). \quad (3.30)$$

Chapter 4

Charged Higgs corrections to $Z \rightarrow b\bar{b}$

In the SM, the $Zb\bar{b}$ couplings receive a correction from the exchange of the longitudinal components of the W^\pm and Z bosons. The Feynman diagrams for these corrections are shown in figure 4.1. We work in the 't Hooft-Feynman gauge, in which the longitudinal components of W^\pm and Z are just the Goldstone bosons G^\pm and G^0 . In this gauge the Goldstone bosons are physical degrees of freedom and have masses M_W and M_Z , respectively. The diagrams in figure 4.1 give the leading m_t^2 contribution to $\delta g^{L,R}$ in the SM. A detailed review of the calculation of these diagrams is given in reference [49]. The diagrams in figure 4.2 also contribute to $\delta g^{L,R}$ but their contributions are suppressed by a factor of m_Z^2/m_t^2 compared to the diagrams of figure 4.1.

In an extended Higgs sector which contains singly charged Higgs states H_i^\pm , the corrections to $\delta g^{L,R}$ arise from the diagrams of figure 4.3, where H_i^\pm runs over all the singly charged states in the Higgs sector, including G^\pm .

In calculating the corrections shown in figure 4.3 we make the following approximation. We keep only the leading term in powers of m_t^2/M_Z^2 . In δg^L this leading term is proportional to m_t^2 , where the two powers of m_t come from the left-handed Higgs-quark couplings $g_{H_i^+tb}^L$. In δg^R the right-handed Higgs-quark couplings are proportional to $m_b^2 \tan^2 \beta$, so the leading term in δg^R does not grow with increasing m_t . This approximation has been used in calculating the large m_t^2 -dependent corrections to R_b in the SM in the classic papers [13,14,15,16], and in calculating the corrections in extended Higgs sectors in references [27,28,29,21,26].

In figure 4.3(d), the W^\pm are longitudinally polarized. The two diagrams in figure 4.3(d) involving a $ZW^+H_i^-$ vertex can be nonzero in models containing Higgs multiplets larger than doublets. However, their contribution to R_b and A_b is suppressed by a factor of m_Z^2/m_t^2 compared to diagrams 4.3(a), (b) and (c), and we will neglect them. Evaluating

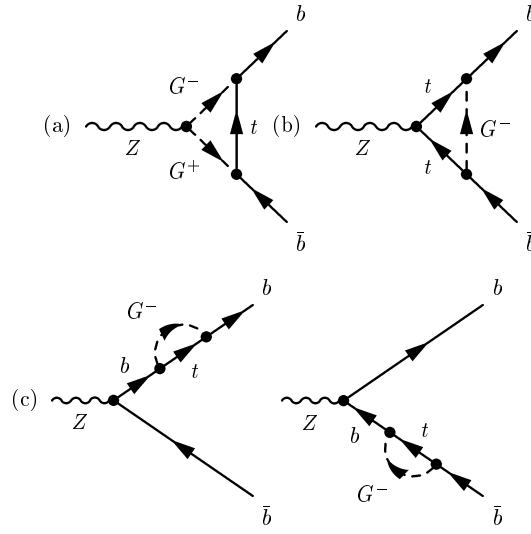


Figure 4.1: Feynman diagrams of the leading m_t^2 contributions to the electroweak corrections to $Z \rightarrow b\bar{b}$ in the SM.

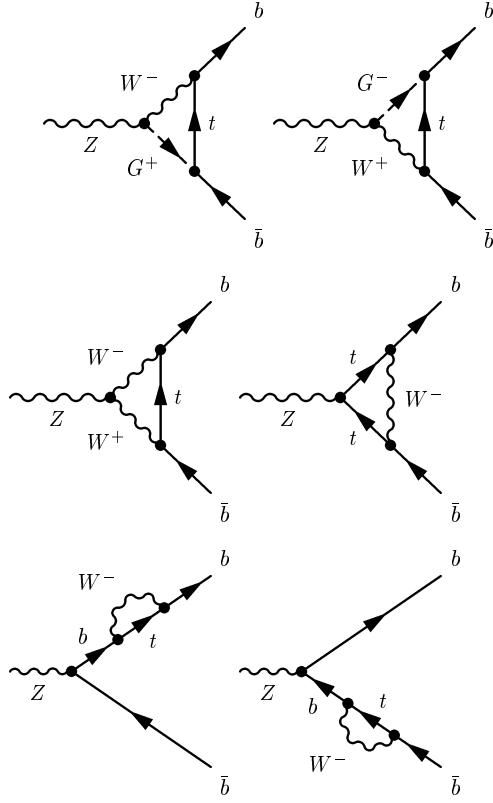


Figure 4.2: Feynman diagrams of the subleading electroweak corrections to $Z \rightarrow b\bar{b}$ in the SM.

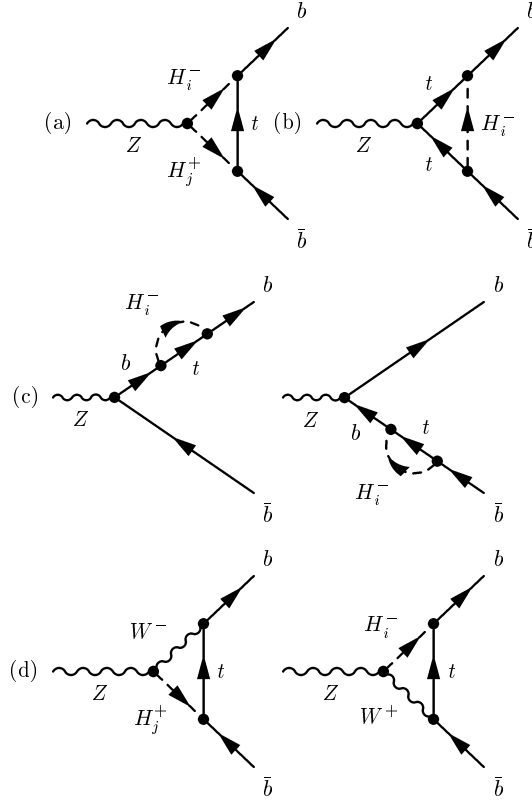


Figure 4.3: Feynman diagrams of the electroweak corrections to $Z \rightarrow b\bar{b}$ in a model with an extended Higgs sector.

diagrams 4.3(a), (b), and (c), we get

$$\delta g^{L,R}(a) = \frac{1}{16\pi^2} \sum_{i,j} g_{H_i^+ \bar{t} b}^{L,R} g_{H_j^+ \bar{t} b}^{L,R} g_{ZH_i^+ H_j^-} \times 2C_{24}(m_b^2, M_Z^2, m_b^2; m_t^2, M_i^2, M_j^2) \quad (4.1)$$

$$\delta g^{L,R}(b) = -\frac{1}{16\pi^2} \sum_i (g_{H_i^+ \bar{t} b}^{L,R})^2 \left\{ -2g_{Zt\bar{t}}^{R,L} C_{24} + \frac{1}{2}g_{Zt\bar{t}}^{R,L} + g_{Zt\bar{t}}^{L,R} m_t^2 C_0 \right\} (m_b^2, M_Z^2, m_b^2; M_i^2, m_t^2, m_t^2) \quad (4.2)$$

$$\delta g^{L,R}(c) = \frac{1}{16\pi^2} \sum_i (g_{H_i^+ \bar{t} b}^{L,R})^2 g_{Zb\bar{b}}^{L,R} B_1(m_b^2; m_t^2, M_i^2). \quad (4.3)$$

The two- and three-point integrals C_{24} , C_0 , and B_1 are defined in appendix F. The sums over i and j run over all the singly charged Higgs mass eigenstates H_i^+ as well as the Goldstone boson G^+ . Where no ambiguity is involved, we have given the arguments of groups of tensor integrals that depend on the same variables only once at the end of the group. These expressions for δg^L agree with those of Kundu *et al.* [26]. For compactness we will drop the first three arguments of the three-point integrals, (m_b^2, M_Z^2, m_b^2) , because these arguments are the same in all the expressions. The first three arguments of the three-point integrals depend only on the masses of the on-shell external particles.

Collecting the results, and expressing the corrections in terms of the quark Yukawa couplings, we obtain for a Type II model,

$$\begin{aligned} \delta g^L &= -\frac{1}{16\pi^2} \lambda_t^2 \frac{e}{s_W c_W} \sum_{i,j} \langle H_i^+ | \phi_2^+ \rangle \langle H_j^+ | \phi_2^+ \rangle \left\{ \sum_{k=1}^N \langle H_i^+ | \phi_k^+ \rangle \langle H_j^+ | \phi_k^+ \rangle T_{\phi_k^+}^3 - s_W^2 \delta_{ij} \right\} \\ &\quad \times 2C_{24}(m_t^2, M_i^2, M_j^2) \\ &\quad - \frac{1}{16\pi^2} \lambda_t^2 \sum_i \langle H_i^+ | \phi_2^+ \rangle^2 \left\{ -2g_{Zt\bar{t}}^{R,L} C_{24} + \frac{1}{2}g_{Zt\bar{t}}^{R,L} + g_{Zt\bar{t}}^{L,R} C_0 \right\} (M_i^2, m_t^2, m_t^2) \\ &\quad + \frac{1}{16\pi^2} \lambda_t^2 g_{Zb\bar{b}}^L \sum_i \langle H_i^+ | \phi_2^+ \rangle^2 B_1(m_b^2; m_t^2, M_i^2) \end{aligned} \quad (4.4)$$

$$\begin{aligned} \delta g^R &= -\frac{1}{16\pi^2} \lambda_b^2 \frac{e}{s_W c_W} \sum_{i,j} \langle H_i^+ | \phi_1^+ \rangle \langle H_j^+ | \phi_1^+ \rangle \left\{ \sum_{k=1}^N \langle H_i^+ | \phi_k^+ \rangle \langle H_j^+ | \phi_k^+ \rangle T_{\phi_k^+}^3 - s_W^2 \delta_{ij} \right\} \\ &\quad \times 2C_{24}(m_t^2, M_i^2, M_j^2) \\ &\quad - \frac{1}{16\pi^2} \lambda_b^2 \sum_i \langle H_i^+ | \phi_1^+ \rangle^2 \left\{ -2g_{Zt\bar{t}}^{L,R} C_{24} + \frac{1}{2}g_{Zt\bar{t}}^{L,R} + g_{Zt\bar{t}}^{R,L} C_0 \right\} (M_i^2, m_t^2, m_t^2) \\ &\quad + \frac{1}{16\pi^2} \lambda_b^2 g_{Zb\bar{b}}^R \sum_i \langle H_i^+ | \phi_1^+ \rangle^2 B_1(m_b^2; m_t^2, M_i^2). \end{aligned} \quad (4.5)$$

The corrections for a Type I model are obtained by replacing ϕ_2^+ with ϕ_1^+ in δg^L .

We see that δg^L is proportional to λ_t^2 and δg^R is proportional to λ_b^2 . Clearly, δg^R is negligible compared to δg^L , except in a Type II model when λ_b is enhanced by small v_1 . In this situation there is also a significant contribution to $\delta g^{L,R}$ coming from loops involving the neutral Higgs bosons, as described in the next section.

In the Type II 2HDM, δg^R is proportional to $(m_b \tan \beta)^2$, while δg^L is proportional to $(m_t \cot \beta)^2$. At large $\tan \beta$, δg^R is enhanced and δg^L is suppressed. λ_t and λ_b are the same size when $\tan \beta = m_t/m_b \simeq 50$. However, because of their different dependence on the $Zq\bar{q}$ couplings, δg^L and δg^R are the same size when $\tan \beta \simeq 10$.

The formulas in equations 4.4 – 4.5 can be simplified a great deal. Electromagnetic gauge invariance requires that the terms proportional to s_W^2 (from the $Zq\bar{q}$ and ZH^+H^- couplings) add to zero in the limit $M_Z^2 \rightarrow 0$. This provides a check on our calculations. In our approximation we neglect terms of order M_Z^2/m_t^2 . Using the expansions for the two- and three-point integrals given in appendix F and neglecting terms of order M_Z^2/m_t^2 in the three-point integrals, we find that the terms proportional to s_W^2 cancel. The corrections can then be written as

$$\begin{aligned} \delta g^{L,R} = & \mp \frac{1}{16\pi^2} \frac{e}{s_W c_W} \sum_i (g_{H_i^+ t b}^{L,R})^2 \frac{1}{2} m_t^2 C_0(M_i^2, m_t^2, m_t^2) \\ & - \frac{1}{16\pi^2} \frac{e}{s_W c_W} \sum_i (g_{H_i^+ t b}^{L,R})^2 \sum_k \langle H_i^+ | \phi_k^+ \rangle^2 (T_{\phi_k^+}^3 - \frac{1}{2}) 2C_{24}(m_t^2, M_i^2, M_i^2) \\ & - \frac{1}{16\pi^2} \frac{e}{s_W c_W} \sum_i \sum_{j \neq i} (g_{H_i^+ t b}^{L,R}) (g_{H_j^+ t b}^{L,R}) \sum_k \langle H_i^+ | \phi_k^+ \rangle \langle H_j^+ | \phi_k^+ \rangle T_{\phi_k^+}^3 \\ & \times 2C_{24}(m_t^2, M_i^2, M_j^2). \end{aligned} \quad (4.6)$$

The third term in equation 4.6 is the sum of the diagrams 4.3(a) for two different charged Higgs bosons H_i^+ and H_j^+ in the loop. It is only nonzero when there are nonzero off-diagonal $ZH_i^+H_j^-$ couplings ($i \neq j$). The second term describes the contribution to diagrams 4.3(a) from diagonal $ZH_i^+H_i^-$ couplings when $T_{\phi_k^+}^3$ is different from 1/2. This term is only nonzero when the Higgs sector contains multiplets larger than doublets. The first term comes from the sum of diagrams 4.3(b) and (c), plus the remaining part of diagram 4.3(a) with $T_{\phi_k^+}^3 = 1/2$. This part of diagram 4.3(a) is what we would get if we replaced all of the ZH^+H^- couplings with the SM ZG^+G^- coupling, $g_{ZG^+G^-} = \frac{-e}{s_W c_W} (\frac{1}{2} - s_W^2)$. Note that for $m_t \gg M_Z$, $C_0(M_i^2, m_t^2, m_t^2)$ is negative (see appendix F). Therefore the first term of δg^L (δg^R) is always positive (negative) definite, which decreases the prediction for R_b .

We can learn much from equation 4.6 about the contributions to $\delta g^{L,R}$ from charged Higgs boson exchange in various types of Higgs sectors. First, if the Higgs sector contains only doublets and singlets, $T_{\phi_k^+}^3 = 1/2$ and there are no off-diagonal ZH^+H^-

couplings. Then the second and third terms of equation 4.6 are zero. We are left with the first term,

$$\begin{aligned}\delta g^{L,R} &= \mp \frac{1}{16\pi^2} \frac{e}{2s_W c_W} \sum_i (g_{H_i^+ t b}^{L,R})^2 m_t^2 C_0(M_i^2, m_t^2, m_t^2) \\ &= \delta g_{SM}^{L,R} \pm \frac{1}{16\pi^2} \frac{e}{2s_W c_W} \sum_{i \neq G^+} (g_{H_i^+ t b}^{L,R})^2 \left[\frac{R_i}{R_i - 1} - \frac{R_i \log R_i}{(R_i - 1)^2} \right]\end{aligned}\quad (4.7)$$

where $R_i \equiv m_t^2/M_i^2$. The correction in the SM due to G^\pm exchange is denoted by $\delta g_{SM}^{L,R}$. The non-SM piece of δg^L (δg^R) is positive (negative) definite, both of which decrease R_b . Therefore, in order for it to be possible to increase R_b through charged Higgs boson loops, we must have a Higgs sector that contains multiplets larger than doublets.

Second, if all the H_i^+ are degenerate with G^+ , we can sum over the complete sets of states in the second and third terms of equation 4.6. These terms cancel and again we are left with,

$$\delta g^L = \frac{\lambda_t^2}{16\pi^2} \frac{e}{2s_W c_W} \left[\frac{R}{R-1} - \frac{R \log R}{(R-1)^2} \right] \quad (4.8)$$

$$\delta g^R = -\frac{\lambda_b^2}{16\pi^2} \frac{e}{2s_W c_W} \left[\frac{R}{R-1} - \frac{R \log R}{(R-1)^2} \right] \quad (4.9)$$

with $R = m_t^2/M_W^2$. This formula includes the SM correction $\delta g_{SM}^{L,R}$. As above, the non-SM piece of δg^L (δg^R) is positive (negative) definite, both of which decrease R_b .

In a Higgs sector that contains only multiplets for which $\rho = 1$ automatically (equation 3.4), the Goldstone boson does not contribute to the second and third terms of equation 4.6 because there are no off-diagonal $ZG^+H_i^-$ couplings and the ZG^+G^- coupling is the same as in the SM. Thus in such a model, if all the H_i^+ (excluding G^+) are degenerate with mass M , we can again sum over the complete sets of states in the second and third terms of equation 4.6. These terms again cancel and we are left with

$$\delta g^L = \frac{\lambda_t^2}{16\pi^2} \left(1 - \frac{v_2^2}{v_{SM}^2} \right) \frac{e}{2s_W c_W} \left[\frac{R}{R-1} - \frac{R \log R}{(R-1)^2} \right] + \delta g_{SM}^L \quad (4.10)$$

$$\delta g^R = -\frac{\lambda_b^2}{16\pi^2} \left(1 - \frac{v_1^2}{v_{SM}^2} \right) \frac{e}{2s_W c_W} \left[\frac{R}{R-1} - \frac{R \log R}{(R-1)^2} \right] + \delta g_{SM}^R \quad (4.11)$$

with $R = m_t^2/M^2$, for a Type II model. The correction in a Type I model is obtained by replacing v_2 with v_1 in equation 4.10. As above, the non-SM piece of δg^L (δg^R) is positive (negative) definite, both of which decrease R_b .

Chapter 5

Neutral Higgs corrections to $Z \rightarrow b\bar{b}$

The corrections to $Z \rightarrow b\bar{b}$ from neutral Higgs boson loops are shown in figure 5.1. As before, we assume that the Higgs sector is CP-conserving. CP-even states are denoted by H_i^0 and CP-odd states are denoted by A_j^0 . These corrections are proportional to λ_b^2 because the neutral Higgs couplings to $b\bar{b}$ are proportional to λ_b . In a Type I model, $\lambda_b \ll \lambda_t$, so the corrections from neutral Higgs loops are negligible compared to the correction from H^+ , which is proportional to λ_t^2 . In a Type II model, however, λ_b increases as v_1 decreases. In the limit of small v_1 , the corrections involving neutral Higgs bosons are significant.

In calculating the corrections due to the diagrams in figure 5.1, we neglect terms proportional to m_b that are not enhanced by small v_1 . The diagrams of figure 5.1(d) are suppressed by a factor of m_b/m_Z compared to diagrams 5.1(a), (b) and (c), and so we neglect them as well. The contributions to $\delta g^{R,L}$ from diagrams 5.1(a), (b), and (c) are

$$\begin{aligned}
\delta g^{R,L}(a) &= \pm \frac{1}{16\pi^2} \sum_{H_i^0, A_j^0} 4g_{ZH_i^0 A_j^0} g_{H_i^0 b\bar{b}}^V g_{A_j^0 b\bar{b}}^A C_{24}(m_b^2, M_i^2, M_j^2) \\
&= \mp \frac{1}{16\pi^2} \lambda_b^2 \frac{e}{s_W c_W} \sum_{H_i^0, A_j^0} \langle H_i^0 | \phi_1^{0,r} \rangle \langle A_j^0 | \phi_1^{0,i} \rangle \\
&\quad \times \sum_{k=1}^N \langle H_i^0 | \phi_k^{0,r} \rangle \langle A_j^0 | \phi_k^{0,i} \rangle T_{\phi_k^0}^3 \times 2C_{24}(m_b^2, M_i^2, M_j^2) \tag{5.1}
\end{aligned}$$

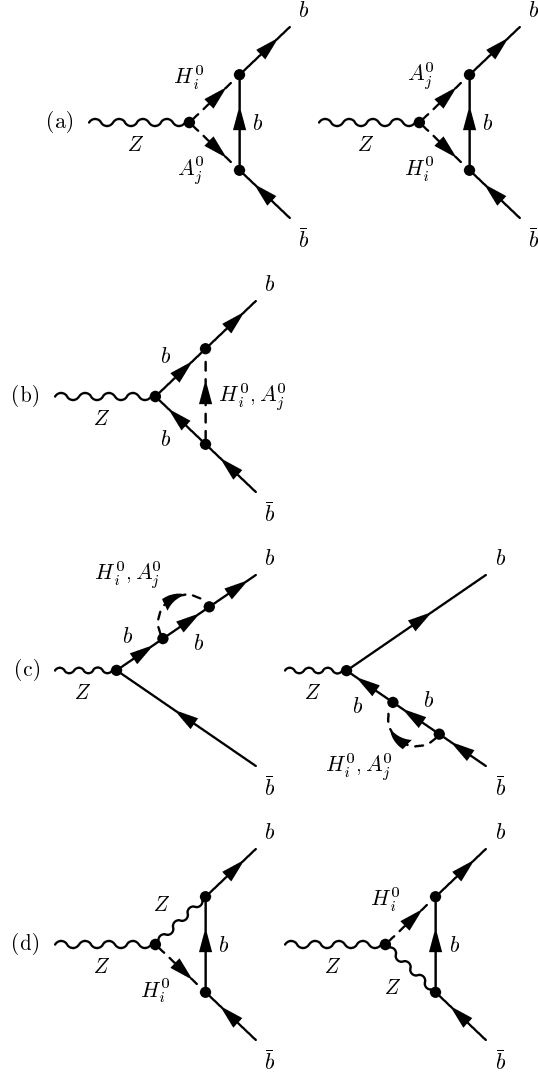


Figure 5.1: Feynman diagrams for the corrections to $Z \rightarrow b\bar{b}$ involving neutral Higgs bosons in the loop.

$$\begin{aligned}
& \delta g^{R,L}(b) \\
&= -\frac{1}{16\pi^2} g_{Zb\bar{b}}^{L,R} \left[\sum_{H_i^0} (g_{H_i^0 b\bar{b}}^V)^2 \left\{ -2C_{24} + \frac{1}{2} - M_Z^2(C_{22} - C_{23}) \right\} (M_i^2, m_b^2, m_b^2) \right. \\
&\quad \left. - \sum_{A_j^0} (g_{A_j^0 b\bar{b}}^A)^2 \left\{ -2C_{24} + \frac{1}{2} - M_Z^2(C_{22} - C_{23}) \right\} (M_j^2, m_b^2, m_b^2) \right] \\
&= -\frac{1}{16\pi^2} g_{Zb\bar{b}}^{L,R} \frac{1}{2} \lambda_b^2 \left[\sum_{H_i^0} \langle H_i^0 | \phi_1^{0,r} \rangle^2 \left\{ -2C_{24} + \frac{1}{2} - M_Z^2(C_{22} - C_{23}) \right\} (M_i^2, m_b^2, m_b^2) \right. \\
&\quad \left. + \sum_{A_j^0} \langle A_j^0 | \phi_1^{0,i} \rangle^2 \left\{ -2C_{24} + \frac{1}{2} - M_Z^2(C_{22} - C_{23}) \right\} (M_j^2, m_b^2, m_b^2) \right] \quad (5.2)
\end{aligned}$$

$$\begin{aligned}
\delta g^{R,L}(c) &= \frac{1}{16\pi^2} g_{Zb\bar{b}}^{R,L} \left[\sum_{H_i^0} (g_{H_i^0 b\bar{b}}^V)^2 B_1(m_b^2; m_b^2, M_i^2) \right. \\
&\quad \left. - \sum_{A_j^0} (g_{A_j^0 b\bar{b}}^A)^2 B_1(m_b^2; m_b^2, M_j^2) \right] \\
&= \frac{1}{16\pi^2} g_{Zb\bar{b}}^{R,L} \frac{1}{2} \lambda_b^2 \left[\sum_{H_i^0} \langle H_i^0 | \phi_1^{0,r} \rangle^2 B_1(m_b^2; m_b^2, M_i^2) \right. \\
&\quad \left. + \sum_{A_j^0} \langle A_j^0 | \phi_1^{0,i} \rangle^2 B_1(m_b^2; m_b^2, M_j^2) \right] \quad (5.3)
\end{aligned}$$

The two- and three-point integrals are specified in appendix F. As in section 4, we drop the first three arguments, (m_b^2, M_Z^2, m_b^2) , of the three-point integrals for compactness. Note that $g_{ZH_i^0 A_j^0}$ and $g_{A_j^0 b\bar{b}}^A$ are imaginary, while $g_{H_i^0 b\bar{b}}^V$ is real. The sum A_j^0 runs over all the CP-odd neutral Higgs bosons, including G^0 . However, the corrections involving G^0 can be neglected because the G^0 coupling to $b\bar{b}$ is not enhanced by large λ_b . In particular, $g_{G^0 b\bar{b}}^A = -m_b/v_{SM}$, independent of the value of v_1 .

As in section 4, we can use electromagnetic gauge invariance to check our calculations. Electromagnetic gauge invariance requires that terms proportional to s_W^2 sum to zero in the limit $M_Z \rightarrow 0$. $\delta g^{R,L}(a)$ is independent of s_W^2 . In the limit $M_Z \rightarrow 0$, we find that $\delta g^{R,L}(b) + \delta g^{R,L}(c) = 0$, independent of the Higgs masses. The terms proportional to s_W^2 indeed vanish in this limit. Although this is a useful formal check, the approximation

$M_Z \rightarrow 0$ cannot be applied to the general formulas in equations 5.1 – 5.3 because terms proportional to M_Z^2 are important here.

We now examine the special case in which all the H_i^0 are degenerate with mass M_H , and all the A_j^0 are degenerate with mass M_A . We neglect G^0 , so that M_A does not have to be equal to M_Z , which is the G^0 mass in the 't Hooft–Feynman gauge. In this case, we can sum over complete sets of states and equations 5.1 – 5.3 simplify to,

$$\delta g^{R,L}(a) = \pm \frac{1}{16\pi^2} \lambda_b^2 \left(\frac{e}{s_W c_W} \right) C_{24}(m_b^2, M_H^2, M_A^2) \quad (5.4)$$

$$\begin{aligned} \delta g^{R,L}(b) = & -\frac{1}{16\pi^2} g_{Zb\bar{b}}^{L,R} \frac{1}{2} \lambda_b^2 \times \\ & \left[\left\{ -2C_{24} + \frac{1}{2} - M_Z^2(C_{22} - C_{23}) \right\} (M_H^2, m_b^2, m_b^2) \right. \\ & \left. + \left\{ -2C_{24} + \frac{1}{2} - M_Z^2(C_{22} - C_{23}) \right\} (M_A^2, m_b^2, m_b^2) \right] \quad (5.5) \end{aligned}$$

$$\delta g^{R,L}(c) = \frac{1}{16\pi^2} g_{Zb\bar{b}}^{R,L} \frac{1}{2} \lambda_b^2 \left[B_1(m_b^2; m_b^2, M_H^2) + B_1(m_b^2; m_b^2, M_A^2) \right]. \quad (5.6)$$

Chapter 6

Corrections to $Z \rightarrow b\bar{b}$ in specific models

In this chapter we calculate the radiative corrections to $Z \rightarrow b\bar{b}$ in specific extended Higgs models. We discuss the form of the corrections in each model. We also show the constraints on the parameter space of each model due to the experimental data.

In section 6.1 we calculate the corrections in models containing only Higgs doublets and/or singlets. We examine the contributions due to both charged Higgs boson and neutral Higgs boson exchange. We discuss the two Higgs doublet model in detail, and describe the effects of adding additional Higgs doublets and singlets. In section 6.2 we calculate the corrections in a number of models containing one or more Higgs multiplets larger than doublets. We discuss two classes of models which take two different approaches to satisfy the experimental constraint on the ρ parameter, $\rho \approx 1$. We first discuss models which are fine-tuned so that the multiplet larger than a doublet has a very small vev. Finally we discuss the models that preserve $SU(2)_c$ symmetry.

We find that the corrections to R_b are large enough that the measurement of R_b can be used to constrain the parameter space of specific models. However, the corrections to A_b are small compared to the uncertainty in the measurement of A_b , and thus cannot be used to further constrain the models.

6.1 Models with Higgs doublets and singlets

6.1.1 Charged Higgs boson contributions

We saw in section 4 that, in a model containing only Higgs doublets and singlets, the radiative corrections due to the charged Higgs bosons are described by equation 4.7. We also saw that these corrections have definite signs; in particular, $\delta g^L > 0$ and $\delta g^R < 0$.

6.1 Models with Higgs doublets and singlets

Both of these give $\Delta R_b < 0$, in worse agreement with experiment than the SM.

In this section, we calculate the corrections due to charged Higgs bosons in specific models containing Higgs doublets or singlets or both. We can then use the measurement of R_b to constrain the models. Note that the corrections due to neutral Higgs boson exchange will also contribute when λ_b is enhanced. They must be taken into account as well in this regime when deriving constraints from the R_b measurement. We first consider the corrections in the two Higgs doublet model (2HDM), then extend the results to multi-doublet models and models with doublets and singlets.

Two Higgs doublet model

The 2HDM contains a single charged Higgs boson, H^+ . Its contribution to $\delta g^{L,R}$ is found from equation 4.7 with only one H^+ in the sum. For the Type II model,

$$\delta g^L = \frac{1}{16\pi^2} \left(\frac{gm_t}{\sqrt{2}M_W} \cot \beta \right)^2 \frac{1}{2} \frac{e}{s_W c_W} \left[\frac{R}{R-1} - \frac{R \log R}{(R-1)^2} \right], \quad (6.1)$$

$$\delta g^R = -\frac{1}{16\pi^2} \left(\frac{gm_b}{\sqrt{2}M_W} \tan \beta \right)^2 \frac{1}{2} \frac{e}{s_W c_W} \left[\frac{R}{R-1} - \frac{R \log R}{(R-1)^2} \right], \quad (6.2)$$

were $R = m_t^2/M_{H^+}^2$. This correction is in addition to the correction due to Goldstone boson exchange, which is the same as in the SM. This agrees with the results of references [27,28,29,21,26]. In the Type II model, δg^L is significant at small $\tan \beta$ and is suppressed at large $\tan \beta$, while δg^R is negligible at small $\tan \beta$ but is significant at large $\tan \beta$.

In a Type I model the result is the same except that $\cot^2 \beta$ is replaced with $\tan^2 \beta$ in δg^L . In this case, δg^R is negligible compared to δg^L at any value of $\tan \beta$. Both δg^L and δg^R grow with increasing $\tan \beta$.

This correction decreases for large M_{H^+} . It goes to zero in the decoupling limit, $M_{H^+} \rightarrow \infty$. (For a discussion of the decoupling limit, see reference [50].)

For small $\tan \beta$, the neutral Higgs couplings to b quarks are small, and contributions to $Z \rightarrow b\bar{b}$ due to neutral Higgs boson exchange can be neglected. In this regime the corrections due to charged Higgs boson exchange can be used to constrain the 2HDM. In figure 6.1 we plot the constraints from R_b on M_{H^+} as a function of $\tan \beta$, for a Type II 2HDM. The input parameters for the calculation are summarized in appendix H. We also show the constraints on the charged Higgs mass from the process $b \rightarrow s\gamma$ [51,52] and the direct searches at LEP (for references and a discussion, see appendix I). The constraint on the charged Higgs mass from the D0 experiment [53] are significantly weaker than the constraint from $b \rightarrow s\gamma$, and are not shown in figure 6.1. R_b provides the strongest constraint on M_{H^+} for $\tan \beta < 1.5$. For larger $\tan \beta$, the constraint from $b \rightarrow s\gamma$ is stronger.

Radiative corrections to the branching ratio $\text{BR}(\bar{B} \rightarrow X_s \gamma)$ involving charged Higgs boson exchange in 2HDMs have been calculated in reference [52]. By comparing

$\text{BR}(\bar{B} \rightarrow X_s \gamma)$ to the value measured at CLEO [51], reference [52] finds a constraint on the charged Higgs boson mass in the Type II 2HDM, as shown in figure 6.1. In the Type I 2HDM, however, the predicted range of $\text{BR}(\bar{B} \rightarrow X_s \gamma)$ falls within the experimental limits. Thus in a Type I 2HDM, there is no constraint on the charged Higgs boson mass from $b \rightarrow s \gamma$.

For large $\tan \beta$, neutral Higgs boson exchange contributes to $Z \rightarrow b\bar{b}$ in addition to charged Higgs boson exchange. The neutral Higgs boson contributions are discussed in section 6.1.2.

We stress that the bounds in figure 6.1 are valid when the only non-SM corrections to $Z \rightarrow b\bar{b}$ are due to H^+ exchange. They cannot be applied to models that contain additional particles which contribute to the corrections. In particular, supersymmetric models give rise to additional corrections to $Z \rightarrow b\bar{b}$ from squark and Higgsino exchange. However, in the limit that the supersymmetric particles are very heavy, their contributions to radiative corrections go to zero, and the bounds in figure 6.1 remain valid.

In the case of a Type I 2HDM, the bound on M_{H^+} from R_b is the same as in figure 6.1, but with $\cot \beta$ replacing $\tan \beta$ on the vertical axis.

Multiple-doublet models and models with singlets

We now consider charged Higgs boson exchange in a model containing multiple Higgs doublets, denoted Φ_k , with hypercharge 1. We can add to this model any number of Higgs singlets with zero hypercharge. These contain only neutral degrees of freedom, and so they have no effect on the charged Higgs sector.

In a Type I model of this type, we let Φ_1 couple to both up- and down-type quarks, and none of the other doublets couple to quarks. In a Type II model, we let Φ_1 couple only to down-type quarks, and Φ_2 couple to up-type quarks. Then the Yukawa couplings are defined in the same way as in the 2HDM, in equations 3.11–3.14.

In a Type II model, the contributions to $Z \rightarrow b\bar{b}$ from charged Higgs boson exchange are

$$\delta g^L = \frac{1}{16\pi^2} \frac{1}{2} \frac{e}{s_W c_W} \left(\frac{gm_t}{\sqrt{2}M_W} \frac{v_{SM}}{v_2} \right)^2 \sum_{i \neq G^+} \langle H_i^+ | \phi_2^+ \rangle^2 \left[\frac{R_i}{R_i - 1} - \frac{R_i \log R_i}{(R_i - 1)^2} \right] \quad (6.3)$$

$$\delta g^R = -\frac{1}{16\pi^2} \frac{1}{2} \frac{e}{s_W c_W} \left(\frac{gm_b}{\sqrt{2}M_W} \frac{v_{SM}}{v_1} \right)^2 \sum_{i \neq G^+} \langle H_i^+ | \phi_1^+ \rangle^2 \left[\frac{R_i}{R_i - 1} - \frac{R_i \log R_i}{(R_i - 1)^2} \right] \quad (6.4)$$

where $R_i \equiv m_t^2/M_{H_i^+}^2$. This contribution is in addition to the contribution due to charged Goldstone boson exchange, which is the same as in the SM. In a Type I model, the

6.1 Models with Higgs doublets and singlets

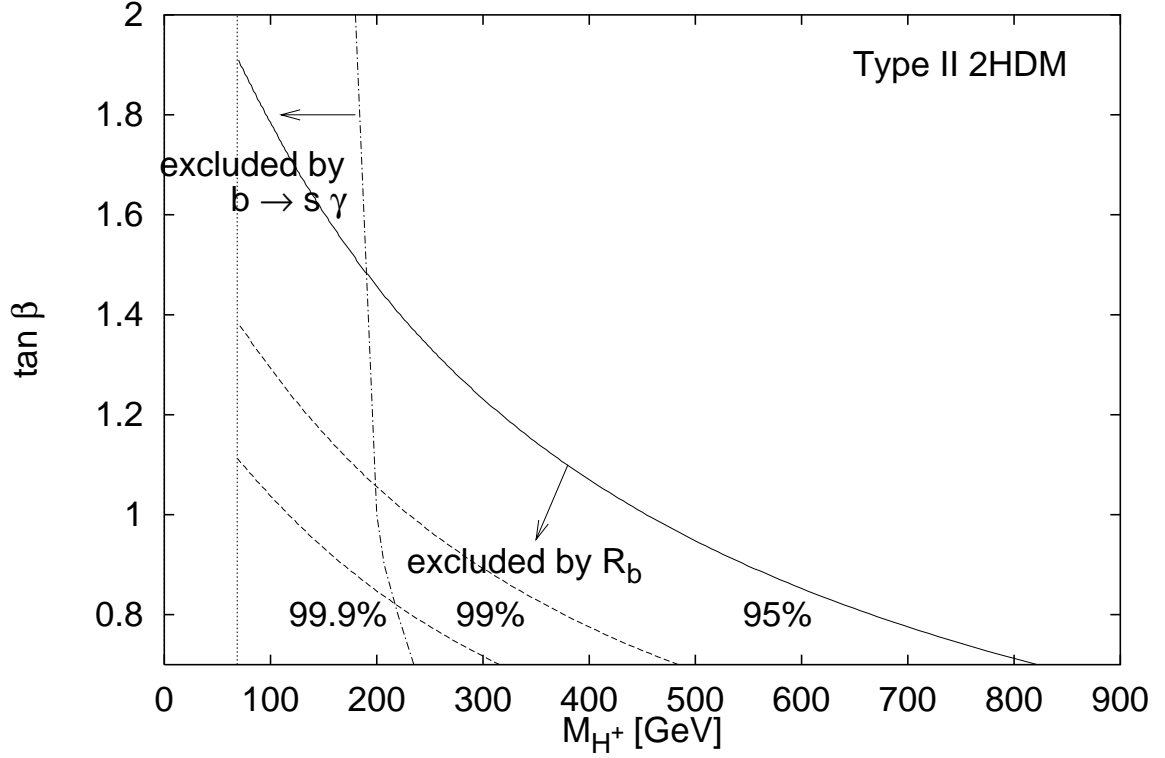


Figure 6.1: Constraints from R_b on the charged Higgs mass and $\tan \beta$ in the Type II 2HDM. The area below the solid line is excluded at 95% confidence level. Also shown are the 99% and 99.9% confidence levels (dashed lines). We also show the 95% confidence level lower bound on M_{H^+} from the $b \rightarrow s \gamma$ branching ratio as measured by CLEO [51,52] (dot-dashed). The vertical dotted line is the direct search bound on the charged Higgs mass from the OPAL collaboration, $M_{H^+} > 68.7$ GeV [54], from LEP data up to $\sqrt{s} = 189$ GeV. (For a discussion of the direct search bound, see appendix I.) A large area below $\tan \beta \approx 1.5$ is excluded by R_b .

contribution is the same except that v_2 is replaced with v_1 and ϕ_2^+ is replaced with ϕ_1^+ in the formula for δg^L .

These corrections to $\delta g^{L,R}$ from charged Higgs boson exchange have the same dependence on the charged Higgs masses as the corrections in the 2HDM. The contribution from each H_i^+ is weighted by the overlap of each H_i^+ with the electroweak eigenstate that couples to the quarks involved.

Note that the Yukawa couplings depend on the ratios v_{SM}/v_2 and v_{SM}/v_1 . This is the same dependence as in the 2HDM. Recall that in the 2HDM, v_1 and v_2 were constrained by the W mass to satisfy the relation, $v_1^2 + v_2^2 = v_{SM}^2$, where $v_{SM} = 246$ GeV. Thus in the 2HDM, v_1 and v_2 cannot both be small at the same time. However, in a model with more than two doublets, the W mass constraint involves the vevs of all the doublets, giving $\sum_k v_k^2 = v_{SM}^2$, where k runs over all the Higgs doublets. In this model, both v_1 and v_2 can be small at the same time, leading to significant contributions to both δg^L and δg^R .

The corrections to $Z \rightarrow b\bar{b}$ in this model can be understood by examining their behavior in certain limits. First, let us examine the limit in which all but one of the H_i^+ are very heavy. The contributions of the heavy H_i^+ to $\delta g^{L,R}$ go to zero as the masses go to infinity. The remaining contribution to $\delta g^{L,R}$ is due to the single light charged Higgs boson, and it is of the same form as in the 2HDM. Comparing with equations 6.1–6.2, we see that in δg^L , $\tan \beta$ is replaced by $\frac{v_2}{v_{SM}\langle H_i^+|\phi_2^+ \rangle}$, and in δg^R , $\tan \beta$ is replaced by $\frac{v_{SM}\langle H_i^+|\phi_1^+ \rangle}{v_1}$. The charged Higgs sector can be constrained by R_b when there are no significant contributions to $Z \rightarrow b\bar{b}$ coming from neutral Higgs boson exchange. This is ensured when v_1 is not too small. In this regime, δg^L can be significant, while δg^R is negligible. The constraint from R_b on the mass of the remaining light charged Higgs boson is the same as in figure 6.1, with $\tan \beta$ replaced by $\frac{v_2}{v_{SM}\langle H_i^+|\phi_2^+ \rangle}$.

If v_2 and $\langle H_i^+|\phi_2^+ \rangle$ are held constant while the masses of the heavy charged Higgs bosons are reduced, the bound shown in figure 6.1 becomes stronger. This happens because the heavy charged Higgs bosons begin to contribute to δg^L , forcing the contribution of the light charged Higgs boson to be smaller in order to be consistent with the measured value of R_b . This is done by raising the mass of the light charged Higgs boson.

Finally, if all the charged Higgs bosons are degenerate, with a common mass M_H , then we can sum over a complete set of states and the corrections simplify to the following, again for a Type II model:

$$\delta g^L = \frac{1}{16\pi^2} \frac{1}{2} \frac{e}{s_W c_W} \left(\frac{gm_t}{\sqrt{2}M_W} \right)^2 \frac{v_{SM}^2 - v_2^2}{v_2^2} \left[\frac{R}{R-1} - \frac{R \log R}{(R-1)^2} \right] \quad (6.5)$$

$$\delta g^R = \frac{1}{16\pi^2} \frac{1}{2} \frac{e}{s_W c_W} \left(\frac{gm_b}{\sqrt{2}M_W} \right)^2 \frac{v_{SM}^2 - v_1^2}{v_1^2} \left[\frac{R}{R-1} - \frac{R \log R}{(R-1)^2} \right], \quad (6.6)$$

6.1 Models with Higgs doublets and singlets

where $R = m_t^2/M_H^2$. These corrections are in addition to the corrections due to charged Goldstone boson exchange in the SM. In a Type I model, v_2 is replaced by v_1 in δg^L .

These corrections are the same as the corrections in the 2HDM, with $\tan\beta$ replaced by $v_2/\sqrt{v_{SM}^2 - v_2^2}$ in δg^L , and $\tan\beta$ replaced by $\sqrt{v_{SM}^2 - v_1^2}/v_1$ in δg^R . As before, the charged Higgs sector can be constrained by R_b when there are no significant contributions to $Z \rightarrow b\bar{b}$ coming from neutral Higgs boson exchange. This is ensured when v_1 is not too small. In this regime, the constraint from R_b on the common charged Higgs mass M_H is the same as in figure 6.1, with $\tan\beta$ replaced by $v_2/\sqrt{v_{SM}^2 - v_2^2}$.

6.1.2 Neutral Higgs boson contributions

As we showed in section 5, the radiative corrections to the process $Z \rightarrow b\bar{b}$ due to neutral Higgs boson exchange are proportional to λ_b^2 . They are negligible compared to the contributions from charged Higgs boson exchange which are proportional to λ_t^2 , except when λ_b is enhanced relative to λ_t . This happens in a Type II model when v_1 is much smaller than v_2 . In what follows we consider only Type II models.

In this section, we calculate the corrections due to neutral Higgs boson exchange in specific models containing Higgs doublets and/or singlets. We can then use the measurement of R_b to constrain the models. Note that when λ_b is enhanced, the corrections to δg^R due to charged Higgs boson exchange will also contribute. We take these into account when deriving constraints from the R_b measurement.

We first consider the corrections in the two Higgs doublet model (2HDM). We also examine the corrections in the 2HDM in the decoupling limit, in which h^0 remains light and its couplings to SM particles approach those of the SM Higgs boson, while all the other Higgs bosons become heavy and decouple from SM particles. We then extend the results to multi-doublet models and models with doublets and singlets. Finally we examine the multi-doublet model when some of the neutral Higgs bosons are degenerate.

Two Higgs doublet model

The corrections due to neutral Higgs boson exchange in the 2HDM depend on the masses of the three neutral Higgs bosons, h^0 , H^0 , and A^0 , the mixing angle α of the two CP-even states h^0 and H^0 , and of course $\tan\beta$, which determines λ_b and the mixing between A^0 and G^0 .

The neutral Higgs couplings in the 2HDM are given in appendix C. Inserting these couplings into equations 5.1–5.3 for the corrections from neutral Higgs boson exchange, we find,

$$\delta g^{R,L}(a) = \pm \frac{1}{16\pi^2} \frac{e}{s_W c_W} \left(\frac{gm_b}{\sqrt{2}M_W} \right)^2 \tan^2 \beta$$

$$\begin{aligned} & \times \left[\frac{s_\alpha}{s_\beta} \cos(\beta - \alpha) C_{24}(m_b^2, M_{h^0}^2, M_{A^0}^2) \right. \\ & \left. + \frac{c_\alpha}{s_\beta} \sin(\beta - \alpha) C_{24}(m_b^2, M_{H^0}^2, M_{A^0}^2) \right] \end{aligned} \quad (6.7)$$

$$\begin{aligned} \delta g^{R,L}(b) &= -\frac{1}{16\pi^2} g_{Zb\bar{b}}^{L,R} \frac{1}{2} \left(\frac{gm_b}{\sqrt{2}M_W} \right)^2 \tan^2 \beta \\ & \times \left[\left(\frac{s_\alpha}{s_\beta} \right)^2 \left[-2C_{24} + \frac{1}{2} - M_Z^2(C_{22} - C_{23}) \right] (M_{h^0}^2, m_b^2, m_b^2) \right. \\ & + \left(\frac{c_\alpha}{s_\beta} \right)^2 \left[-2C_{24} + \frac{1}{2} - M_Z^2(C_{22} - C_{23}) \right] (M_{H^0}^2, m_b^2, m_b^2) \\ & \left. + \left[-2C_{24} + \frac{1}{2} - M_Z^2(C_{22} - C_{23}) \right] (M_{A^0}^2, m_b^2, m_b^2) \right] \end{aligned} \quad (6.8)$$

$$\begin{aligned} \delta g^{R,L}(c) &= \frac{1}{16\pi^2} g_{Zb\bar{b}}^{R,L} \frac{1}{2} \left(\frac{gm_b}{\sqrt{2}M_W} \right)^2 \tan^2 \beta \left[\left(\frac{s_\alpha}{s_\beta} \right)^2 B_1(m_b^2; m_b^2, M_{h^0}^2) \right. \\ & \left. + \left(\frac{c_\alpha}{s_\beta} \right)^2 B_1(m_b^2; m_b^2, M_{H^0}^2) + B_1(m_b^2; m_b^2, M_{A^0}^2) \right], \end{aligned} \quad (6.9)$$

where $s_\alpha = \sin \alpha$, $c_\alpha = \cos \alpha$, $s_\beta = \sin \beta$, and $c_\beta = \cos \beta$.

The contribution of these corrections to R_b can be either positive or negative, depending on the neutral Higgs masses and the mixing angle α . We plot the corrections for various sets of parameters.

In figures 6.2 and 6.3, we plot the constraints on the neutral Higgs sector from R_b . The parameters in these plots are $\tan \beta = 50$, $\cos^2(\beta - \alpha) = 1/2$, and $M_{H^0} = 200$ GeV. With $\cos^2(\beta - \alpha) = 1/2$, the Zh^0A^0 and ZH^0A^0 couplings are equal, and h^0 , H^0 , and A^0 all contribute to the corrections. The charged Higgs boson can also contribute. If the charged Higgs boson were taken to be very heavy, its contribution to R_b would go to zero and only the effects of the neutral Higgs bosons would remain. However, a large mass splitting between the charged Higgs boson and the neutral Higgs bosons results in large radiative corrections to the ρ parameter (see, e.g., reference [55] and appendix C). Using the formula for $\Delta\rho_{\text{new}}$ from neutral Higgs exchange in the 2HDM given in appendix C, and requiring that $-4.7 \times 10^{-3} < \Delta\rho_{\text{new}} < 3.0 \times 10^{-3}$ (see section 6.2.1 for further details), we find that for the parameters of figures 6.2 and 6.3, the charged Higgs boson must be lighter than 270 GeV. The lower bound on the charged Higgs mass at large $\tan \beta$

6.1 Models with Higgs doublets and singlets

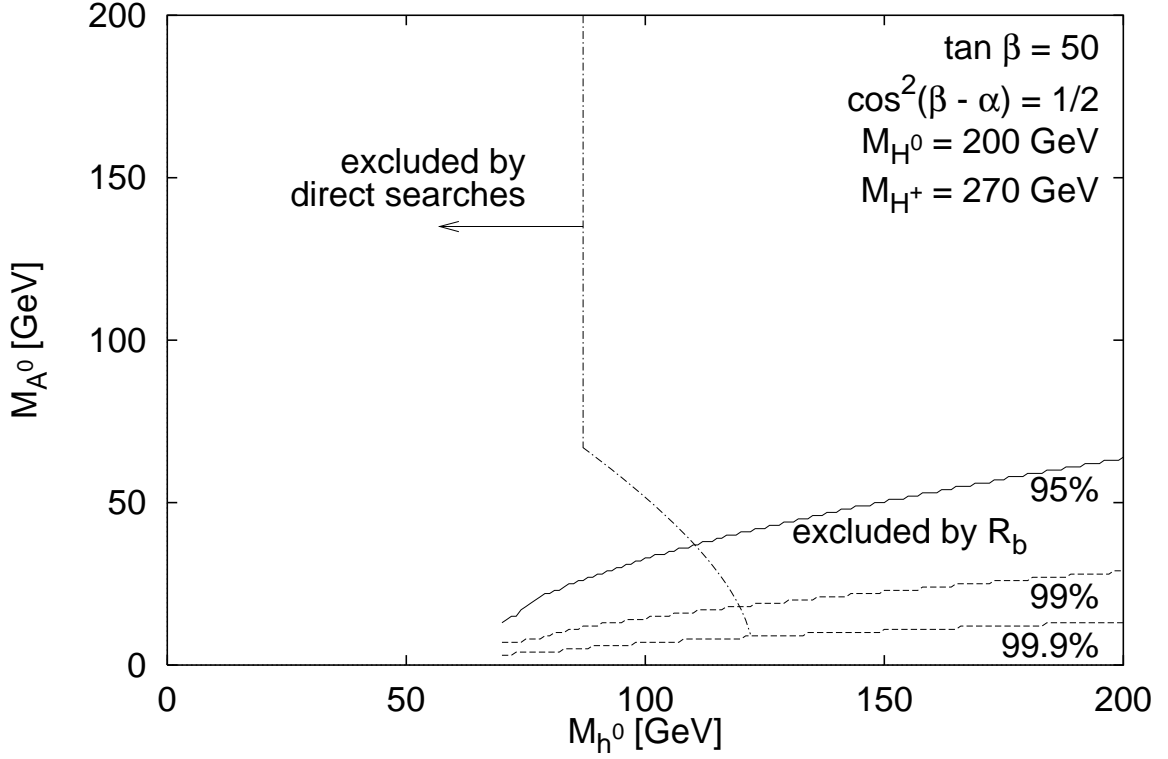


Figure 6.2: R_b in the Type II 2HDM with $\tan \beta = 50$, $\cos^2(\beta - \alpha) = 1/2$, $M_{H^0} = 200 \text{ GeV}$, and $M_{H^\pm} = 270 \text{ GeV}$. The axes are M_{A^0} and M_{h^0} . $\Delta R_b < 0$ for all allowed masses, so this model is in worse agreement with experiment than the SM. The solid line is the 95% confidence level lower bound on M_{A^0} from R_b . We also plot the 99% and 99.9% confidence level contours (dashed lines). The dot-dashed line is the lower bound on M_{h^0} from direct searches, as discussed in appendix I.

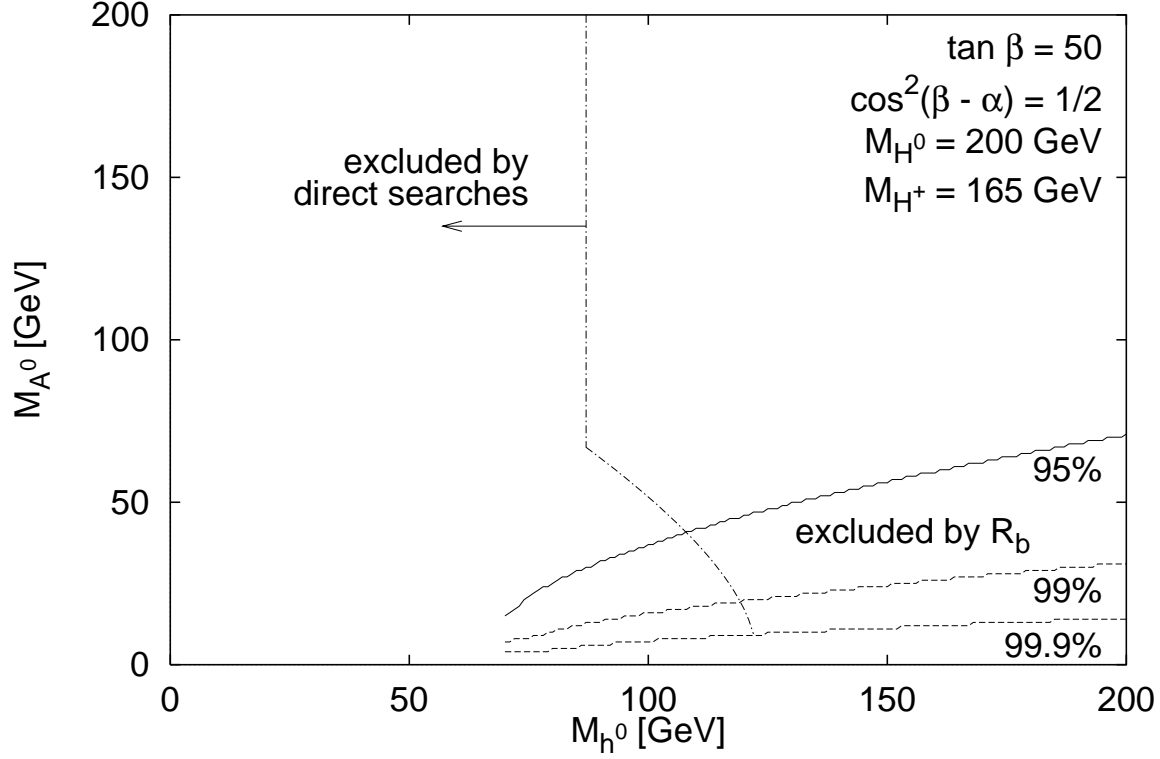


Figure 6.3: R_b in the 2HDM with $M_{H^+} = 165$ GeV (the lower limit from $b \rightarrow s\gamma$ [52]), and other parameters the same as in figure 6.2. Since $\Delta R_b < 0$ from H^+ , the 95% confidence level exclusion curve from R_b (solid line) moves upward compared to $M_{H^+} \rightarrow \infty$. Also shown are the 99% and 99.9% confidence levels (dashed lines). The dot-dashed line is the lower bound on M_{h^0} from direct searches as in figure 6.2.

6.1 Models with Higgs doublets and singlets

is $M_{H^+} > 165$ GeV, from $b \rightarrow s\gamma$ [51,52]. In figure 6.2 we take $M_{H^+} = 270$ GeV, and in figure 6.3 we take $M_{H^+} = 165$ GeV, in order to show the full allowed range of charged Higgs boson contributions. For large $\tan\beta$, the charged Higgs boson contributions to δg^L are negligible. The charged Higgs boson contributions to δg^R are negative, which reduces R_b .

For these parameters, the range of masses of h^0 and A^0 in which $\Delta R_b > 0$ is already excluded by direct searches. For all remaining allowed h^0 and A^0 masses, $\Delta R_b < 0$, in worse agreement with experiment than the SM. Since the corrections from both the charged and neutral Higgs bosons are proportional to $\tan^2\beta$, we can vary $\tan\beta$ within the large $\tan\beta$ regime and ΔR_b will still be negative. Since the corrections grow with $\tan^2\beta$, the region ruled out by R_b gets larger as $\tan\beta$ increases.

The correction to A_b is very small compared to the experimental uncertainty in the A_b measurement. For these parameters, $|\Delta A_b| < 0.003$. Also, $\Delta A_b > 0$ in the regions allowed by the direct search bounds, in worse agreement with experiment than the SM. For $M_{H^+} = 270$ GeV, we find that $0.936 < A_b < 0.937$ in the allowed region. For $M_{H^+} = 165$ GeV, we find that $0.937 < A_b < 0.938$ in the allowed region.

For $\cos^2(\beta - \alpha) = 1/2$, the lower bound on M_{h^0} from direct searches is 87 GeV for arbitrary M_{A^0} , as discussed in appendix I. Combining the direct search bound and the constraint from R_b , we find that for these parameters with $M_{H^+} = 270$ GeV, the lower bound on the A^0 mass is $M_{A^0} > 37$ GeV (shown in figure 6.2). For an h^0 mass of 200 GeV or greater, $M_{A^0} > 64$ GeV. Similarly, if $M_{H^+} = 165$ GeV, we find that the lower bound on the A^0 mass increases to 40 GeV, as shown in figure 6.3. In this case, for an h^0 mass of 200 GeV or greater, $M_{A^0} > 71$ GeV.

In figures 6.4 and 6.5, we again plot the constraints on the neutral Higgs sector from R_b . This time, the parameters in these plots are $\tan\beta = 50$ and $\cos(\beta - \alpha) = 1$. For $\cos(\beta - \alpha) = 1$, the ZH^0A^0 coupling is zero and the $H^0b\bar{b}$ coupling is not enhanced over the SM $H^0b\bar{b}$ coupling, so the contribution of H^0 to the corrections is negligible. As before, the charged Higgs mass is constrained by the ρ parameter. For the parameters of figures 6.4 and 6.5, we find that the charged Higgs boson must be lighter than 250 GeV. In figure 6.4 we take $M_{H^+} = 250$ GeV, and in figure 6.5 we take $M_{H^+} = 165$ GeV, which is the lower bound from $b \rightarrow s\gamma$ [51,52].

For these parameters with $M_{H^+} = 250$ GeV, there is a very small allowed range of h^0 and A^0 masses in which $\Delta R_b > 0$, in better agreement with experiment than the SM. This range is on the verge of being ruled out experimentally. This is shown in figure 6.4. For $M_{H^+} = 165$ GeV, the corrections from charged Higgs boson exchange give a negative contribution to R_b . The region where $\Delta R_b > 0$ becomes smaller, and is excluded by the direct search limits.

If we combine the constraint from R_b with the direct search bounds, we find absolute lower limits on the h^0 and A^0 masses for $\cos(\beta - \alpha) = 1$. For $M_{H^+} = 250$ GeV,

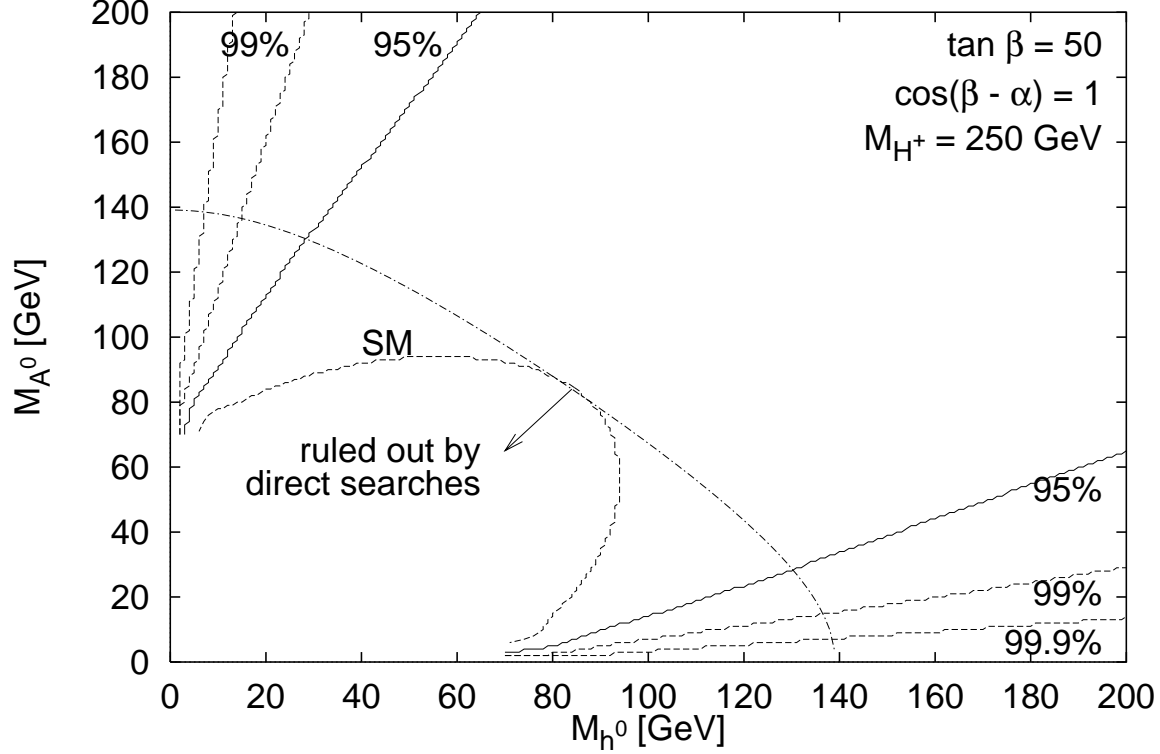


Figure 6.4: R_b in the Type II 2HDM with $\tan \beta = 50$, $\cos(\beta - \alpha) = 1$, and $M_{H^+} = 250$ GeV. The axes are M_{A^0} and M_{h^0} . The solid lines are the 95% confidence level lower bounds on M_{A^0} and M_{h^0} from R_b . The dashed lines labelled “99%” and “99.9%” are the 99% and 99.9% confidence level bounds from R_b . The dashed line labelled “SM” is where R_b is the same as in the SM. The region below this line, in which $\Delta R_b > 0$, is almost entirely excluded by direct searches. The dot-dashed line is the bound from direct searches, described in appendix I.

6.1 Models with Higgs doublets and singlets

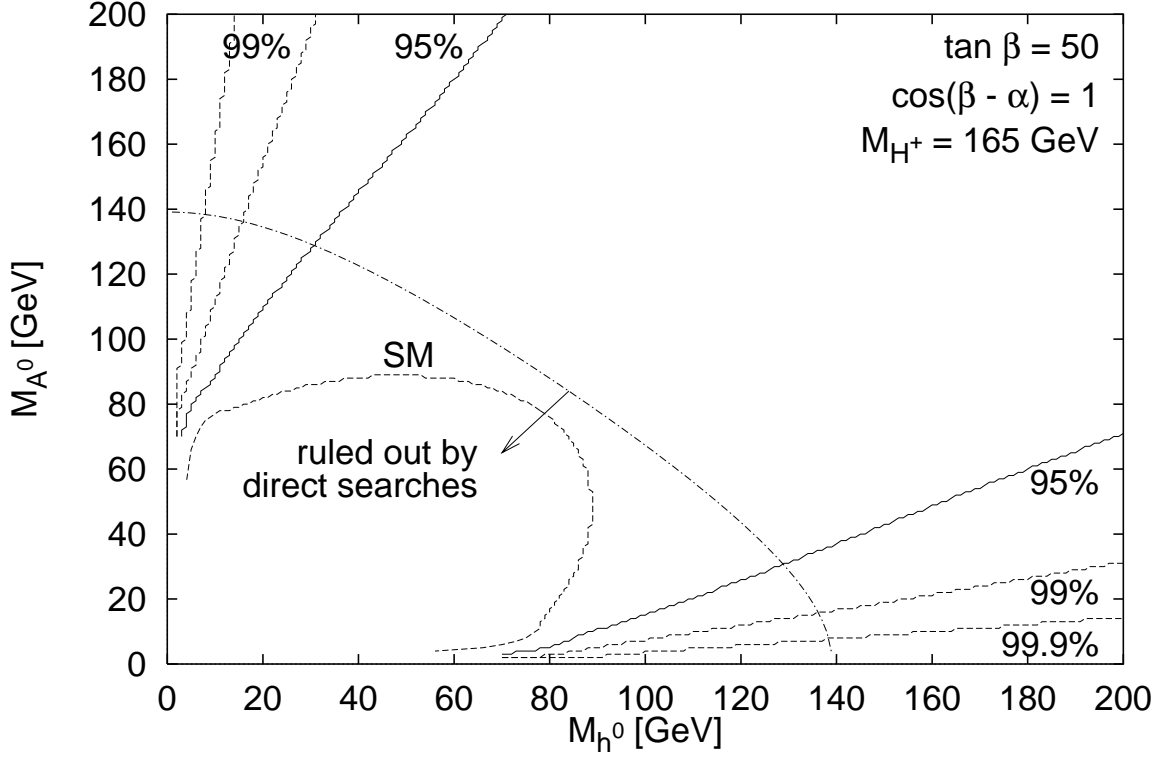


Figure 6.5: R_b in the 2HDM with $M_{H^+} = 165 \text{ GeV}$ (the lower limit from $b \rightarrow s\gamma$ [52]) and other parameters the same as in figure 6.4. Since $\Delta R_b < 0$ from H^+ , a larger area is excluded by R_b at 95% confidence level (solid lines), and the region in which $\Delta R_b > 0$ is now entirely excluded by direct searches. Also shown are the 99% and 99.9% confidence level contours (dashed). The dot-dashed line is the bound from direct searches as in figure 6.4.

both h^0 and A^0 must be heavier than 28 GeV. Similarly, for $M_{H^+} = 165$ GeV, both h^0 and A^0 must be heavier than 30 GeV. The direct search bounds are discussed in appendix I. The corrections to R_b are negative for large splittings between M_{h^0} and M_{A^0} . Thus areas of low M_{h^0} and high M_{A^0} , and of low M_{A^0} and high M_{h^0} , are ruled out by the R_b measurement.

Since both the charged and neutral Higgs boson corrections at large $\tan\beta$ are proportional to $\tan^2\beta$, varying $\tan\beta$ will not change the combinations of M_{h^0} and M_{A^0} for which $\Delta R_b = 0$. Thus the line where R_b is equal to its SM value stays the same as we vary $\tan\beta$, as long as we remain in the large $\tan\beta$ regime. Since the corrections grow with $\tan\beta$, the regions ruled out by R_b in figures 6.4 and 6.5 get larger as $\tan\beta$ increases.

For $\cos(\beta - \alpha) = 1$, the correction to A_b is again very small compared to the experimental uncertainty in the A_b measurement. For these parameters, $|\Delta A_b| < 0.004$. For $M_{H^+} = 250$ GeV, $0.935 < A_b < 0.937$ in the allowed region. For $M_{H^+} = 165$ GeV, $0.936 < A_b < 0.938$ in the allowed region. This is in slightly worse agreement with experiment than the SM.

In the decoupling limit, $\cos(\beta - \alpha) \rightarrow 0$, as discussed in reference [50]. Thus the case $\cos(\beta - \alpha) = 1$ is the opposite of the decoupling limit, and the Higgs sector may develop large, nonperturbative scalar quartic couplings as we try to take the charged Higgs mass large. However, we can take $\cos(\beta - \alpha) = 0$ while interchanging h^0 and H^0 in figures 6.4 and 6.5, and the results for R_b and A_b will remain the same. This is shown in figure 6.6. In the limit $\cos(\beta - \alpha) = 0$, the couplings of h^0 go to their SM values. Therefore, the mass of h^0 is constrained by the SM bound, $M_{h^0} > 95.2$ GeV [56]. This is the bound on the SM Higgs mass from LEP running at $\sqrt{s} = 189$ GeV. H^0 is, by definition, the heavier CP-even neutral Higgs boson, so $M_{H^0} > M_{h^0} > 95.2$ GeV. The mass of H^0 is also constrained by the search for $H^0 A^0$ production, as discussed in appendix I. When $\cos(\beta - \alpha) = 0$, the $Z h^0 A^0$ coupling is zero and the $h^0 b\bar{b}$ coupling is not enhanced over the SM coupling, so h^0 does not contribute significantly to the corrections. We will neglect it.

As discussed before, a large mass splitting between the charged Higgs boson and the neutral Higgs bosons results in large radiative corrections to the ρ parameter. For this reason, we set $M_{H^+} = M_{A^0}$ in figure 6.6, for $M_{A^0} > 165$ GeV. For $M_{A^0} < 165$ GeV, we set $M_{H^+} = 165$ GeV, which is the lower bound on the charged Higgs mass from $b \rightarrow s\gamma$ [51,52].

For $\cos(\beta - \alpha) = 0$, the R_b measurement rules out areas where the mass splitting between H^0 and A^0 is large. For example, if the H^0 (A^0) mass is 1000 GeV, then A^0 (H^0) must be heavier than about 300 GeV.

Two Higgs doublet model in the decoupling limit

In the decoupling limit of the 2HDM, h^0 remains light and its couplings to the SM particles approach those of the SM Higgs boson, while all the other Higgs bosons become

6.1 Models with Higgs doublets and singlets

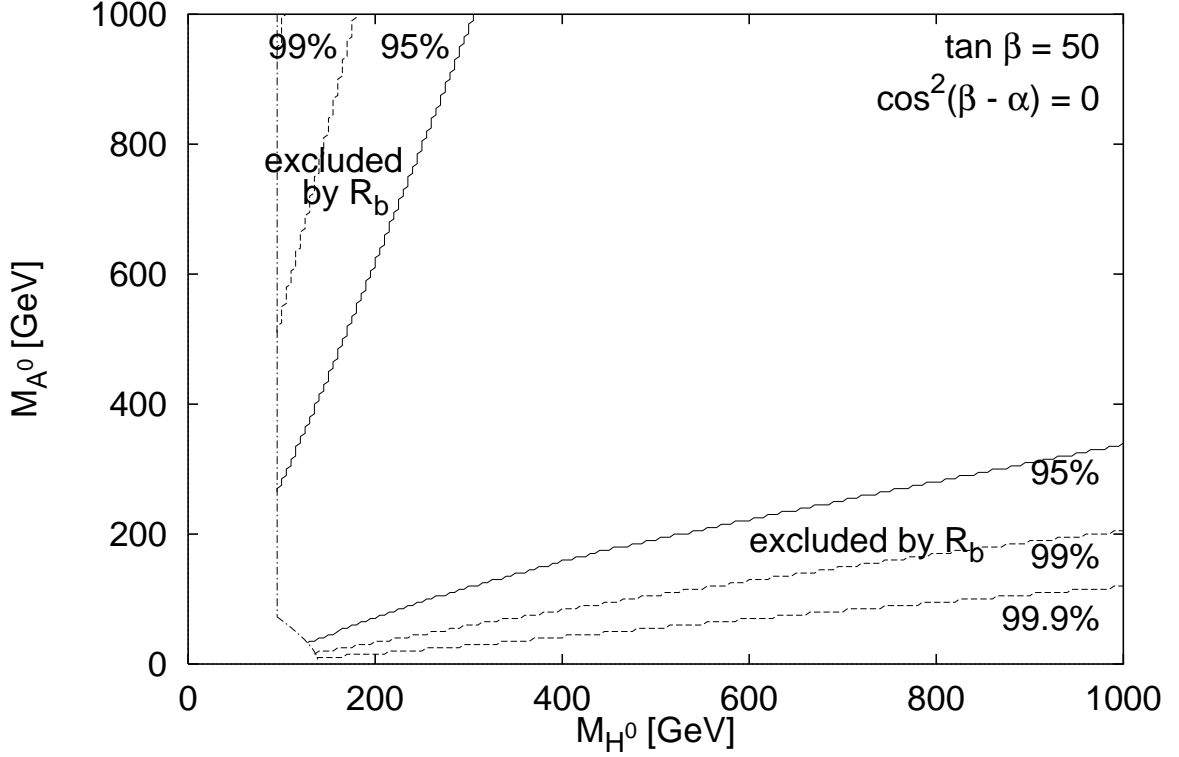


Figure 6.6: R_b in the 2HDM with $\tan \beta = 50$ and $\cos(\beta - \alpha) = 0$. The axes are M_{H^0} and M_{A^0} . For $M_{A^0} > 165$ GeV, the charged Higgs mass is set equal to M_{A^0} , while for $M_{A^0} < 165$ GeV, the charged Higgs mass is set equal to 165 GeV. The solid lines are the 95% confidence level lower bounds on M_{A^0} and M_{H^0} from R_b . The dashed lines labelled “99%” and “99.9%” are the 99% and 99.9% confidence level bounds from R_b . The dot-dashed line is the bound from direct searches, described in appendix I.

heavy and decouple from the SM particles. This limit is discussed in reference [50]. In particular, in the decoupling limit,

$$M_{h^0} \sim \mathcal{O}(M_Z), \quad (6.10)$$

$$M_{H^0} \simeq M_{A^0}, \quad (6.11)$$

$$|M_{H^0}^2 - M_{A^0}^2| \sim \mathcal{O}(M_Z^2), \quad (6.12)$$

$$\cos(\beta - \alpha) \sim \mathcal{O}\left(\frac{M_Z^2}{M_{A^0}^2}\right), \quad (6.13)$$

where $M_{A^0} \gg M_Z$. We can expand the corrections to $Z \rightarrow b\bar{b}$ from neutral Higgs boson exchange in the 2HDM in this limit. We use the expansions of the three-point integrals given in appendix F. To leading order in $M_Z^2/M_{A^0}^2$,

$$\begin{aligned} \delta g^L &\simeq \frac{1}{16\pi^2} \left(\frac{e}{s_W c_W}\right) \left(\frac{gm_b}{\sqrt{2}M_W}\right)^2 \tan^2 \beta \times \frac{M_Z^2}{M_{A^0}^2} \\ &\times \left[-\frac{1}{36} + \frac{1}{9}s_W^2 \left(\frac{1}{3} + \log\left(\frac{M_{A^0}^2}{M_Z^2}\right) + i\pi \right) \right] \end{aligned} \quad (6.14)$$

$$\begin{aligned} \delta g^R &\simeq \frac{1}{16\pi^2} \left(\frac{e}{s_W c_W}\right) \left(\frac{gm_b}{\sqrt{2}M_W}\right)^2 \tan^2 \beta \times \frac{M_Z^2}{M_{A^0}^2} \\ &\times \left[-\frac{1}{36} - \frac{1}{6} \left(\log\left(\frac{M_{A^0}^2}{M_Z^2}\right) + i\pi \right) + \frac{1}{9}s_W^2 \left(\frac{1}{3} + \log\left(\frac{M_{A^0}^2}{M_Z^2}\right) + i\pi \right) \right]. \end{aligned} \quad (6.15)$$

For $\tan \beta = 50$ and $M_{A^0} = 200$ GeV, these corrections give $\Delta R_b = -0.00037$, which is half the size of the experimental error on the R_b measurement. As M_{A^0} increases, the correction decreases; for $M_{A^0} = 500$ GeV, $\Delta R_b = -0.00015$.

This limit is approached in figure 6.6 when M_{H^0} and M_{A^0} are large and similar in size.

Multiple-doublet models

We now consider neutral Higgs boson exchange in a model containing multiple Higgs doublets, denoted Φ_k , with hypercharge $Y = 1$.

In a Type I model of this type, we let Φ_1 couple to both up- and down-type quarks, and none of the other doublets couple to quarks. In a Type II model, we let Φ_1 couple only to down-type quarks, and Φ_2 couple to up-type quarks. Then the Yukawa couplings are defined in the same way as in the 2HDM, in equations 3.11–3.14. As always, the contributions to $Z \rightarrow b\bar{b}$ from neutral Higgs boson exchange are only significant in a Type II model, when λ_b is enhanced by small v_1 . We will only consider Type II multi-doublet models with small v_1 .

6.1 Models with Higgs doublets and singlets

The contributions from neutral Higgs boson exchange in the multi-doublet model are more complicated than in the 2HDM, simply because there are more neutral Higgs states. Only the states which have a nonzero overlap with Φ_1 can couple to b quarks, so only these states contribute. The corrections depend on the overlap of each neutral state with Φ_1 and the mass of each state. As in the 2HDM, the region of parameter space in which the correction to R_b is positive is almost entirely ruled out by direct searches.

Multiple-doublet models with Higgs singlets

We can also consider adding a number of Higgs singlets, with hypercharge zero, to the multi-doublet model. The singlets do not couple to Z or to quarks. Their vevs are also unconstrained by the W mass. In general, the singlets will mix with the neutral components of the doublets to form mass eigenstates. The couplings of the physical states to $b\bar{b}$ still depend only on v_1 , which fixes λ_b , and on the overlap of each state with Φ_1 . The couplings of physical states to Z are no longer the same as in a model containing only doublets. Instead, they are equal to the Z coupling for doublet states weighted by the overlap of each state with doublets. Explicitly,

$$g_{ZH_i^0 A_j^0} = \frac{-i}{2} \frac{e}{s_W c_W} \sum_k \langle H_i^0 | \phi_k^{0,r} \rangle \langle A_j^0 | \phi_k^{0,i} \rangle, \quad (6.16)$$

where k runs only over the Higgs doublets.

In order to understand the effects of singlets on the corrections to $Z \rightarrow b\bar{b}$, let us imagine replacing each Higgs singlet with the neutral component of a doublet, with the appropriate CP quantum number, while holding the masses and mixings of the physical states constant. Then, the couplings of each state to $b\bar{b}$ remain the same. However, the couplings of the states to Z are now equal to,

$$g_{ZH_i^0 A_j^0} = \frac{-i}{2} \frac{e}{s_W c_W}, \quad (6.17)$$

which is the coupling in a model containing only Higgs doublets. Comparing this to equation 6.16, we see that $\delta g^{R,L}(a)$ in the model with singlets must be smaller in magnitude than in the model in which the singlets are replaced by doublets.

Degenerate neutral Higgs bosons in a general extended Higgs sector

The corrections to $Z \rightarrow b\bar{b}$ due to neutral Higgs boson exchange in a general model are quite complicated. They depend on the couplings and masses of all the neutral Higgs bosons in the model. However, the corrections can be simplified if some of the neutral Higgs bosons are degenerate in mass. We describe these simplifications in this section.

In this section we consider a general extended Higgs sector, which can contain Higgs singlets, doublets, and larger multiplets. We require that the model be Type II, and that λ_b be enhanced relative to λ_t . A Type II model must contain at least two Higgs doublets, Φ_1 and Φ_2 , to couple to down- and up-type quarks, respectively.

Only the neutral Higgs bosons with large couplings to $b\bar{b}$ give significant contributions to the corrections. In what follows we will only consider these. States without enhanced $b\bar{b}$ couplings, such as G^0 , do not contribute significantly. We will ignore them, and therefore it does not matter what their masses are.

If all the CP-even neutral Higgs bosons are degenerate with mass M_H , and all the CP-odd neutral Higgs bosons are degenerate with mass M_A , then we can take the two- and three-point integrals outside of the sums in equations 5.1–5.3. Then we can sum the couplings over complete sets of states. Using the couplings in a general model from equations 3.22, 3.23, and 3.26, we find

$$\sum_{H_i^0, A_j^0} g_{ZH_i^0 A_j^0} g_{H_i^0 b\bar{b}}^V g_{A_j^0 b\bar{b}}^A = \frac{1}{2} \frac{e}{s_W c_W} \left(\frac{gm_b}{\sqrt{2}M_W} \right)^2 \left(\frac{v_{SM}}{v_1} \right)^2 \quad (6.18)$$

$$\sum_{H_i^0} (g_{H_i^0 b\bar{b}}^V)^2 = - \sum_{A_j^0} (g_{A_j^0 b\bar{b}}^A)^2 = \left(\frac{gm_b}{\sqrt{2}M_W} \right)^2 \left(\frac{v_{SM}}{v_1} \right)^2. \quad (6.19)$$

These sums over the couplings are related to certain couplings in the 2HDM, as follows. On the left-hand side are the couplings in the general model with degenerate neutral Higgs bosons, and on the right-hand side are the couplings in the 2HDM with $\cos(\beta - \alpha) = 1$.

$$\sum_{H_i^0, A_j^0} g_{ZH_i^0 A_j^0} g_{H_i^0 b\bar{b}}^V g_{A_j^0 b\bar{b}}^A = g_{Zh^0 A^0} g_{h^0 b\bar{b}}^V g_{A^0 b\bar{b}}^A \quad (6.20)$$

$$\sum_{H_i^0} (g_{H_i^0 b\bar{b}}^V)^2 = (g_{h^0 b\bar{b}}^V)^2 \quad (6.21)$$

$$- \sum_{A_j^0} (g_{A_j^0 b\bar{b}}^A)^2 = -(g_{A^0 b\bar{b}}^A)^2. \quad (6.22)$$

Therefore, when all the CP-even neutral Higgs bosons are degenerate with mass M_H , and all the CP-odd neutral Higgs bosons are degenerate with mass M_A , the contributions to $Z \rightarrow b\bar{b}$ are the same as the contributions from the 2HDM with $M_{h^0} = M_H$, $M_{A^0} = M_A$, and $\cos(\beta - \alpha) = 1$. The parameter corresponding to $\tan \beta$ in the extended model is,

$$\sqrt{\frac{v_{SM}^2 - v_1^2}{v_1^2}} = \tan \beta. \quad (6.23)$$

If there are no contributions from the charged Higgs bosons, the corrections to R_b and A_b in this situation are the same as those for the 2HDM shown in figure 6.4, for $\tan \beta = 50$.

6.2 Models with Higgs multiplets larger than doublets

Similarly, the corrections can be simplified if only the CP-even states, or only the CP-odd states, are degenerate. If the CP-even states are degenerate, we can sum over the H_i^0 couplings. We then get the same result as if the CP-even neutral Higgs sector consisted of a single state H^0 , which consists entirely of $\phi_1^{0,r}$. Recall that $\phi_1^{0,r}$ is the CP-even neutral component of the doublet which couples to down-type quarks. If, instead, the CP-odd states are degenerate, we can sum over the A_j^0 couplings. We get the same result as if the CP-odd neutral Higgs sector consisted of a single state A^0 , which consists entirely of $\phi_1^{0,i}$ (up to the small mixing of $\phi_1^{0,i}$ with G^0 , which is negligible in the small v_1 regime).

6.2 Models with Higgs multiplets larger than doublets

We now consider Higgs sectors which contain one or more multiplets larger than doublets. We consider two types of models which use two different approaches to satisfy $\rho \approx 1$. We first consider models in which the vevs of the multiplets larger than doublets are fine-tuned to be very small, so that their contribution to the ρ parameter is negligible. Second, we consider models which preserve $SU(2)_c$ symmetry, ensuring that $\rho = 1$ at tree level.

In section 6.2.1 we examine a model containing one Higgs doublet and one triplet, and in section 6.2.2 we examine a model containing two Higgs doublets and one triplet. In both of these models, the vev of the Higgs triplet must be very small in order to be consistent with the measured value of the ρ parameter. The model with two doublets and one triplet is also discussed further in appendix D.

In section 6.2.3 we examine the model with Higgs triplets and $SU(2)_c$ symmetry introduced by Georgi and Machacek [42]. The $SU(2)_c$ symmetry ensures that $\rho = 1$ at tree level in this model, as explained in detail in appendix E. We then extend the results to a class of generalized Georgi–Machacek models which preserve $SU(2)_c$ symmetry.

6.2.1 Models with one Higgs doublet and one triplet

In this section we describe the minimal extension of the Higgs sector to include multiplets larger than doublets. The Higgs sector consists of the complex, $Y = 1$ doublet of the SM, denoted by Φ , plus a triplet field. The vev of the triplet field must be fine-tuned very small in order to be consistent with the measured value of the ρ parameter, $\rho \approx 1$. The triplet field can either be a real triplet with $Y = 0$, or a complex triplet with $Y = 2$. Here we investigate both possibilities.

These two models contain only one Higgs doublet, which couples to both up- and down-type quarks, so they are necessarily Type I models. Thus $\lambda_b \ll \lambda_t$, and the only non-negligible contributions to $Z \rightarrow b\bar{b}$ come from the contributions to δg^L from charged

Higgs boson exchange.

We first consider the “ $Y = 0$ model” with one doublet and one real triplet field with $Y = 0$. The triplet field is $\xi = (\xi^+, \xi^0, \xi^-)$. We define the doublet and triplet vevs by $\langle \phi^0 \rangle = v_\phi/\sqrt{2}$ and $\langle \xi^0 \rangle = v_\xi$. The vevs are constrained by the W mass to satisfy,

$$v_{SM}^2 = v_\phi^2 + 4v_\xi^2, \quad (6.24)$$

where $v_{SM} = 246$ GeV. It is convenient to parameterize the ratio of the vevs by,

$$\tan \theta_0 = \frac{v_\phi}{2v_\xi}. \quad (6.25)$$

In this model, the tree-level ρ parameter is,

$$\rho = \frac{v_\phi^2 + 4v_\xi^2}{v_\phi^2} = 1 + \frac{4v_\xi^2}{v_\phi^2} \equiv 1 + \Delta\rho. \quad (6.26)$$

In terms of $\tan \theta_0$, we find

$$\Delta\rho = \frac{1}{\tan^2 \theta_0}. \quad (6.27)$$

We see that in order to have $\rho \approx 1$, the triplet vev must be very small, giving large $\tan \theta_0$. The charged states mix to form the charged Goldstone boson and a single charged physical state,

$$G^+ = \sin \theta_0 \phi^+ + \cos \theta_0 \xi^+ \quad (6.28)$$

$$H^+ = \cos \theta_0 \phi^+ - \sin \theta_0 \xi^+. \quad (6.29)$$

We next consider the “ $Y = 2$ model” with one doublet and one complex triplet field with $Y = 2$. The triplet field is $\chi = (\chi^{++}, \chi^+, \chi^0)$. We define the vev of this triplet field by $\langle \chi^0 \rangle = v_\chi/\sqrt{2}$. The vevs are constrained by the W mass to satisfy,

$$v_{SM}^2 = v_\phi^2 + 2v_\chi^2. \quad (6.30)$$

It is convenient to parameterize the ratio of the doublet and triplet vevs by,

$$\tan \theta_2 = \frac{v_\phi}{\sqrt{2}v_\chi}. \quad (6.31)$$

In this model, the tree-level ρ parameter is,

$$\rho = \frac{v_\phi^2 + 2v_\chi^2}{v_\phi^2 + 4v_\chi^2} = 1 - \frac{2v_\chi^2}{v_\phi^2 + 4v_\chi^2} \equiv 1 + \Delta\rho. \quad (6.32)$$

6.2 Models with Higgs multiplets larger than doublets

In terms of $\tan \theta_2$, we find

$$\Delta\rho = -\frac{1}{\tan^2 \theta_2 + 2}. \quad (6.33)$$

We see that in order to have $\rho \approx 1$, the triplet vev must be very small, giving large $\tan \theta_2$. The charged states mix to form the charged Goldstone boson and a single charged physical state,

$$G^+ = \sin \theta_2 \phi^+ + \cos \theta_2 \xi^+ \quad (6.34)$$

$$H^+ = \cos \theta_2 \phi^+ - \sin \theta_2 \xi^+. \quad (6.35)$$

The Higgs couplings to quarks and the Z boson can be parameterized as follows. We let θ denote θ_0 in the $Y = 0$ model and θ_2 in the $Y = 2$ model. We also define a factor ϵ such that $\epsilon = +1$ in the $Y = 0$ model and $\epsilon = -1$ in the $Y = 2$ model. The charged Higgs couplings to quarks are,

$$g_{G^+ \bar{t} b}^L = \frac{gm_t}{\sqrt{2}M_W} \quad (6.36)$$

$$g_{H^+ \bar{t} b}^L = \frac{gm_t}{\sqrt{2}M_W} \cot \theta. \quad (6.37)$$

The $ZH_i^+ H_j^-$ couplings are,

$$g_{ZG^+ G^-} = -\frac{e}{s_W c_W} \left(\frac{1}{2} - s_W^2 + \frac{\epsilon}{2} \cos^2 \theta_2 \right) \quad (6.38)$$

$$g_{ZG^+ H^-} = \frac{e}{s_W c_W} \frac{\epsilon}{2} \sin \theta_2 \cos \theta_2 \quad (6.39)$$

$$g_{ZH^+ H^-} = -\frac{e}{s_W c_W} \left(\frac{1}{2} - s_W^2 + \frac{\epsilon}{2} \sin^2 \theta_2 \right). \quad (6.40)$$

The $ZH_i^+ H_j^-$ couplings are different in the two models because the hypercharge of the triplet is different.

Contributions to $Z \rightarrow b\bar{b}$

In both the $Y = 0$ and the $Y = 2$ models, there is an off-diagonal $ZG^+ H^-$ coupling, and the diagonal $ZH^+ H^-$ and $ZG^+ G^-$ couplings differ from their values in models containing only Higgs doublets and singlets. These couplings contribute to the second and third terms of δg^L in equation 4.6.

The resulting contribution to δg^L is,

$$\begin{aligned} \delta g^L &= \frac{1}{16\pi^2} \left(\frac{gm_t}{\sqrt{2}M_W} \right)^2 \frac{1}{2} \frac{e}{s_W c_W} \cos^2 \theta \left\{ \frac{1}{\sin^2 \theta} \left[\frac{R}{R-1} - \frac{R \log R}{(R-1)^2} \right] \right. \\ &\quad \left. - 2\epsilon \left[C_{24}(m_t^2, M_W^2, M_W^2) + C_{24}(m_t^2, M_H^2, M_H^2) - 2C_{24}(m_t^2, M_W^2, M_H^2) \right] \right\} \end{aligned} \quad (6.41)$$

in addition to the SM contribution to δg_{SM}^L from G^+ exchange. We have defined $R \equiv m_t^2/M_H^2$, M_H is the mass of H^+ . As before, in the $Y = 0$ model, $\theta = \theta_0$ and $\epsilon = +1$, while in the $Y = 2$ model, $\theta = \theta_2$ and $\epsilon = -1$.

Note that δg^L is proportional to $\cos^2 \theta$, which goes to zero in the large $\tan \theta$ limit. This is due to the fact that in the limit of small triplet vev in either of these models, the overlap of H^+ with the doublet is proportional to $\cos \theta$. As a result, in the large $\tan \theta$ limit, H^+ is almost entirely triplet and so its couplings to quarks are very small. Also in the large $\tan \theta$ limit, the off-diagonal ZG^+H^- coupling goes to zero, and the ZG^+G^- coupling approaches its SM value.

Constraints from the ρ parameter

We must also take into account the constraint on $\tan \theta$ from the ρ parameter in each of the models. Since $\Delta\rho$ depends differently on $\tan \theta_0$ than on $\tan \theta_2$, the constraint on $\tan \theta$ will be different in the $Y = 0$ model than in the $Y = 2$ model.

The experimental constraints on $\Delta\rho$ are taken from reference [5], in which $\Delta\rho = \epsilon_1$. Reference [5] finds,

$$\Delta\rho = (3.9 \pm 1.2) \times 10^{-3}. \quad (6.42)$$

However, we cannot take this directly as a constraint on $\tan \theta_0$ and $\tan \theta_2$, because the ρ parameter gets radiative corrections from SM particles. We must take into account these radiative corrections in order to extract limits on $\Delta\rho$ from new physics.

In the SM, the radiative corrections to ρ depend on the masses of the top quark and the SM Higgs boson. If the top quark and the SM Higgs boson are taken to lie in certain mass ranges, a range can be found for the SM prediction for the radiative corrections to ρ . From reference [5], if the mass ranges are taken to be $170 \text{ GeV} < m_t < 180 \text{ GeV}$ and $70 \text{ GeV} < m_H < 1000 \text{ GeV}$, then the SM predictions for $\Delta\rho$ from radiative corrections are,

$$3.32 \times 10^{-3} < \Delta\rho_{SM} < 6.19 \times 10^{-3}. \quad (6.43)$$

We must take this into account in order to find the experimental limits on $\Delta\rho$ due to new physics. Varying the SM prediction for $\Delta\rho$ within this range, we find the following limits on $\Delta\rho$ from new physics, at the 2σ level:

$$-4.7 \times 10^{-3} < \Delta\rho_{\text{new}} < 3.0 \times 10^{-3}. \quad (6.44)$$

We now use $\Delta\rho_{\text{new}}$ to constrain $\tan \theta_0$ and $\tan \theta_2$. We ignore the radiative corrections from the non-minimal Higgs sector. Note that $\Delta\rho_{\text{new}}$ can be either positive or negative. In the $Y = 0$ model, $\Delta\rho_{\text{new}}$ is positive, while in the $Y = 2$ model, $\Delta\rho_{\text{new}}$ is negative. The resulting 2σ limits on $\tan \theta_0$ and $\tan \theta_2$ are,

$$\tan \theta_0 > 18 \quad (6.45)$$

$$\tan \theta_2 > 15. \quad (6.46)$$

6.2 Models with Higgs multiplets larger than doublets

Results

The contribution to δg^L in both the $Y = 0$ model and the $Y = 2$ model is proportional to $\cos^2 \theta$ (equation 6.41). When the constraints on $\tan \theta$ from the ρ parameter are imposed, the corrections to R_b and A_b are very small. In the $Y = 0$ model, for $\tan \theta_0 = 18$ and M_{H^+} varying between 10 and 1000 GeV, $-6.7 \times 10^{-6} < \Delta R_b < 7.2 \times 10^{-6}$ and $-2.5 \times 10^{-6} < \Delta A_b < 2.7 \times 10^{-6}$. In the $Y = 2$ model, for $\tan \theta_2 = 15$ and again M_{H^+} varying between 10 and 1000 GeV, $-1.2 \times 10^{-5} < \Delta R_b < -5.9 \times 10^{-6}$ and $-4.6 \times 10^{-6} < \Delta A_b < -2.2 \times 10^{-6}$. These corrections are minuscule compared to the experimental error on the R_b and A_b measurements (equations 2.26 and 2.27).

In general, the contribution to δg^L vanishes in the large $\tan \theta$ limit in any model in which the charged Goldstone boson is made up almost entirely of the doublet that couples to quarks. Then the overlap of the other charged Higgs states with the doublet is very small, so the other charged Higgs states couple very weakly to quarks. This occurs in any model that contains only one scalar doublet, plus any number of singlets and multiplets larger than doublets, as long as the vevs of the multiplets larger than doublets are forced to be small.

The contributions of multiplets larger than doublets to $Z \rightarrow b\bar{b}$ can be large only if the larger multiplets mix significantly with doublets, so that the resulting Higgs states have non-negligible couplings to quarks. This can happen in two ways. First, if the model contains more than one doublet, then the charged Goldstone boson will not necessarily be made up almost entirely of the doublet which couples to quarks. In fact, in a Type II model, one doublet couples to up-type quarks and a different one couples to down-type quarks. In this case, there is no way that the charged Goldstone boson can consist entirely of both the doublets. The remaining parts of the doublets which couple to quarks can then be mixed into the physical charged Higgs states, giving them non-negligible couplings to quarks. A model of this type is discussed in section 6.2.2. Second, if the multiplets larger than doublets have sizeable vevs, then the charged Goldstone boson must contain some admixture of the larger multiplets, leaving part of the doublet free to mix into the physical charged Higgs states. However, in order for the multiplets larger than doublets to have sizeable vevs without violating the constraint from the ρ parameter, the model must preserve $SU(2)_c$ symmetry. Models of this type are discussed in section 6.2.3.

6.2.2 Models with two doublets and one triplet

We now consider a Higgs sector consisting of two doublets and one triplet. As in section 6.2.1, the triplet can be real with $Y = 0$ or complex with $Y = 2$. The couplings for these models are listed in appendix D. With two doublets, we can construct either a Type I model or a Type II model. In this section we consider a Type II model, but we also note the changes in the formulas that must be made to recover a Type I model.

We will consider both the corrections due to charged Higgs boson exchange and the corrections due to neutral Higgs boson exchange. The corrections from neutral Higgs boson exchange can be significant in a Type II model with large $\tan\beta$. We define $\tan\beta$ in this model exactly as in the 2HDM, $\tan\beta = v_2/v_1$, where the vevs of the doublets are $\langle\phi_1^0\rangle = v_1/\sqrt{2}$ and $\langle\phi_2^0\rangle = v_2/\sqrt{2}$.

Charged Higgs boson contributions

We first consider the corrections due to charged Higgs boson exchange in the model with two doublets and one real triplet field with $Y = 0$. We will refer to this model as the $Y = 0$ model. The triplet field is $\xi = (\xi^+, \xi^0, \xi^-)$. We define the triplet vev by $\langle\xi^0\rangle = v_\xi$. In the $Y = 0$ model we parameterize the vevs by,

$$\tan\theta_0 = \frac{\sqrt{v_1^2 + v_2^2}}{2v_\xi}, \quad (6.47)$$

in analogy to section 6.2.1.

The charged Higgs states are defined as follows. The Goldstone boson is,

$$G^+ = \sin\theta_0(\cos\beta\phi_1^+ + \sin\beta\phi_2^+) + \cos\theta_0\xi^+. \quad (6.48)$$

In addition we define two orthogonal states,

$$H_1^{+'} = \cos\theta_0(\cos\beta\phi_1^+ + \sin\beta\phi_2^+) - \sin\theta_0\xi^+ \quad (6.49)$$

$$H_2^{+'} = -\sin\beta\phi_1^+ + \cos\beta\phi_2^+, \quad (6.50)$$

which will mix by an angle δ to form the mass eigenstates. Before mixing them, however, let us take the limit of large $\tan\theta_0$ in order to satisfy the experimental constraint on the ρ parameter. We make the approximation $\sin\theta_0 \approx 1$ and $\cos\theta_0 \approx 0$. Then the states are,

$$G^+ \simeq \cos\beta\phi_1^+ + \sin\beta\phi_2^+ \quad (6.51)$$

$$H_1^{+'} \simeq -\xi^+ \quad (6.52)$$

$$H_2^{+'} = -\sin\beta\phi_1^+ + \cos\beta\phi_2^+. \quad (6.53)$$

These states mix by an angle δ to form the mass eigenstates, which are,

$$H_1^+ \simeq \sin\delta(-\sin\beta\phi_1^+ + \cos\beta\phi_2^+) - \cos\delta\xi^+ \quad (6.54)$$

$$H_2^+ \simeq \cos\delta(-\sin\beta\phi_1^+ + \cos\beta\phi_2^+) + \sin\delta\xi^+. \quad (6.55)$$

The exact states are listed in appendix D, where we do not make the large $\tan\theta_0$ approximation.

6.2 Models with Higgs multiplets larger than doublets

We next consider the corrections due to charged Higgs boson exchange in the model with two doublets and one complex triplet field with $Y = 2$. We will refer to this model as the $Y = 2$ model. The triplet field is $\chi = (\chi^{++}, \chi^+, \chi^0)$. We define the triplet vev by $\langle \chi^0 \rangle = v_\chi / \sqrt{2}$. In the $Y = 2$ model we parameterize the vevs by,

$$\tan \theta_2 = \frac{\sqrt{v_1^2 + v_2^2}}{\sqrt{2}v_\chi}, \quad (6.56)$$

again in analogy to section 6.2.1.

The charged Higgs states in the $Y = 2$ model are parameterized in the same way as the states in the $Y = 0$ model. The Goldstone boson is,

$$G^+ = \sin \theta_2 (\cos \beta \phi_1^+ + \sin \beta \phi_2^+) + \cos \theta_2 \chi^+. \quad (6.57)$$

In addition we define two orthogonal states,

$$H_1^{+'} = \cos \theta_2 (\cos \beta \phi_1^+ + \sin \beta \phi_2^+) - \sin \theta_2 \chi^+ \quad (6.58)$$

$$H_2^{+'} = -\sin \beta \phi_1^+ + \cos \beta \phi_2^+ \quad (6.59)$$

which will mix by an angle δ to form the mass eigenstates. Before mixing them, however, let us take the limit of large $\tan \theta_2$ in order to satisfy the experimental constraint on the ρ parameter. We make the approximation $\sin \theta_2 \approx 1$ and $\cos \theta_2 \approx 0$. Then the states are,

$$G^+ \simeq \cos \beta \phi_1^+ + \sin \beta \phi_2^+ \quad (6.60)$$

$$H_1^{+'} \simeq -\chi^+ \quad (6.61)$$

$$H_2^{+'} = -\sin \beta \phi_1^+ + \cos \beta \phi_2^+. \quad (6.62)$$

These states mix by an angle δ to form the mass eigenstates, which are,

$$H_1^+ \simeq \sin \delta (-\sin \beta \phi_1^+ + \cos \beta \phi_2^+) - \cos \delta \chi^+ \quad (6.63)$$

$$H_2^+ \simeq \cos \delta (-\sin \beta \phi_1^+ + \cos \beta \phi_2^+) + \sin \delta \chi^+. \quad (6.64)$$

The exact states are listed in appendix D, where we do not make the large $\tan \theta_2$ approximation.

We now calculate the corrections to $Z \rightarrow b\bar{b}$ from charged Higgs boson exchange in the Type II $Y = 0$ and $Y = 2$ models. As in section 6.2.1, we introduce the parameter $\epsilon = +1$ in the $Y = 0$ model, and $\epsilon = -1$ in the $Y = 2$ model. The contributions to δg^L are,

$$\delta g^L \simeq \frac{1}{16\pi^2} \frac{1}{2} \frac{e}{s_W c_W} \left(\frac{gm_t}{\sqrt{2}M_W} \right)^2 \cot^2 \beta$$

$$\begin{aligned}
& \times \left[\sin^2 \delta \left[\frac{R_1}{R_1 - 1} - \frac{R_1 \log R_1}{(R_1 - 1)^2} \right] + \cos^2 \delta \left[\frac{R_2}{R_2 - 1} - \frac{R_2 \log R_2}{(R_2 - 1)^2} \right] \right] \\
& - \frac{\epsilon}{16\pi^2} \frac{e}{s_W c_W} \left(\frac{gm_t}{\sqrt{2}M_W} \right)^2 \cot^2 \beta \sin^2 \delta \cos^2 \delta \left[C_{24}(m_t^2, M_{H_1^+}^2, M_{H_1^+}^2) \right. \\
& \left. + C_{24}(m_t^2, M_{H_2^+}^2, M_{H_2^+}^2) - 2C_{24}(m_t^2, M_{H_1^+}^2, M_{H_2^+}^2) \right], \tag{6.65}
\end{aligned}$$

in addition to the SM correction due to charged Goldstone boson exchange. We have defined $R_i = m_t^2/M_{H_i^+}^2$. In the Type I models, δg^L is the same as above with $\cot^2 \beta$ replaced by $\tan^2 \beta$.

The first term of equation 6.65 is the same as the correction in a three Higgs doublet model (3HDM), given in equation 6.3. It is positive, which gives a negative contribution to R_b , taking it farther from the measured value. The second term comes from the effects of the triplet. This second term is proportional to $\sin^2 \delta \cos^2 \delta$, so it is only significant for δ near $\pi/4$, which corresponds to maximal mixing between the charged doublet and triplet states in H_1^+ and H_2^+ . The second term is zero if H_1^+ and H_2^+ have the same mass.

The sign of the second term depends on the hypercharge of the Higgs triplet. In the $Y = 0$ model, the second term is negative. However, the second term is smaller in magnitude than the first term, so the overall contribution to δg^L is positive in the $Y = 0$ model.

In figure 6.7, we plot the constraints on $M_{H_1^+}$ and $M_{H_2^+}$ from the R_b measurement in the $Y = 0$ model, for maximal doublet–triplet mixing ($\delta = \pi/4$) and $\tan \beta = 1$. In order for the $Y = 0$ model with maximal doublet–triplet mixing to be consistent with the R_b measurement, one or both of the charged Higgs bosons must be very heavy.

In the $Y = 2$ model, the second term of equation 6.65 is positive, resulting in a positive δg^L which is larger than in the $Y = 0$ model. As a result, a larger area of parameter space is excluded by the R_b measurement in the $Y = 2$ model than in the $Y = 0$ model.

In figure 6.8, we plot the constraints on $M_{H_1^+}$ and $M_{H_2^+}$ from the R_b measurement on the $Y = 2$ model, for maximal doublet–triplet mixing ($\delta = \pi/4$) and $\tan \beta = 1$. From the R_b constraint with these parameters, we find that both of the charged Higgs bosons must be heavier than 410 GeV. If δ is varied or $\tan \beta$ is increased, this bound becomes lower. Note that we do not plot a direct search bound on the H^+ mass. In this model, the bound on the charged Higgs mass quoted by LEP does not apply, as explained in appendix I.

For completeness, we also write the contributions to δg^R , which are only signifi-

6.2 Models with Higgs multiplets larger than doublets

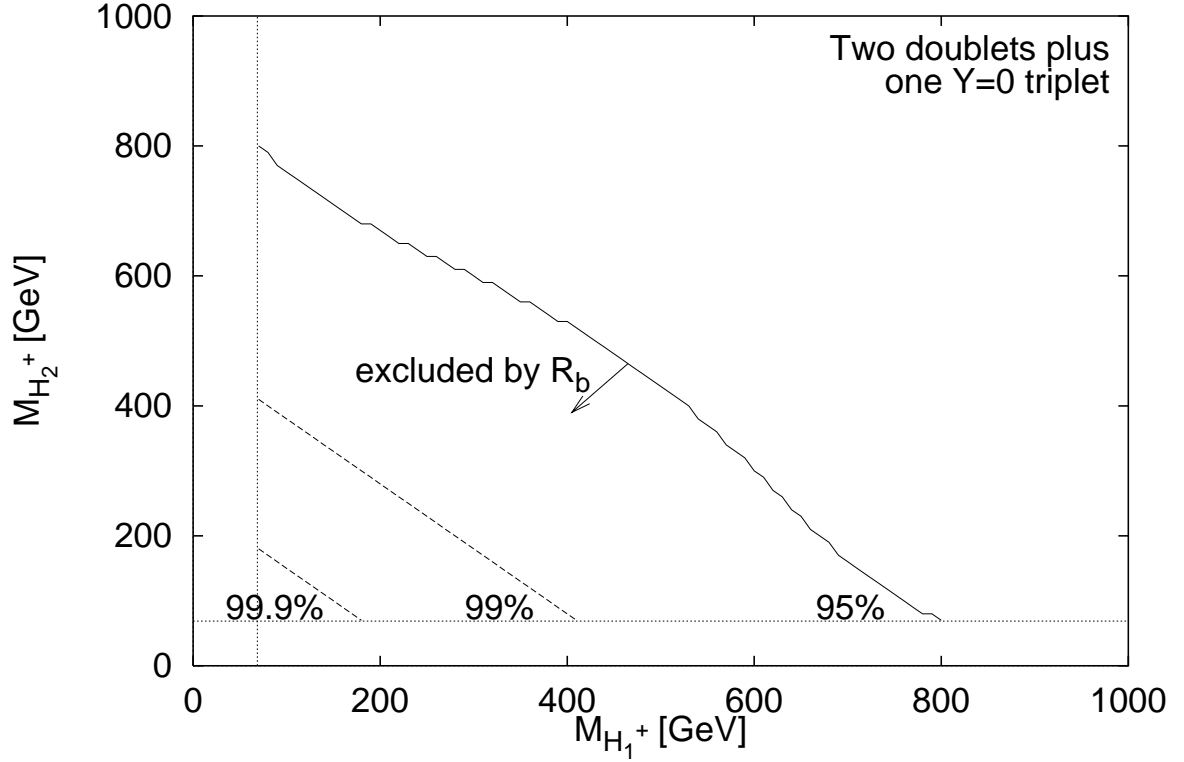


Figure 6.7:

Constraints from R_b on the masses of the two charged Higgs states H_1^+ and H_2^+ in the model with two doublets and one real $Y = 0$ triplet, with $\tan\beta = 1$ and $\delta = \pi/4$. The area below the solid line is excluded at 95% confidence level. Also shown are the 99% and 99.9% confidence levels (dashed). The dotted lines are the direct search bounds on the H^+ mass from the OPAL collaboration, $M_{H^+} > 68.7$ GeV [54], from LEP data up to $\sqrt{s} = 189$ GeV. (For a discussion of the direct search bound, see appendix I.)

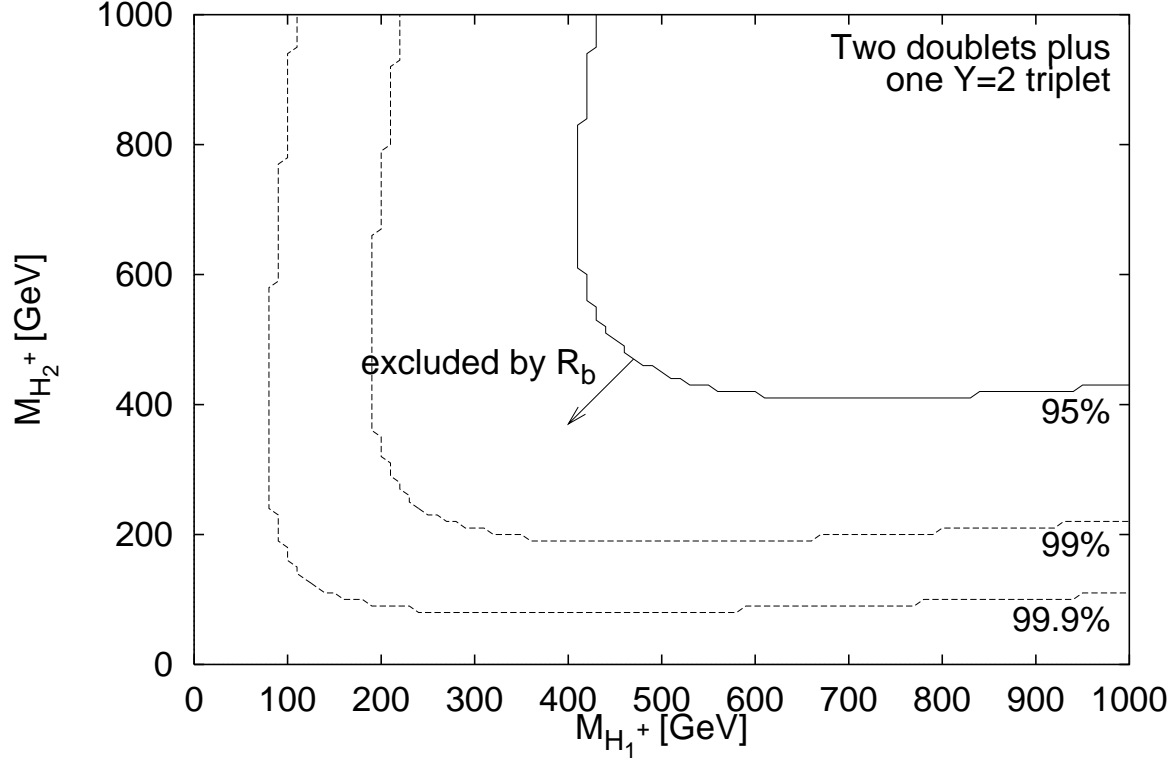


Figure 6.8: Constraints from R_b on the masses of the two charged Higgs states H_1^+ and H_2^+ in the model with two doublets and one complex $Y = 2$ triplet, with $\tan\beta = 1$ and $\delta = \pi/4$. The area below the solid line is excluded at 95% confidence level. For these values of $\tan\beta$ and δ , H^+ masses below 410 GeV are ruled out. Also shown are the 99% and 99.9% confidence levels (dashed).

6.2 Models with Higgs multiplets larger than doublets

cant at large $\tan \beta$. For both the Type I and Type II models, they are,

$$\begin{aligned} \delta g^R \simeq & -\frac{1}{16\pi^2} \frac{1}{2} \frac{e}{s_W c_W} \left(\frac{gm_b}{\sqrt{2}M_W} \right)^2 \tan^2 \beta \\ & \times \left[\sin^2 \delta \left[\frac{R_1}{R_1 - 1} - \frac{R_1 \log R_1}{(R_1 - 1)^2} \right] + \cos^2 \delta \left[\frac{R_2}{R_2 - 1} - \frac{R_2 \log R_2}{(R_2 - 1)^2} \right] \right] \\ & - \frac{\epsilon}{16\pi^2} \frac{e}{s_W c_W} \left(\frac{gm_b}{\sqrt{2}M_W} \right)^2 \tan^2 \beta \sin^2 \delta \cos^2 \delta \left[C_{24}(m_t^2, M_{H_1^+}^2, M_{H_1^+}^2) \right. \\ & \left. + C_{24}(m_t^2, M_{H_2^+}^2, M_{H_2^+}^2) - 2C_{24}(m_t^2, M_{H_1^+}^2, M_{H_2^+}^2) \right], \end{aligned} \quad (6.66)$$

where again $\epsilon = +1$ in the $Y = 0$ model and $\epsilon = -1$ in the $Y = 2$ model. The first term of equation 6.66 is the same as the correction in a 3HDM. The second term comes from the effects of the triplet.

Neutral Higgs boson contributions

Now let us consider the contributions to $Z \rightarrow b\bar{b}$ from neutral Higgs boson exchange in these models. The corrections can only be significant in the Type II models when $\tan \beta$ is large. For this reason, we disregard the Type I models here.

The real triplet with $Y = 0$ has no CP-odd neutral component, so there is no $Z\xi^0 A^0$ coupling. For this reason, ξ^0 has the same couplings as a Higgs singlet. (The neutral Higgs couplings for this model are listed in appendix D.) The corrections from neutral Higgs boson exchange in the $Y = 0$ model thus have the same form as in a model containing two doublets and a real singlet with $Y = 0$. Models of this type were discussed in section 6.1.2.

In the $Y = 2$ model, the triplet has both a CP-even and a CP-odd neutral component, and there is a nonzero $Z\chi^{0,r}\chi^{0,i}$ coupling. The neutral Higgs states and couplings in this model are listed in appendix D. We find that the contributions of the neutral Higgs bosons in this model can be split into two pieces. The first piece is the same as the contribution in a 3HDM, in which the neutral Higgs states are given by equations D.104, D.107–D.108, and D.111–D.113, but with the triplet states $\chi^{0,r}$ and $\chi^{0,i}$ replaced by the neutral states of the third doublet. This piece is denoted by $\delta g_{3\text{HDM}}^{R,L}$. The second piece contains the additional contribution due to the effects of the isospin and hypercharge of the triplet, and is denoted $\delta g_{\text{triplet}}^{R,L}$. That is,

$$\delta g^{R,L} = \delta g_{3\text{HDM}}^{R,L} + \delta g_{\text{triplet}}^{R,L}. \quad (6.67)$$

We calculate the contributions to $\delta g^{L,R}$ in the limit of large $\tan \theta_2$. In this limit, the contributions to $\delta g^{L,R}$ are as follows. The mixing angles α , γ , and ω , which parameterize

the mixing of the neutral states, are defined in appendix D. They depend on the details of the Higgs potential. The contribution in the 3HDM is,

$$\begin{aligned}
\delta g_{3\text{HDM}}^{R,L}(a) &\simeq \mp \frac{1}{16\pi^2} \frac{e}{s_W c_W} \left(\frac{gm_b}{\sqrt{2}M_W} \right)^2 \tan^2 \beta \\
&\times \left[-\cos \gamma \cos \alpha \sin \omega (\cos \gamma \cos \alpha \sin \omega + \sin \gamma \cos \omega) C_{24}(m_b^2, M_{H_1^0}^2, M_{A_1^0}^2) \right. \\
&+ \sin \gamma \cos \alpha \sin \omega (-\sin \gamma \cos \alpha \sin \omega + \cos \gamma \cos \omega) C_{24}(m_b^2, M_{H_2^0}^2, M_{A_1^0}^2) \\
&- \sin^2 \alpha \sin^2 \omega C_{24}(m_b^2, M_{H_3^0}^2, M_{A_1^0}^2) \\
&- \cos \gamma \cos \alpha \cos \omega (\cos \gamma \cos \alpha \cos \omega - \sin \gamma \sin \omega) C_{24}(m_b^2, M_{H_1^0}^2, M_{A_2^0}^2) \\
&+ \sin \gamma \cos \alpha \cos \omega (-\sin \gamma \cos \alpha \cos \omega - \cos \gamma \sin \omega) C_{24}(m_b^2, M_{H_2^0}^2, M_{A_2^0}^2) \\
&\left. - \sin^2 \alpha \cos^2 \omega C_{24}(m_b^2, M_{H_3^0}^2, M_{A_2^0}^2) \right] \quad (6.68)
\end{aligned}$$

$$\begin{aligned}
\delta g_{3\text{HDM}}^{R,L}(b) &\simeq -\frac{1}{16\pi^2} g_{Zb\bar{b}}^{L,R} \frac{1}{2} \left(\frac{gm_b}{\sqrt{2}M_W} \right)^2 \tan^2 \beta \\
&\times \left[\cos^2 \gamma \cos^2 \alpha \left(-2C_{24} + \frac{1}{2} - M_Z^2(C_{22} - C_{23}) \right) (M_{H_1^0}^2, m_b^2, m_b^2) \right. \\
&+ \sin^2 \gamma \cos^2 \alpha \left(-2C_{24} + \frac{1}{2} - M_Z^2(C_{22} - C_{23}) \right) (M_{H_2^0}^2, m_b^2, m_b^2) \\
&+ \sin^2 \alpha \left(-2C_{24} + \frac{1}{2} - M_Z^2(C_{22} - C_{23}) \right) (M_{H_3^0}^2, m_b^2, m_b^2) \\
&+ \sin^2 \omega \left(-2C_{24} + \frac{1}{2} - M_Z^2(C_{22} - C_{23}) \right) (M_{A_1^0}^2, m_b^2, m_b^2) \\
&\left. + \cos^2 \omega \left(-2C_{24} + \frac{1}{2} - M_Z^2(C_{22} - C_{23}) \right) (M_{A_2^0}^2, m_b^2, m_b^2) \right] \quad (6.69)
\end{aligned}$$

$$\begin{aligned}
\delta g_{3\text{HDM}}^{R,L}(c) &\simeq \frac{1}{16\pi^2} g_{Zb\bar{b}}^{R,L} \frac{1}{2} \left(\frac{gm_b}{\sqrt{2}M_W} \right)^2 \tan^2 \beta \\
&\times \left[\cos^2 \gamma \cos^2 \alpha B_1(m_b^2; m_b^2, M_{H_1^0}^2) + \sin^2 \gamma \cos^2 \alpha B_1(m_b^2; m_b^2, M_{H_2^0}^2) \right. \\
&+ \sin^2 \alpha B_1(m_b^2; m_b^2, M_{H_3^0}^2) + \sin^2 \omega B_1(m_b^2; m_b^2, M_{A_1^0}^2) \\
&\left. + \cos^2 \omega B_1(m_b^2; m_b^2, M_{A_2^0}^2) \right]. \quad (6.70)
\end{aligned}$$

The additional contribution due to the effects of the triplet is,

$$\begin{aligned}
\delta g_{\text{triplet}}^{R,L} &\simeq \pm \frac{1}{16\pi^2} \frac{e}{s_W c_W} \left(\frac{gm_b}{\sqrt{2}M_W} \right)^2 \tan^2 \beta \cos \alpha \cos \gamma \sin \gamma \cos \omega \sin \omega \\
&\times \left[C_{24}(m_b^2, M_{H_1^0}^2, M_{A_1^0}^2) + C_{24}(m_b^2, M_{H_2^0}^2, M_{A_2^0}^2) \right]
\end{aligned}$$

6.2 Models with Higgs multiplets larger than doublets

$$-C_{24}(m_b^2, M_{H_1^0}^2, M_{A_2^0}^2) - C_{24}(m_b^2, M_{H_2^0}^2, M_{A_1^0}^2) \Big]. \quad (6.71)$$

Note that $\delta g_{\text{triplet}}^{R,L}$ is only significant near maximal doublet–triplet mixing in both the CP–odd and CP–even sectors, which occurs when ω and γ are both near $\pm\pi/4$. In addition, $\delta g_{\text{triplet}}^{R,L}$ is zero if $M_{H_1^0} = M_{H_2^0}$ or $M_{A_1^0} = M_{A_2^0}$. Its sign depends on the mixing angles and the Higgs masses. For all the neutral Higgs bosons lighter than about 200 GeV and maximal doublet–triplet mixing, the contribution to R_b from $\delta g_{\text{triplet}}^{R,L}$ is smaller than the contribution to R_b from $\delta g_{3\text{HDM}}^{R,L}$ over most of the parameter space. The contribution to R_b from $\delta g_{3\text{HDM}}^{R,L}$ is of the same order of magnitude as the contribution to R_b from the neutral sector of the 2HDM.

6.2.3 Georgi–Machacek model with $\text{SU}(2)_c$ symmetry

In order to obtain $\rho = 1$ at tree level the electroweak symmetry breaking must preserve a “custodial” $\text{SU}(2)$ symmetry, called $\text{SU}(2)_c$, that ensures equal masses are given to the W^\pm and W^3 . We refer to models with this property as Georgi–Machacek models, after the extended model of this type with Higgs triplets created by Georgi and Machacek [42]. This class of models, and in particular the triplet Georgi–Machacek model, is described in detail in appendix E, which also contains details on the $\text{SU}(2)_L \times \text{SU}(2)_R$ transformations and how $\text{SU}(2)_c$ is preserved after electroweak symmetry breaking. In appendix E we also explain how models that preserve $\text{SU}(2)_c$ automatically lead to $\rho = 1$ at tree level, and derive certain Higgs couplings to fermions and gauge bosons in a general Georgi–Machacek model.

The triplet Georgi–Machacek model contains a complex $Y = 1$ doublet Φ , a real $Y = 0$ triplet ξ , and a complex $Y = 2$ triplet χ . The Higgs fields take the form

$$\Phi = \begin{pmatrix} \phi^{0*} & \phi^+ \\ -\phi^{+*} & \phi^0 \end{pmatrix} \quad (6.72)$$

$$\chi = \begin{pmatrix} \chi^{0*} & \xi^+ & \chi^{++} \\ -\chi^{+*} & \xi^0 & \chi^+ \\ \chi^{++*} & \xi^- & \chi^0 \end{pmatrix} \quad (6.73)$$

where $\xi^- = -(\xi^+)^*$, which transform under $\text{SU}(2)_L \times \text{SU}(2)_R$ as $(1/2, 1/2)$ and $(1, 1)$ representations, respectively. The electroweak symmetry breaking preserves $\text{SU}(2)_c$ when the vevs of the fields are diagonal, $\langle \chi \rangle = v_\chi \mathbf{I}$ and $\langle \phi^0 \rangle = (v_\phi/\sqrt{2})\mathbf{I}$, where \mathbf{I} is the unit matrix.

Under the electroweak symmetry breaking, the $\text{SU}(2)_L \times \text{SU}(2)_R$ symmetry is broken down to $\text{SU}(2)_c$. A representation (T, T) of $\text{SU}(2)_L \times \text{SU}(2)_R$ decomposes into a set of representations of $\text{SU}(2)_c$, in particular, $2T \oplus 2T - 1 \oplus \cdots \oplus 1 \oplus 0$. In the triplet

Georgi–Machacek model, Φ breaks down to a triplet and a singlet of $SU(2)_c$, and χ breaks down to a fiveplet, a triplet, and a singlet of $SU(2)_c$. The W^\pm and Z bosons are given mass by absorbing the $SU(2)_c$ triplet of Goldstone bosons, $G_3^{+,0,-}$. The remaining physical states are a fiveplet $H_5^{++,+,0,-,-}$, a threeplet $H_3^{+,0,-}$, and two singlets H_1^0 and H_1^0 . If the Higgs potential is chosen to preserve $SU(2)_c$, then states transforming in different representations of $SU(2)_c$ cannot mix, and the states in each representation are degenerate.

This model contains only one doublet Φ which gives mass to both the top- and bottom-type quarks. Therefore it is a Type I model and $\lambda_b \ll \lambda_t$. Thus the only sizeable correction to the $Zb\bar{b}$ vertex in this model will come from the left-handed charged Higgs boson loops.

The two singly-charged Higgs bosons and G^+ can be written in terms of the combinations of triplet fields

$$\psi^+ = \frac{1}{\sqrt{2}}(\chi^+ - \xi^+), \quad (6.74)$$

which transforms in a triplet of $SU(2)_c$, and

$$\zeta^+ = \frac{1}{\sqrt{2}}(\chi^+ + \xi^+), \quad (6.75)$$

which transforms in a fiveplet of $SU(2)_c$. We denote the ratio of the vevs of χ and ϕ as

$$\tan \theta_H \equiv \frac{2\sqrt{2}v_\chi}{v_\phi}. \quad (6.76)$$

Then in terms of the sine and cosine of this angle, denoted by s_H and c_H , the singly charged Higgs bosons are

$$G_3^+ = c_H \phi^+ + s_H \psi^+, \quad (6.77)$$

$$H_3^+ = -s_H \phi^+ + c_H \psi^+, \quad (6.78)$$

$$H_5^+ = \zeta^+. \quad (6.79)$$

If the Higgs potential is chosen to preserve $SU(2)_c$ then H_3^+ and H_5^+ are mass eigenstates because they transform in different representations of $SU(2)_c$ [43]. Such a potential is desirable because it preserves $SU(2)_c$ (and $\rho = 1$) to all orders in the Higgs self-couplings. However, renormalization of the parameters in the Higgs potential at the one loop level introduces quadratically divergent terms that break $SU(2)_c$ [45]. These terms lead to quadratically divergent contributions to the ρ parameter and to the mixing of some of the Higgs states, including H_3^+ and H_5^+ . In order to cancel the divergent corrections, $SU(2)_c$ -breaking counterterms must be introduced in the bare Lagrangian and fine-tuned to restore $\rho \approx 1$. These $SU(2)_c$ -violating corrections arise at the two-loop level in R_b , so they will be neglected here.

6.2 Models with Higgs multiplets larger than doublets

The couplings in this model have been given in [44,11]. We have also derived them in appendix E for a general Georgi–Machacek model containing one multiplet $\Phi = (1/2, 1/2)$ and one larger multiplet $X = (T, T)$. The doublet field Φ is the only field with quark Yukawa couplings. Under $SU(2)_c$ the doublet decomposes into a singlet and a triplet. Thus only $SU(2)_c$ singlets and triplets can contain a doublet admixture and couple to quarks. This is a general feature of any model whose Higgs sector obeys a custodial $SU(2)_c$ symmetry. In the triplet Georgi–Machacek model the charged Higgs couplings to quarks are,

$$g_{G^+ \bar{t} b}^L = \frac{gm_t}{\sqrt{2}M_W} \quad (6.80)$$

$$g_{H_3^+ \bar{t} b}^L = \frac{-gm_t}{\sqrt{2}M_W} \tan \theta_H \quad (6.81)$$

$$g_{H_5^+ \bar{t} b}^L = 0. \quad (6.82)$$

These couplings also hold in a general Georgi–Machacek model containing $\Phi = (1/2, 1/2)$ and $X = (T, T)$, if $\tan \theta_H$ is defined as

$$\tan \theta_H = \frac{v_X \sqrt{\frac{4}{3}T(T+1)(2T+1)}}{v_\phi}. \quad (6.83)$$

The loop corrections to R_b will only involve the charged Higgs states that appear in the triplet representations of $SU(2)_c$; namely, H_3^+ and G^+ .

The relevant ZH^+H^- couplings for charged Higgs bosons in a triplet of $SU(2)_c$ are given below, for any model which preserves $SU(2)_c$.

$$g_{ZG^+G^-} = \frac{-e}{s_W c_W} \left(\frac{1}{2} - s_W^2 \right) \quad (6.84)$$

$$g_{ZG^+H_3^-} = 0 \quad (6.85)$$

$$g_{ZH_3^+H_3^-} = \frac{-e}{s_W c_W} \left(\frac{1}{2} - s_W^2 \right), \quad (6.86)$$

as we show in appendix E. The loop corrections to R_b involving H^+ are particularly simple because the $ZG^+H_3^-$ coupling is zero.

In any model which preserves $SU(2)_c$ and contains only two multiplets Φ and X , the correction to δg^L is, in addition to the SM correction due to the charged Goldstone loops,

$$\delta g^L = \frac{1}{16\pi^2} \left(\frac{gm_t}{\sqrt{2}M_W} \right)^2 \tan^2 \theta_H \frac{1}{2} \frac{e}{s_W c_W} \left[\frac{R}{R-1} - \frac{R \log R}{(R-1)^2} \right] \quad (6.87)$$

from loops involving H_3^+ , where $R \equiv m_t^2/M_{H_3^+}^2$. This correction is positive definite and has the same form as the correction in the 2HDM (equation 6.1).

In general for a model with custodial $SU(2)_c$ and more than one exotic multiplet X , the correction becomes

$$\delta g^L = \sum_{H_{3i}^+} \frac{1}{16\pi^2} (g_{H_{3i}^+ \bar{t} b}^L)^2 \frac{1}{2} \frac{e}{s_W c_W} \left[\frac{R_i}{R_i - 1} - \frac{R_i \log R_i}{(R_i - 1)^2} \right], \quad (6.88)$$

which is positive definite. Thus when the Higgs potential is invariant under $SU(2)_c$, the corrections always decrease R_b .

As in the 2HDM, the R_b measurement can be used to set a lower bound on the mass of the $SU(2)_c$ triplet H_3 , which varies with $\tan \theta_H$. This bound is independent of the isospin of the exotic $SU(2)_L \times SU(2)_R$ multiplet X (or χ in the triplet Georgi–Machacek model). In figure 6.9 we plot the bound on M_{H_3} as a function of $\tan \theta_H$.

For H_3 lighter than about 1 TeV, the R_b measurement puts an upper limit on $\tan \theta_H$, $\tan \theta_H < 2.0$. In the triplet Georgi–Machacek model, this corresponds to an upper limit on the triplet vev of $v_\chi/v_\phi < 0.7$. As in the Type I 2HDM, the charged Higgs boson contribution to $b \rightarrow s\gamma$ is small compared to the contribution in the Type II 2HDM [57], and the $b \rightarrow s\gamma$ measurement does not provide additional bounds on the parameter space.

In most of the region allowed by R_b , $0.9345 < A_b < 0.935$. There is a small region of larger A_b , up to 0.937, for $\tan \theta_H$ very small.

Higgs potential without $SU(2)_c$ invariance

If the requirement of $SU(2)_c$ symmetry is relaxed, it is no longer meaningful to write the Higgs fields in $SU(2)_L \times SU(2)_R$ matrices. In the triplet model we must define the vevs of the two $SU(2)_L$ triplets separately, $\langle \chi^0 \rangle = v_\chi$, and $\langle \xi^0 \rangle = v_\xi$. Then $SU(2)_c$ symmetry corresponds to $v_\chi = v_\xi$. The triplet model can still satisfy $\rho = 1$ if the Higgs potential is fine-tuned so that $v_\chi = v_\xi$. In this situation the two physical charged Higgs bosons H_3^+ and H_5^+ can mix with each other. If we parameterize this mixing with an angle α , the new mass eigenstates are

$$H_1^+ = \sin \alpha H_3^+ + \cos \alpha H_5^+ \quad (6.89)$$

$$H_2^+ = \cos \alpha H_3^+ - \sin \alpha H_5^+ \quad (6.90)$$

and their couplings to the Z and quark pairs are

$$g_{H_1^+ \bar{t} b}^L = \frac{gm_t}{\sqrt{2}M_W} \tan \theta_H \sin \alpha \quad (6.91)$$

$$g_{H_2^+ \bar{t} b}^L = \frac{gm_t}{\sqrt{2}M_W} \tan \theta_H \cos \alpha \quad (6.92)$$

6.2 Models with Higgs multiplets larger than doublets

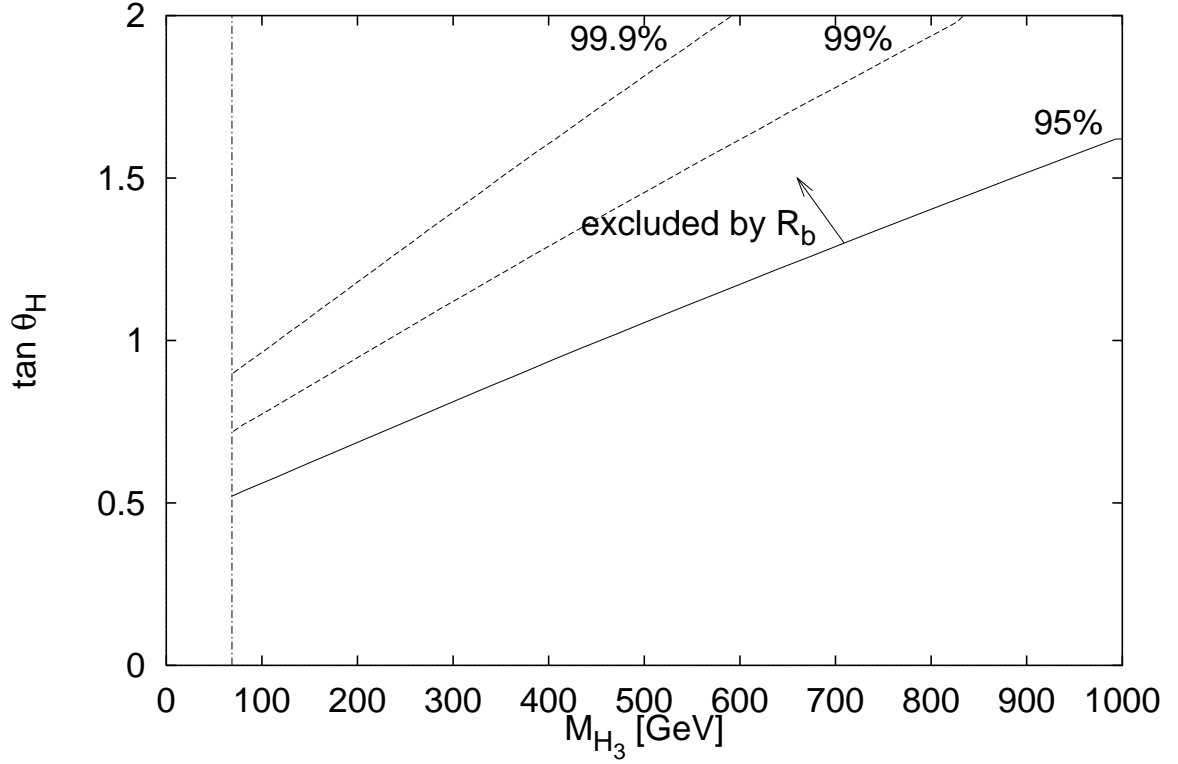


Figure 6.9: Bounds from R_b on the Georgi–Machacek model with Higgs triplets and $SU(2)_c$ symmetry. On the vertical axis we plot $\tan \theta_H$. On the horizontal axis we plot the mass of the $SU(2)_c$ triplet H_3^\pm, H_3^0 . The area above the solid line is ruled out at 95% confidence level by R_b . Also shown (top to bottom) are the 99.9%, 99% and 68% confidence level contours (dashed). The dot-dashed line is the direct search bound on the charged Higgs mass from the OPAL collaboration, $M_{H^\pm} > 68.7$ GeV [54], from LEP data up to $\sqrt{s} = 189$ GeV. (For a discussion of the direct search bound, see appendix I.)

$$g_{ZG^+H_1^-} = \frac{-e}{s_W c_W} \frac{1}{2} s_H \cos \alpha \quad (6.93)$$

$$g_{ZG^+H_2^-} = \frac{e}{s_W c_W} \frac{1}{2} s_H \sin \alpha \quad (6.94)$$

$$g_{ZH_1^+H_1^-} = \frac{-e}{s_W c_W} \left(\frac{1}{2} - s_W^2 - c_H \sin \alpha \cos \alpha \right) \quad (6.95)$$

$$g_{ZH_1^+H_2^-} = \frac{-e}{s_W c_W} \frac{1}{2} c_H (\sin^2 \alpha - \cos^2 \alpha) \quad (6.96)$$

$$g_{ZH_2^+H_2^-} = \frac{-e}{s_W c_W} \left(\frac{1}{2} - s_W^2 + c_H \sin \alpha \cos \alpha \right). \quad (6.97)$$

Now both of the singly charged Higgs bosons couple to quarks instead of just one. There are now off-diagonal $ZH_i^+H_j^-$ couplings with $i \neq j$ and non-SM-like terms in the diagonal couplings which contribute to δg^L .

The correction is

$$\begin{aligned} \delta g_{H^+}^L &= \delta g_{G^+}^L(SM) \\ &+ \frac{1}{16\pi^2} \frac{1}{2} \frac{e}{s_W c_W} \left(\frac{gm_t}{\sqrt{2}M_W} \right)^2 \tan^2 \theta_H \left\{ \sin^2 \alpha \left[\frac{R_1}{R_1 - 1} - \frac{R_1 \log R_1}{(R_1 - 1)^2} \right] \right. \\ &\quad \left. + \cos^2 \alpha \left[\frac{R_2}{R_2 - 1} - \frac{R_2 \log R_2}{(R_2 - 1)^2} \right] \right\} \\ &+ \frac{1}{16\pi^2} \left(\frac{e}{s_W c_W} \right) \left(\frac{gm_t}{\sqrt{2}M_W} \right)^2 \tan^2 \theta_H \times 2c_H \sin \alpha \cos \alpha \\ &\quad \times \left\{ C_{24}(m_t^2, M_W^2, M_2^2) - C_{24}(m_t^2, M_W^2, M_1^2) \right. \\ &\quad \left. + \sin^2 \alpha [C_{24}(m_t^2, M_1^2, M_1^2) - C_{24}(m_t^2, M_1^2, M_2^2)] \right. \\ &\quad \left. + \cos^2 \alpha [C_{24}(m_t^2, M_1^2, M_2^2) - C_{24}(m_t^2, M_2^2, M_2^2)] \right\}, \end{aligned} \quad (6.98)$$

where $R_i = m_t^2/M_i^2$. The first term is the SM correction due to G^+ . The second term is positive definite and has the same mass dependence as the charged Higgs boson correction in the 2HDM. The third term arises from the off-diagonal ZH^+H^- couplings and the non-SM parts of the diagonal ZH^+H^- couplings. This third term can be positive or negative, depending on the mixing angle α . It is negative for $M_{H_2^+} > M_{H_1^+}$ when $\sin \alpha \cos \alpha$ is positive, and grows with increasing splitting between $M_{H_1^+}$ and $M_{H_2^+}$ and between M_W and the charged Higgs masses.

This model is fine tuned to $v_\chi = v_\xi$ to give $\rho = 1$; when the parameters of the Higgs potential are renormalized this fine tuning will be lost. In order to satisfy the

6.2 Models with Higgs multiplets larger than doublets

experimental bounds on $\Delta\rho$ [5], we must have

$$-4.7 \times 10^{-3} < \Delta\rho = \frac{4(v_\xi^2 - v_\chi^2)}{v_\phi^2 + 8v_\chi^2} < 3.0 \times 10^{-3} \quad (6.99)$$

or $-(8.4\text{GeV})^2 < v_\xi^2 - v_\chi^2 < (6.7\text{GeV})^2$. For the model to be “natural” we require the parameters to be of the same order as their fine tuning, or $v_\chi \sim v_\xi \sim 8 \text{ GeV}$. Then $\tan\theta_H \sim 0.09$ and the correction in equation 6.98 is suppressed by a factor of $\tan^2\theta_H \sim 0.008$.

Chapter 7

Conclusions

Radiative corrections to the process $Z \rightarrow b\bar{b}$ arise in extended Higgs sectors due to the exchange of the additional singly-charged and neutral Higgs bosons in such models. Because the radiative corrections affect the predictions for R_b and A_b , the measurements of these quantities can in principle be used to constrain the parameter space of the models. The radiative corrections to R_b from extended Higgs sectors are typically of the same order of magnitude as the experimental error in the R_b measurement. Thus R_b can be used to constrain the models. However, the radiative corrections to A_b from extended Higgs sectors are much smaller than the experimental error in the A_b measurement. They are also much smaller than the deviation of the A_b measurement from the SM prediction. We conclude that if $A_b \neq A_b^{SM}$, the deviation does not arise from the contributions of an extended Higgs sector.

In this thesis we obtained general formulas for the corrections to the $Zb\bar{b}$ vertex, and then used the general formulas to calculate the contributions to R_b and A_b in specific models. Here we summarize our conclusions for the various models.

The contributions from neutral Higgs boson exchange are only significant in a Type II model with enhanced λ_b . The regions of parameter space in which the contribution to R_b from neutral Higgs boson exchange can be positive is almost ruled out by direct Higgs boson searches, as shown in figure 6.4. Otherwise, the contribution to R_b is negative, giving a worse agreement with experiment than the SM. A pair of neutral Higgs states, H^0 and A^0 , with a significant ZH^0A^0 coupling and a large mass splitting, gives a large negative contribution to R_b . The R_b measurement can then be used to exclude these regions of parameter space.

The contributions to R_b from charged Higgs boson exchange are negative in models which contain only doublets and singlets, and in any model whose Higgs sector

preserves $SU(2)_c$ symmetry. If the contributions from neutral Higgs boson exchange in these models are not significant (e.g., if λ_b is small), then R_b sets a lower bound on the masses of the charged Higgs states. The lower bound depends on λ_t and the charged Higgs mixing angles.

The contribution to R_b from charged Higgs boson exchange can only be positive if the model contains one of two features. It must either contain off-diagonal $ZH_i^+H_j^-$ couplings in which both of the charged Higgs bosons couple to quarks and have different masses, or it must contain diagonal $ZH_i^+H_i^-$ couplings which differ from the couplings in doublet models, or both. This can only happen in models which contain Higgs multiplets larger than doublets and are not constrained by $SU(2)_c$ symmetry. In such a model, the vevs of the multiplets larger than doublets must be very small in order for the model to be consistent with the measured value of the ρ parameter. With this constraint, the contribution to R_b can only be positive when the model contains more than one doublet and there is significant mixing between the doublets and the larger multiplets.

The precision of the R_b and A_b measurements is not likely to improve significantly in the near future. LEP is no longer running at the Z pole and most of LEP's Z pole data has been analyzed. SLD will soon stop taking data. Thus future constraints on extended Higgs sectors must come from other sources.

The ongoing direct search for Higgs bosons at LEP will discover an SM Higgs boson at the 5σ level if its mass is below 104 GeV, or exclude an SM Higgs boson at the 95% confidence level up to a mass of 108 GeV [58]. The upcoming search at the Tevatron Run 2 will have a significantly greater Higgs mass reach. With 10–30 fb^{-1} of data per detector, the Tevatron will discover an SM Higgs boson at the $3\text{--}5\sigma$ level if its mass is below 190 GeV. If there is no SM Higgs boson lighter than 190 GeV, the Tevatron will be able to exclude it at 95% confidence level with 10 fb^{-1} of data [59].

New virtual constraints on extended Higgs sectors will come from measurements of b quark decays at BaBar. For example, the processes $b \rightarrow s\gamma$ and $b \rightarrow sl^+l^-$ acquire radiative corrections from charged Higgs boson exchange. In addition, the process $b \rightarrow s\tau^+\tau^-$ receives a contribution from a neutral Higgs boson coupled to the $\tau^+\tau^-$ pair. The process $b \rightarrow c\tau\nu$ receives a contribution from tree-level charged Higgs boson exchange [60,61,62].

Appendix A

Tree-level $Zq\bar{q}$ couplings in the Standard Model

In this section we summarize our conventions for the tree-level couplings of Z to fermions. The tree-level $Zq\bar{q}$ vertex is,

$$-i\gamma_\mu(g_{Zq\bar{q}}^L P_L + g_{Zq\bar{q}}^R P_R) \quad (\text{A.1})$$

where $P_{R,L}$ are the right and left handed projection operators, $P_{R,L} = (1 \pm \gamma_5)/2$, and $g_{Zq\bar{q}}^{R,L}$ are the right and left handed $Zq\bar{q}$ couplings.

The tree-level $Zb\bar{b}$ and $Zt\bar{t}$ couplings in the SM are,

$$g_{Zb\bar{b}}^L = \frac{e}{s_W c_W} \left(-\frac{1}{2} + \frac{1}{3} s_W^2 \right) \quad (\text{A.2})$$

$$g_{Zb\bar{b}}^R = \frac{e}{s_W c_W} \left(\frac{1}{3} s_W^2 \right) \quad (\text{A.3})$$

$$g_{Zt\bar{t}}^L = \frac{e}{s_W c_W} \left(\frac{1}{2} - \frac{2}{3} s_W^2 \right) \quad (\text{A.4})$$

$$g_{Zt\bar{t}}^R = \frac{e}{s_W c_W} \left(-\frac{2}{3} s_W^2 \right). \quad (\text{A.5})$$

Appendix B

Higgs–Vector boson couplings

In this section we list general formulas for the couplings of Higgs bosons to vector bosons. These couplings come from the covariant derivatives in the kinetic terms for the Higgs bosons in the Lagrangian,

$$\mathcal{L} = (\mathcal{D}_\mu \Phi_k)^\dagger (\mathcal{D}^\mu \Phi_k) + \frac{1}{2} (\mathcal{D}_\mu \eta_i)^T (\mathcal{D}^\mu \eta_i), \quad (\text{B.1})$$

where the Φ_k are complex Higgs multiplets with isospin T_k and hypercharge Y_k , and the η_i are real Higgs multiplets with isospin T_i and hypercharge zero. The covariant derivative is

$$\mathcal{D}_\mu = \partial_\mu - igW_\mu^a T^a - ig' \frac{Y}{2} B_\mu \quad (\text{B.2})$$

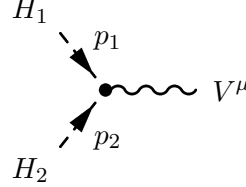
$$= \partial_\mu - i \frac{g}{\sqrt{2}} (W_\mu^+ T^+ + W_\mu^- T^-) - i \frac{g}{\cos \theta_W} Z_\mu (T^3 - \sin^2 \theta_W Q) - ieQ A_\mu \quad (\text{B.3})$$

where T^a are the SU(2) isospin generators, $Q = T^3 + Y/2$ is the electric charge in units of the positron charge, $T^\pm = (T^1 \pm iT^2)$, θ_W is the weak mixing angle given by $\tan \theta_W = g'/g$, and $e = gg'/\sqrt{g^2 + g'^2} = g \sin \theta_W$ is the electromagnetic coupling. The Higgs–Vector boson couplings are thus entirely determined by the SU(2) \times U(1) quantum numbers of the Higgs states and the mixing angles which determine the mass eigenstates.

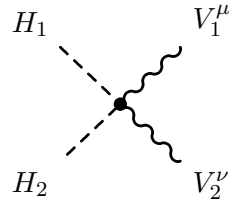
We list the Higgs–Vector boson couplings for electroweak eigenstates in sections B.1 and B.2 below. Section B.1 contains the coupling rules for complex Higgs representations, and section B.2 contains the coupling rules for real Higgs representations (with

hypercharge zero). Finally in section B.3 we list the formulas for the couplings of Higgs mass eigenstates in terms of the couplings of electroweak eigenstates.

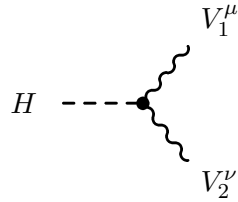
The couplings are defined as follows, with all particles incoming to the vertex:



$$= ig_{H_1 H_2 V} (p_1 - p_2)^\mu \quad (\text{B.4})$$



$$= ig_{H_1 H_2 V_1 V_2} g^{\mu\nu} \quad (\text{B.5})$$



$$= ig_{H V_1 V_2} g^{\mu\nu} \quad (\text{B.6})$$

The Higgs–Higgs–Vector (HHV) couplings come from the terms in the lagrangian involving two Higgs fields, one vector field and one partial derivative. The momentum dependence of the vertex comes from the partial derivative. Because of the momentum structure of the vertex, the coupling g_{HHV} is antisymmetric under interchange of the two Higgs fields.

The Higgs–Higgs–Vector–Vector (HHVV) couplings come from the terms in the lagrangian involving two Higgs fields and two vector fields.

The Higgs–Vector–Vector (HVV) couplings come from the terms in the lagrangian involving one Higgs field, one Higgs vev, and two vector fields. Therefore if a multiplet has zero vev, its members will have no HVV couplings. The HVV couplings can be immediately obtained from the HHVV couplings which involve the CP-even neutral Higgs boson $\phi^{0,r}$. This is done by replacing $\phi^{0,r}$ with $\phi^{0,r} + v$ in the lagrangian and keeping terms with one Higgs field and one vev. In order to conserve electric charge, the HVV couplings can only involve Higgs bosons of charge +2, +1, 0, -1, or -2.

We note also that in the electroweak basis, the HHV and HHVV couplings can only involve two Higgs bosons from the same multiplet.

B.1 Higgs–Vector couplings for complex Higgs representations

We use the Condon–Shortley phase convention for the $SU(2)$ generators T^\pm :

$$T^\pm |T, T^3\rangle = [(T \mp T^3)(T \pm T^3 + 1)]^{1/2} |T, T^3 \pm 1\rangle \quad (\text{B.7})$$

where $|T, T^3\rangle$ represents a state with isospin T and third component of isospin T^3 . The electric charge of a state is related to its hypercharge and third component of isospin by $Q = T^3 + Y/2$. Using this, we can write the couplings entirely in terms of the quantum numbers of the entire Higgs multiplet, Y and T , and the electric charge Q of the particular Higgs state involved.

B.1 Higgs–Vector couplings for complex Higgs representations

In this section we list the Higgs–Vector boson couplings for complex Higgs representations. We list separately the couplings involving neutral Higgs bosons and those involving only charged Higgs bosons because the neutral Higgs states must be separated into CP–even and CP–odd states.

Our notation is as follows. We denote the vev of the Higgs multiplet by v , where $\phi^0 = \frac{1}{\sqrt{2}}(\phi^{0,r} + v + i\phi^{0,i})$ and v is real. Using this notation, in the Standard Model $v = \frac{2M_W}{g} = 246$ GeV. We denote the complex conjugate of a Higgs state ϕ^Q of charge Q by $(\phi^Q)^*$. Note that $(\phi^Q)^*$ is a state of charge $-Q$, but differs from ϕ^{-Q} .

B.1.1 Higgs–Higgs–Vector couplings

In this section we list the HHV couplings, following the notation of equation B.4. We first list the couplings involving only charged Higgs bosons.

$$g_{\phi^Q(\phi^Q)^*\gamma} = -eQ \quad (\text{B.8})$$

$$g_{\phi^Q(\phi^Q)^*Z} = -\frac{g}{c_W} \left(c_W^2 Q - \frac{Y}{2} \right) \quad (\text{B.9})$$

$$g_{\phi^Q(\phi^{Q+1})^*W^+} = -\frac{g}{\sqrt{2}} \left[\left(T - \frac{Y}{2} + 1 + Q \right) \left(T + \frac{Y}{2} - Q \right) \right]^{1/2} \quad (\text{B.10})$$

Note that the W^- coupling can be obtained from equation B.10 by taking the hermitian conjugate of the Lagrangian. The couplings are related by,

$$g_{H_1^* H_2^* W^-} = -(g_{H_1 H_2 W^+})^*. \quad (\text{B.11})$$

Note that all the couplings are real except for those involving $\phi^{0,i}$. In this case,

$$g_{(\phi^Q)^*\phi^{Q+1}W^-} = +\frac{g}{\sqrt{2}} \left[\left(T - \frac{Y}{2} + 1 + Q \right) \left(T + \frac{Y}{2} - Q \right) \right]^{1/2}. \quad (\text{B.12})$$

We now list the couplings involving one or more neutral Higgs bosons. The neutral Higgs couplings to the photon are zero. Since the Z is CP-odd, it can only couple to one CP-even and one CP-odd Higgs boson:

$$g_{\phi^0, r \phi^0, i Z} = -\frac{ig}{c_W} \frac{Y}{2} \quad (\text{B.13})$$

The W –Higgs–Higgs couplings are,

$$g_{\phi^0, r(\phi^+)^* W^+} = -\frac{g}{2} \left[\left(T + \frac{Y}{2} \right) \left(T - \frac{Y}{2} + 1 \right) \right]^{1/2} \quad (\text{B.14})$$

$$g_{\phi^0, i(\phi^+)^* W^+} = -i\frac{g}{2} \left[\left(T + \frac{Y}{2} \right) \left(T - \frac{Y}{2} + 1 \right) \right]^{1/2} \quad (\text{B.15})$$

$$g_{\phi^-, \phi^0, r W^+} = -\frac{g}{2} \left[\left(T - \frac{Y}{2} \right) \left(T + \frac{Y}{2} + 1 \right) \right]^{1/2} \quad (\text{B.16})$$

$$g_{\phi^-, \phi^0, i W^+} = i\frac{g}{2} \left[\left(T - \frac{Y}{2} \right) \left(T + \frac{Y}{2} + 1 \right) \right]^{1/2} \quad (\text{B.17})$$

$$(\text{B.18})$$

Again, the W^- couplings are obtained by using equation B.11.

B.1.2 Higgs–Higgs–Vector–Vector couplings

In this section we list the HHVV couplings, following the notation of equation B.5. We first list the couplings involving only charged Higgs bosons.

$$g_{\phi^Q(\phi^Q)^* \gamma \gamma} = 2e^2 Q^2 \quad (\text{B.19})$$

$$g_{\phi^Q(\phi^Q)^* Z Z} = \frac{2g^2}{c_W^2} \left(c_W^2 Q - \frac{Y}{2} \right)^2 \quad (\text{B.20})$$

$$g_{\phi^Q(\phi^Q)^* Z \gamma} = \frac{2Qeg}{c_W} \left(c_W^2 Q - \frac{Y}{2} \right) \quad (\text{B.21})$$

$$g_{\phi^Q(\phi^Q)^* W^+ W^-} = g^2 \left[\left(T + \frac{Y}{2} - Q \right) \left(T - \frac{Y}{2} + Q \right) + T \right] \quad (\text{B.22})$$

$$\begin{aligned} g_{\phi^Q(\phi^{Q+2})^* W^+ W^+} &= g^2 \left[\left(T + \frac{Y}{2} - Q \right) \left(T - \frac{Y}{2} + Q + 1 \right) \right]^{1/2} \\ &\times \left[\left(T + \frac{Y}{2} - Q - 1 \right) \left(T - \frac{Y}{2} + Q + 2 \right) \right]^{1/2} \end{aligned} \quad (\text{B.23})$$

$$g_{\phi^Q(\phi^{Q+1})^* W^+ Z} = \frac{g^2}{\sqrt{2}c_W} (c_W^2 (2Q + 1) - Y)$$

B.1 Higgs–Vector couplings for complex Higgs representations

$$\times \left[\left(T + \frac{Y}{2} - Q \right) \left(T - \frac{Y}{2} + 1 + Q \right) \right]^{1/2} \quad (\text{B.24})$$

$$g_{\phi^Q(\phi^{Q+1})^*W+\gamma} = \frac{ge}{\sqrt{2}}(2Q+1) \left[\left(T + \frac{Y}{2} - Q \right) \left(T - \frac{Y}{2} + 1 + Q \right) \right]^{1/2} \quad (\text{B.25})$$

The Higgs coupling to W^- pairs can be obtained from equation B.23 using

$$g_{H_1^*H_2W^-W^-} = (g_{H_1H_2^*W^+W^+})^*, \quad (\text{B.26})$$

and the Higgs couplings to W^-V where $V = Z, \gamma$ can be obtained from equations B.24 and B.25 using

$$g_{H_1^*H_2W^-V} = (g_{H_1H_2^*W^+V})^*. \quad (\text{B.27})$$

We now list the couplings involving one or more neutral Higgs bosons. The neutral Higgs couplings to $\gamma\gamma$ and $Z\gamma$ are zero.

$$g_{\phi^0,r\phi^0,rZZ} = g_{\phi^0,i\phi^0,iZZ} = \frac{g^2}{c_W^2} \frac{Y^2}{2} \quad (\text{B.28})$$

$$g_{\phi^0,r\phi^0,iZZ} = 0 \quad (\text{B.29})$$

$$g_{\phi^0,r\phi^0,rW^+W^-} = g_{\phi^0,i\phi^0,iW^+W^-} = \frac{g^2}{2} \left[2T(T+1) - \frac{Y^2}{4} \right] \quad (\text{B.30})$$

$$g_{\phi^0,r(\phi^{+2})^*W^+W^+} = -ig_{\phi^0,i(\phi^{+2})^*W^+W^+} \quad (\text{B.31})$$

$$\begin{aligned} &= \frac{g^2}{\sqrt{2}} \left[\left(T + \frac{Y}{2} \right) \left(T - \frac{Y}{2} + 1 \right) \right]^{1/2} \\ &\times \left[\left(T + \frac{Y}{2} - 1 \right) \left(T - \frac{Y}{2} + 2 \right) \right]^{1/2} \end{aligned} \quad (\text{B.32})$$

$$g_{\phi^0,r\phi^{-2}W^+W^+} = ig_{\phi^0,i\phi^{-2}W^+W^+} \quad (\text{B.33})$$

$$\begin{aligned} &= \frac{g^2}{\sqrt{2}} \left[\left(T - \frac{Y}{2} \right) \left(T + \frac{Y}{2} + 1 \right) \right]^{1/2} \\ &\times \left[\left(T - \frac{Y}{2} - 1 \right) \left(T + \frac{Y}{2} + 2 \right) \right]^{1/2} \end{aligned} \quad (\text{B.34})$$

$$g_{\phi^0,r(\phi^+)^*W^+Z} = -ig_{\phi^0,i(\phi^+)^*W^+Z} \quad (\text{B.35})$$

$$= \frac{g^2}{2c_W} (c_W^2 - Y) \left[\left(T + \frac{Y}{2} \right) \left(T - \frac{Y}{2} + 1 \right) \right]^{1/2} \quad (\text{B.36})$$

$$g_{\phi^0,r\phi^-W^+Z} = ig_{\phi^0,i\phi^-W^+Z} \quad (\text{B.37})$$

$$= -\frac{g^2}{2c_W} (c_W^2 + Y) \left[\left(T - \frac{Y}{2} \right) \left(T + \frac{Y}{2} + 1 \right) \right]^{1/2} \quad (\text{B.38})$$

$$g_{\phi^{0,r}(\phi^+)^*W^+\gamma} = -ig_{\phi^{0,i}(\phi^+)^*W^+\gamma} \quad (\text{B.39})$$

$$= \frac{ge}{2} \left[\left(T + \frac{Y}{2} \right) \left(T - \frac{Y}{2} + 1 \right) \right]^{1/2} \quad (\text{B.40})$$

$$g_{\phi^{0,r}\phi^-W^+\gamma} = ig_{\phi^{0,i}\phi^-W^+\gamma} \quad (\text{B.41})$$

$$= -\frac{ge}{2} \left[\left(T - \frac{Y}{2} \right) \left(T + \frac{Y}{2} + 1 \right) \right]^{1/2} \quad (\text{B.42})$$

$$(\text{B.43})$$

The Higgs coupling to W^- pairs can be obtained from equations B.32 and B.34 using equation B.26 and remembering that $(\phi^{0,r})^* = \phi^{0,r}$ and $(\phi^{0,i})^* = \phi^{0,i}$. Similarly the Higgs couplings to W^-V where $V = Z, \gamma$ can be obtained from equations B.36 – B.42 using equation B.27.

B.1.3 Higgs–Vector–Vector couplings

In this section we list the HVV couplings, following the notation of equation B.6. The neutral Higgs couplings are,

$$g_{\phi^{0,r}ZZ} = \frac{g^2v}{c_W^2} \frac{Y^2}{2} \quad (\text{B.44})$$

$$g_{\phi^{0,r}W^+W^-} = g^2v \left(T(T+1) - \frac{Y^2}{4} \right). \quad (\text{B.45})$$

$\phi^{0,i}$ does not couple to gauge boson pairs.

The charged Higgs couplings are,

$$g_{\phi^+W^-Z} = \frac{g^2v}{2c_W}(c_W^2 - Y) \left[\left(T + \frac{Y}{2} \right) \left(T - \frac{Y}{2} + 1 \right) \right]^{1/2} \quad (\text{B.46})$$

$$g_{\phi^+W^-\gamma} = \frac{egv}{2} \left[\left(T + \frac{Y}{2} \right) \left(T - \frac{Y}{2} + 1 \right) \right]^{1/2} \quad (\text{B.47})$$

$$g_{\phi^-W^+Z} = -\frac{g^2v}{2c_W}(c_W^2 + Y) \left[\left(T - \frac{Y}{2} \right) \left(T + \frac{Y}{2} + 1 \right) \right]^{1/2} \quad (\text{B.48})$$

$$g_{\phi^-W^+\gamma} = -\frac{egv}{2} \left[\left(T - \frac{Y}{2} \right) \left(T + \frac{Y}{2} + 1 \right) \right]^{1/2} \quad (\text{B.49})$$

$$\begin{aligned} g_{\phi^{\pm 2}W^-W^-} &= \frac{g^2v}{\sqrt{2}} \left[\left(T - \frac{Y}{2} + 2 \right) \left(T + \frac{Y}{2} - 1 \right) \right]^{1/2} \\ &\times \left[\left(T - \frac{Y}{2} + 1 \right) \left(T + \frac{Y}{2} \right) \right]^{1/2} \end{aligned} \quad (\text{B.50})$$

B.2 Higgs–Vector couplings for real, $Y = 0$ Higgs representations

$$g_{\phi^{-2}W^+W^+} = \frac{g^2 v}{\sqrt{2}} \left[\left(T + \frac{Y}{2} + 2 \right) \left(T - \frac{Y}{2} - 1 \right) \right]^{1/2} \times \left[\left(T + \frac{Y}{2} + 1 \right) \left(T - \frac{Y}{2} \right) \right]^{1/2} \quad (\text{B.51})$$

$$(\text{B.52})$$

The couplings for the conjugate Higgs states $(\phi^Q)^*$ are obtained using the following equations ($V = Z, \gamma$),

$$g_{(H^\pm)^*W^\pm V} = (g_{H^\pm W^\mp V})^* \quad (\text{B.53})$$

$$g_{(H^{\pm 2})^*W^\pm W^\pm} = (g_{H^{\pm 2}W^\mp W^\mp})^*. \quad (\text{B.54})$$

B.2 Higgs–Vector couplings for real, $Y = 0$ Higgs representations

In this section we list the Higgs–Vector boson couplings for real Higgs representations. We consider only real representations with $Y = 0$ so that each electrically charged Higgs boson has an antiparticle of opposite charge.

Our notation is as follows. The real Higgs representation is denoted by η . We denote the vev of the Higgs multiplet by v , where $\eta^0 \rightarrow \eta^0 + v$, and v is real.

The complex conjugate of a Higgs state η^Q is related to the state of opposite charge by $(\eta^Q)^* = \epsilon_Q \eta^{-Q}$ where $\epsilon_Q = (-1)^Q$. This relation is derived in section B.2.4. We list the Higgs–Vector boson couplings for two incoming Higgs bosons, η^Q and $\eta^{Q'}$. Note that an incoming η^Q corresponds to an outgoing $(\eta^Q)^* = \epsilon_Q \eta^{-Q}$. This will be important for finding the correct sign of diagrams involving a Higgs state that couples to vector bosons at both ends.

The Higgs–Vector couplings for a real Higgs representation will differ from the couplings for a complex representation because of the phase relation between $(\eta^Q)^*$ and η^{-Q} . The Higgs–Vector–Vector couplings will also differ because of the different normalization of the vev of a real representation.

B.2.1 Higgs–Higgs–Vector couplings

In this section we list the HHV couplings, following the notation of equation B.4.

$$g_{\eta^Q \eta^{-Q} \gamma} = -\epsilon_Q e Q \quad (\text{B.55})$$

$$g_{\eta^Q \eta^{-Q} Z} = -\epsilon_Q g_{CW}^Q \quad (\text{B.56})$$

$$g_{\eta^Q \eta^{-Q-1} W^+} = \epsilon_Q \frac{g}{\sqrt{2}} [(T - Q)(T + Q + 1)]^{1/2} \quad (\text{B.57})$$

$$g_{\eta^Q \eta^{-Q+1} W^-} = \epsilon_Q \frac{g}{\sqrt{2}} [(T+Q)(T-Q+1)]^{1/2} \quad (\text{B.58})$$

These couplings are related to the couplings for complex Higgs representations given in section B.1.1 as follows. Using $\eta^Q = \epsilon_Q (\eta^{-Q})^*$, $(\epsilon_Q)^2 = 1$, and $\epsilon_Q \epsilon_{Q+1} = -1$,

$$g_{\eta^Q (\eta^Q)^* \gamma} = \epsilon_Q g_{\eta^Q \eta^{-Q} \gamma} = -eQ \quad (\text{B.59})$$

$$g_{\eta^Q (\eta^Q)^* Z} = \epsilon_Q g_{\eta^Q \eta^{-Q} Z} = -g_{CW} Q \quad (\text{B.60})$$

$$\begin{aligned} g_{\eta^Q (\eta^{Q+1})^* W^+} &= \epsilon_{Q+1} g_{\eta^Q \eta^{-Q-1} W^+} \\ &= -\frac{g}{\sqrt{2}} [(T-Q)(T+Q+1)]^{1/2} \end{aligned} \quad (\text{B.61})$$

$$g_{(\eta^Q)^* \eta^{Q+1} W^-} = \epsilon_Q g_{\eta^{-Q} \eta^{Q+1} W^-} = \frac{g}{\sqrt{2}} [(T-Q)(T+Q+1)]^{1/2} \quad (\text{B.62})$$

which are the same as the corresponding couplings for a complex Higgs representation, with $Y = 0$.

Note that the W^+ and W^- couplings are related by

$$g_{\eta^Q \eta^{-Q-1} W^+} = g_{\eta^{-Q} \eta^{Q+1} W^-} \quad (\text{B.63})$$

$$= -(g_{(\eta^Q)^* (\eta^{-Q-1})^* W^-})^*, \quad (\text{B.64})$$

just as for a complex representation.

B.2.2 Higgs–Higgs–Vector–Vector couplings

In this section we list the HHVV couplings, following the notation of equation B.5.

$$g_{\eta^Q \eta^{-Q} \gamma \gamma} = 2\epsilon_Q e^2 Q^2 \quad (\text{B.65})$$

$$g_{\eta^Q \eta^{-Q} Z Z} = 2\epsilon_Q g^2 c_W^2 Q^2 \quad (\text{B.66})$$

$$g_{\eta^Q \eta^{-Q} Z \gamma} = 2\epsilon_Q e g_{CW} Q^2 \quad (\text{B.67})$$

$$g_{\eta^Q \eta^{-Q} W^+ W^-} = \epsilon_Q g^2 [T(T+1) - Q^2] \quad (\text{B.68})$$

$$\begin{aligned} g_{\eta^Q \eta^{-Q-2} W^+ W^+} &= \epsilon_Q g^2 [(T-Q)(T+Q+1)]^{1/2} \\ &\quad \times [(T-Q-1)(T+Q+2)]^{1/2} \end{aligned} \quad (\text{B.69})$$

$$g_{\eta^Q \eta^{-Q-1} W^+ Z} = -\epsilon_Q \frac{g^2}{\sqrt{2}} c_W (2Q+1) [(T-Q)(T+Q+1)]^{1/2} \quad (\text{B.70})$$

$$g_{\eta^Q \eta^{-Q-1} W^+ \gamma} = -\epsilon_Q \frac{ge}{\sqrt{2}} (2Q+1) [(T-Q)(T+Q+1)]^{1/2} \quad (\text{B.71})$$

The Higgs coupling to W^- pairs can be obtained from equation B.69 using

$$g_{\eta^{-Q} \eta^{Q+2} W^- W^-} = g_{\eta^Q \eta^{-Q-2} W^+ W^+} = (g_{(\eta^{-Q})^* (\eta^{Q+2})^* W^+ W^+})^* \quad (\text{B.72})$$

B.2 Higgs–Vector couplings for real, $Y = 0$ Higgs representations

and the Higgs couplings to W^-V where $V = Z, \gamma$ can be obtained from equations B.70 and B.71 using

$$g_{\eta^{-Q}\eta^{Q+1}W^-V} = -g_{\eta^Q\eta^{-Q-1}W^+V} = (g_{(\eta^{-Q})^*(\eta^{Q+1})^*W^+V})^*, \quad (\text{B.73})$$

the same as for a complex representation. Note that the couplings for the real representation are always real; we write $(g_{HHVV})^*$ in equations B.72 and B.73 in order to compare with equations B.26 and B.27 for the complex representation.

These couplings are related to the couplings for a complex Higgs representation given in section B.1.2 as follows.

$$g_{\eta^Q(\eta^Q)^*\gamma\gamma} = \epsilon_Q g_{\eta^Q\eta^{-Q}\gamma\gamma} = 2e^2 Q^2 \quad (\text{B.74})$$

$$g_{\eta^Q(\eta^Q)^*ZZ} = \epsilon_Q g_{\eta^Q\eta^{-Q}ZZ} = 2g^2 c_W^2 Q^2 \quad (\text{B.75})$$

$$g_{\eta^Q(\eta^Q)^*Z\gamma} = \epsilon_Q g_{\eta^Q\eta^{-Q}Z\gamma} = 2egc_W Q^2 \quad (\text{B.76})$$

$$g_{\eta^Q(\eta^Q)^*W^+W^-} = \epsilon_Q g_{\eta^Q\eta^{-Q}W^+W^-} = g^2 [T(T+1) - Q^2] \quad (\text{B.77})$$

$$\begin{aligned} g_{\eta^Q(\eta^{Q+2})^*W^+W^+} &= \epsilon_{Q+2} g_{\eta^Q\eta^{-Q-2}W^+W^+} \\ &= g^2 [(T-Q)(T+Q+1)]^{1/2} \\ &\quad \times [(T-Q-1)(T+Q+2)]^{1/2} \end{aligned} \quad (\text{B.78})$$

$$\begin{aligned} g_{\eta^Q(\eta^{Q+1})^*W^+Z} &= \epsilon_{Q+1} g_{\eta^Q\eta^{-Q-1}W^+Z} \\ &= \frac{g^2}{\sqrt{2}} c_W (2Q+1) [(T-Q)(T+Q+1)]^{1/2} \end{aligned} \quad (\text{B.79})$$

$$\begin{aligned} g_{\eta^Q(\eta^{Q+1})^*W^+\gamma} &= \epsilon_{Q+1} g_{\eta^Q\eta^{-Q-1}W^+\gamma} \\ &= \frac{ge}{\sqrt{2}} (2Q+1) [(T-Q)(T+Q+1)]^{1/2} \end{aligned} \quad (\text{B.80})$$

which are the same as the corresponding couplings for a complex Higgs representation, with $Y = 0$.

B.2.3 Higgs–Vector–Vector couplings

In this section we list the HVV couplings, following the notation of equation B.6. The neutral Higgs couplings to ZZ , $\gamma\gamma$, and $Z\gamma$ are zero. The neutral Higgs coupling to W^+W^- is,

$$g_{\eta^0 W^+ W^-} = g^2 v [T(T+1)]. \quad (\text{B.81})$$

The charged Higgs couplings are,

$$g_{\eta^+ W^- Z} = \frac{g^2 c_W v}{\sqrt{2}} [T(T+1)]^{1/2} \quad (\text{B.82})$$

$$g_{\eta^+ W^- \gamma} = \frac{gev}{\sqrt{2}} [T(T+1)]^{1/2} \quad (\text{B.83})$$

$$g_{\eta^{+2} W^- W^-} = g^2 v [T(T+1)]^{1/2} [(T+2)(T-1)]^{1/2} \quad (\text{B.84})$$

The couplings for η^- and η^{-2} are obtained using the following equations, with $V = Z, \gamma$,

$$g_{\eta^- W^+ V} = -g_{(\eta^+)^* W^+ V} = -(g_{\eta^+ W^- V})^* \quad (\text{B.85})$$

$$g_{\eta^{-2} W^+ W^+} = g_{(\eta^{+2})^* W^+ W^+} = (g_{\eta^{+2} W^- W^-})^* \quad (\text{B.86})$$

where we have used $\epsilon_1 = -1$ and $\epsilon_2 = +1$. Note that these relations are the same as for a complex representation.

Notice that the HVV couplings for a real multiplet are not the same as the corresponding couplings for a complex multiplet with $Y = 0$, given in section B.1.3. The couplings of η^\pm and $\eta^{\pm 2}$ differ from the corresponding couplings of a complex multiplet by a factor of $\sqrt{2}$. This difference comes from the factor of $\sqrt{2}$ difference in the normalization of the vev of the real multiplet compared to that of the complex multiplet.

B.2.4 Derivation of ϵ_Q

In this section we derive the phase relation between the states of a real Higgs representation in the electric charge basis.

The lagrangian for a real Higgs representation,

$$\mathcal{L} = \frac{1}{2} (\mathcal{D}_\mu \eta)^T (\mathcal{D}^\mu \eta) \quad (\text{B.87})$$

is written in a Cartesian basis, in which η is real and the $\text{SU}(2)$ generators T^a are imaginary and antisymmetric. However, the Feynman rules are most useful written in terms of charge eigenstates. In the charge basis, equation B.87 becomes

$$\mathcal{L} = \frac{1}{2} \sum_{Q=-T}^T ((\mathcal{D}_\mu \eta)^Q)^* (\mathcal{D}^\mu \eta)^Q \quad (\text{B.88})$$

where $(\mathcal{D}^\mu \eta)^Q$ has isospin $T^3 = Q$. We introduce this notation in order to treat terms which involve the raising and lowering operators T^\pm correctly.

Let us first examine the kinetic terms for the Higgs states. The kinetic part of the Lagrangian is

$$\mathcal{L} = \frac{1}{2} \sum_{Q=-T}^T \partial_\mu (\eta^Q)^* \partial^\mu \eta^Q \quad (\text{B.89})$$

B.2 Higgs–Vector couplings for real, $Y = 0$ Higgs representations

$$= \frac{1}{2} \partial_\mu (\eta^0)^* \partial^\mu \eta^0 + \sum_{Q=1}^T \partial_\mu (\eta^Q)^* \partial^\mu \eta^Q \quad (\text{B.90})$$

$$= \frac{1}{2} \epsilon_0 \partial_\mu \eta^0 \partial^\mu \eta^0 + \sum_{Q=1}^T \epsilon_Q \partial_\mu \eta^{-Q} \partial^\mu \eta^Q \quad (\text{B.91})$$

We have introduced the notation $(\eta^Q)^* = \epsilon_Q \eta^{-Q}$, where $\epsilon_Q = \pm 1$ is a phase factor. Examining the kinetic term for η^0 , we see immediately that $\epsilon_0 = 1$, or $(\eta^0)^* = \eta^0$, as is required for a real representation.

We now derive ϵ_Q for general Q . Consider the following term, in which ρ and η are two real multiplets,

$$\rho^T T^+ \eta = \sum_{Q=-T+1}^T (\rho^Q)^* (T^+ \eta)^Q \quad (\text{B.92})$$

$$= \sum_{Q=-T+1}^T \epsilon_Q \rho^{-Q} [(T+Q)(T-Q+1)]^{1/2} \eta^{Q-1} \quad (\text{B.93})$$

Taking the complex conjugate of equation B.93,

$$(\rho^T T^+ \eta)^* = \sum_{Q=-T+1}^T \epsilon_Q (\rho^{-Q})^* [(T+Q)(T-Q+1)]^{1/2} (\eta^{Q-1})^* \quad (\text{B.94})$$

$$= \sum_{Q=-T+1}^T \epsilon_{Q-1} \rho^Q [(T+Q)(T-Q+1)]^{1/2} \eta^{-Q+1}, \quad (\text{B.95})$$

where we have used $\epsilon_{-Q} = \epsilon_Q$ and $(\epsilon_Q)^2 = 1$. The complex conjugate of equation B.93 can be derived as follows. Writing the real Higgs multiplets in a Cartesian basis, the SU(2) generators T^a can be chosen to be imaginary and antisymmetric. Using

$$T^\pm = T^1 \pm iT^2, \quad (\text{B.96})$$

we find that

$$(T^+)^* = -T^1 + iT^2 = -T^-. \quad (\text{B.97})$$

The complex conjugate of equation B.93 can be written as,

$$(\rho^T T^+ \eta)^* = -\rho^T T^- \eta \quad (\text{B.98})$$

$$= - \sum_{Q'=-T}^{T-1} (\rho^{Q'})^* (T^- \eta)^{Q'} \quad (\text{B.99})$$

$$= - \sum_{Q'=-T}^{T-1} (\rho^{Q'})^* [(T-Q')(T+Q'+1)]^{1/2} \eta^{Q'+1} \quad (\text{B.100})$$

$$= - \sum_{Q'=-T}^{T-1} \epsilon_{Q'} \rho^{-Q'} [(T-Q')(T+Q'+1)]^{1/2} \eta^{Q'+1}. \quad (\text{B.101})$$

Changing the summation index to $Q = -Q'$ and using the fact that $\epsilon_{-Q} = \epsilon_Q$,

$$(\rho^T T^+ \eta)^* = - \sum_{Q=-T+1}^T \epsilon_Q \rho^Q [(T+Q)(T-Q+1)]^{1/2} \eta^{-Q+1}. \quad (\text{B.102})$$

Comparing equations B.95 and B.102, we see that $\epsilon_{Q-1} = -\epsilon_Q$. Together with $\epsilon_0 = 1$, this gives us a general expression for ϵ_Q ,

$$\epsilon_Q = (-1)^Q. \quad (\text{B.103})$$

B.3 Higgs–Vector couplings for Higgs mass eigenstates

In computing the amplitudes for real processes we are interested in the couplings of Higgs mass eigenstates to vector bosons. In general, the Higgs mass eigenstates will not correspond to electroweak eigenstates. The couplings of Higgs mass eigenstates to vector bosons are obtained from the couplings given in sections B.1 and B.2 above using the following formulas. H_i is a Higgs mass eigenstate and ϕ_i is a Higgs electroweak eigenstate.

$$g_{H V_1 V_2} = \sum_{\phi_i} \langle H | \phi_i \rangle g_{\phi_i V_1 V_2} \quad (\text{B.104})$$

$$g_{H_1 H_2 V} = \sum_{\phi_i} \sum_{\phi_j} \langle H_1 | \phi_i \rangle \langle H_2 | \phi_j \rangle g_{\phi_i \phi_j V} \quad (\text{B.105})$$

and the $H_1 H_2 V_1 V_2$ coupling is given by equation B.105 with V replaced by $V_1 V_2$.

Appendix C

The two Higgs doublet model

In this section we summarize the couplings and the corrections to the ρ parameter in the two Higgs doublet model (2HDM). The physical spectrum contains one charged Higgs state,

$$H^\pm = -\sin \beta \phi_1^\pm + \cos \beta \phi_2^\pm, \quad (\text{C.1})$$

one CP-odd neutral state,

$$A^0 = -\sin \beta \phi_1^{0,i} + \cos \beta \phi_2^{0,i}, \quad (\text{C.2})$$

and two CP-even neutral states,

$$h^0 = -\sin \alpha \phi_1^{0,r} + \cos \alpha \phi_2^{0,r} \quad (\text{C.3})$$

$$H^0 = \cos \alpha \phi_1^{0,r} + \sin \alpha \phi_2^{0,r} \quad (\text{C.4})$$

where α is a mixing angle and $M_{h^0} < M_{H^0}$. There are also the three Goldstone bosons,

$$G^0 = \cos \beta \phi_1^{0,i} + \sin \beta \phi_2^{0,i} \quad (\text{C.5})$$

$$G^\pm = \cos \beta \phi_1^\pm + \sin \beta \phi_2^\pm. \quad (\text{C.6})$$

The Higgs Yukawa couplings in the Type II 2HDM are of the form

$$i(g_{H\bar{q}q}^L P_L + g_{H\bar{q}q}^R P_R) = i(g_{H\bar{q}q}^V + g_{H\bar{q}q}^A \gamma_5). \quad (\text{C.7})$$

The quark couplings for each Higgs state are,

$$g_{G^+ \bar{t} b}^L = \frac{gm_t}{\sqrt{2}M_W} \quad (\text{C.8})$$

$$g_{G^+\bar{t}b}^R = -\frac{gm_b}{\sqrt{2}M_W} \quad (\text{C.9})$$

$$g_{H^+\bar{t}b}^L = \frac{gm_t}{\sqrt{2}M_W} \cot \beta \quad (\text{C.10})$$

$$g_{H^+\bar{t}b}^R = \frac{gm_b}{\sqrt{2}M_W} \tan \beta \quad (\text{C.11})$$

$$g_{h^0 b\bar{b}}^V = \frac{gm_b}{2M_W} \frac{\sin \alpha}{\cos \beta} \quad (\text{C.12})$$

$$g_{H^0 b\bar{b}}^V = -\frac{gm_b}{2M_W} \frac{\cos \alpha}{\cos \beta} \quad (\text{C.13})$$

$$g_{G^0 b\bar{b}}^A = -\frac{igm_b}{2M_W} \quad (\text{C.14})$$

$$g_{A^0 b\bar{b}}^A = \frac{igm_b}{2M_W} \tan \beta. \quad (\text{C.15})$$

All the Higgs couplings in the Type I model are the same as in the Type II model except for

$$g_{H^+\bar{t}b}^L = -\frac{gm_t}{\sqrt{2}M_W} \tan \beta. \quad (\text{C.16})$$

The Z –Higgs–Higgs couplings take the form,

$$ig_{ZH_i H_j} (p_i - p_j)_\mu, \quad (\text{C.17})$$

where p_i (p_j) is the incoming momentum of H_i (H_j). The couplings are,

$$g_{ZG^+G^-} = -\frac{e}{s_W c_W} \left(\frac{1}{2} - s_W^2 \right) \quad (\text{C.18})$$

$$g_{ZH^+H^-} = -\frac{e}{s_W c_W} \left(\frac{1}{2} - s_W^2 \right) \quad (\text{C.19})$$

$$g_{ZG^+H^-} = 0 \quad (\text{C.20})$$

$$g_{Zh^0 G^0} = -\frac{i}{2} \frac{e}{s_W c_W} \sin(\beta - \alpha) \quad (\text{C.21})$$

$$g_{ZH^0 G^0} = -\frac{i}{2} \frac{e}{s_W c_W} \cos(\beta - \alpha) \quad (\text{C.22})$$

$$g_{Zh^0 A^0} = -\frac{i}{2} \frac{e}{s_W c_W} \cos(\beta - \alpha) \quad (\text{C.23})$$

$$g_{ZH^0 A^0} = \frac{i}{2} \frac{e}{s_W c_W} \sin(\beta - \alpha). \quad (\text{C.24})$$

We now give the one-loop contribution of the 2HDM Higgs bosons to the ρ parameter, from reference [55]. This contribution is defined relative to the SM in which the SM Higgs mass is taken equal to M_{h^0} . We have corrected a typographical error in the formula for $\Delta\rho$ in reference [55].

$$\begin{aligned} \Delta\rho = & \frac{\alpha}{16\pi M_W^2 s_W^2} \left\{ F(M_{H^\pm}^2, M_{A^0}^2) + \sin^2(\beta - \alpha) \left[F(M_{H^\pm}^2, M_{H^0}^2) - F(M_{A^0}^2, M_{H^0}^2) \right] \right. \\ & + \cos^2(\beta - \alpha) \left[F(M_{H^\pm}^2, M_{h^0}^2) - F(M_{A^0}^2, M_{h^0}^2) + F(M_W^2, M_{H^0}^2) \right. \\ & - F(M_W^2, M_{h^0}^2) - F(M_Z^2, M_{H^0}^2) + F(M_Z^2, M_{h^0}^2) \\ & + 4M_Z^2 \left[B_0(0; M_Z^2, M_{H^0}^2) - B_0(0; M_Z^2, M_{h^0}^2) \right] \\ & \left. \left. - 4M_W^2 \left[B_0(0; M_W^2, M_{H^0}^2) - B_0(0; M_W^2, M_{h^0}^2) \right] \right] \right\} \end{aligned} \quad (\text{C.25})$$

where $s_W \equiv \sin \theta_W$, and

$$B_0(0; m_1^2, m_2^2) = \frac{A_0(m_1^2) - A_0(m_2^2)}{m_1^2 - m_2^2} \quad (\text{C.26})$$

$$A_0(m^2) \equiv m^2(\Delta + 1 - \log m^2) \quad (\text{C.27})$$

$$F(m_1^2, m_2^2) \equiv \frac{1}{2}(m_1^2 + m_2^2) - \frac{m_1^2 m_2^2}{m_1^2 - m_2^2} \log \left(\frac{m_1^2}{m_2^2} \right). \quad (\text{C.28})$$

Appendix D

Details of the models with two Higgs doublets and one triplet

In this chapter we summarize the details of the models with two doublets and one triplet, discussed in section 6.2.2. We list the Higgs mass eigenstates, and their couplings which are relevant in the calculation of the corrections to $Z \rightarrow b\bar{b}$.

The Higgs sector in these models consists of two complex, $Y = 1$ Higgs doublets, denoted by Φ_1 and Φ_2 , plus a triplet field. The triplet field can either be a real triplet with $Y = 0$, or a complex triplet with $Y = 2$. We thus have four possible models to consider: a Type I model with a $Y = 0$ triplet, a Type II model with a $Y = 0$ triplet, a Type I model with a $Y = 2$ triplet, and a Type II model with a $Y = 2$ triplet. We will refer to the models with a $Y = 0$ triplet as the $Y = 0$ models, and to the models with a $Y = 2$ triplet as the $Y = 2$ models.

We will treat the $Y = 0$ and $Y = 2$ models separately. In what follows we will assume that the models are Type II, but will also give the couplings in the Type I models where they differ from those in the Type II models.

We define $\tan\beta$ in these models exactly as in the 2HDM: $\tan\beta = v_2/v_1$, where the vevs of the doublets are $\langle\phi_1^0\rangle = v_1/\sqrt{2}$ and $\langle\phi_2^0\rangle = v_2/\sqrt{2}$. The vev of the triplet field must be fine-tuned very small in order to be consistent with the measured value of the ρ parameter, $\rho \approx 1$.

D.1 $Y = 0$ model

We first consider the model with one doublet and one real triplet field with $Y = 0$. The triplet field is $\xi = (\xi^+, \xi^0, \xi^-)$. We define the triplet vev as $\langle\xi^0\rangle = v_\xi$. The vevs are

D.1 $Y = 0$ model

constrained by the W mass to satisfy,

$$v_{SM}^2 = v_1^2 + v_2^2 + 4v_\xi^2, \quad (\text{D.1})$$

where $v_{SM} = 246$ GeV. It is convenient to parameterize the ratio of the vevs by,

$$\tan \theta_0 = \frac{\sqrt{v_1^2 + v_2^2}}{2v_\xi}. \quad (\text{D.2})$$

In this model, the tree-level ρ parameter is,

$$\rho = \frac{v_1^2 + v_2^2 + 4v_\xi^2}{v_1^2 + v_2^2} = 1 + \frac{4v_\xi^2}{v_1^2 + v_2^2} = 1 + \Delta\rho. \quad (\text{D.3})$$

Writing this in terms of $\tan \theta_0$, we find

$$\Delta\rho = \frac{1}{\tan^2 \theta_0}. \quad (\text{D.4})$$

We see that in order to have $\rho \approx 1$, the triplet vev must be very small, giving large $\tan \theta_0$.

This model contains three charged states, one from each of the doublets and one from the triplet. The charged Higgs states mix to form the Goldstone boson,

$$G^+ = \sin \theta_0 (\cos \beta \phi_1^+ + \sin \beta \phi_2^+) + \cos \theta_0 \xi^+, \quad (\text{D.5})$$

and two orthogonal states which are the physical charged Higgs bosons. We define two orthogonal states,

$$H_1^{+'} = \cos \theta_0 (\cos \beta \phi_1^+ + \sin \beta \phi_2^+) - \sin \theta_0 \xi^+ \quad (\text{D.6})$$

$$H_2^{+'} = -\sin \beta \phi_1^+ + \cos \beta \phi_2^+ \quad (\text{D.7})$$

which will mix by an angle δ to form the mass eigenstates. The mixing angle δ depends on the details of the Higgs potential. The mass eigenstates then take the complicated form,

$$H_1^+ = (\cos \delta \cos \theta_0 \cos \beta - \sin \delta \sin \beta) \phi_1^+ + (\cos \delta \cos \theta_0 \sin \beta + \sin \delta \cos \beta) \phi_2^+ - \cos \delta \sin \theta_0 \xi^+ \quad (\text{D.8})$$

$$H_2^+ = (-\sin \delta \cos \theta_0 \cos \beta - \cos \delta \sin \beta) \phi_1^+ + (-\sin \delta \cos \theta_0 \sin \beta + \cos \delta \cos \beta) \phi_2^+ + \sin \delta \sin \theta_0 \xi^+. \quad (\text{D.9})$$

The Higgs couplings to quarks are of the form,

$$i(g_{H\bar{q}q}^L P_L + g_{H\bar{q}q}^R P_R) = i(g_{H\bar{q}q}^V + g_{H\bar{q}q}^A \gamma_5). \quad (\text{D.10})$$

Details of the models with two Higgs doublets and one triplet

In the Type II model, the charged Higgs couplings to $\bar{t}b$ are,

$$g_{G^+\bar{t}b}^L = \frac{gm_t}{\sqrt{2}M_W} \quad (D.11)$$

$$g_{G^+\bar{t}b}^R = -\frac{gm_b}{\sqrt{2}M_W} \quad (D.12)$$

$$g_{H_1^+\bar{t}b}^L = \frac{gm_t}{\sqrt{2}M_W} \frac{(\cos \delta \cos \theta_0 \sin \beta + \sin \delta \cos \beta)}{\sin \beta \sin \theta_0} \quad (D.13)$$

$$g_{H_1^+\bar{t}b}^R = -\frac{gm_b}{\sqrt{2}M_W} \frac{(\cos \delta \cos \theta_0 \cos \beta - \sin \delta \sin \beta)}{\cos \beta \sin \theta_0} \quad (D.14)$$

$$g_{H_2^+\bar{t}b}^L = \frac{gm_t}{\sqrt{2}M_W} \frac{(-\sin \delta \cos \theta_0 \sin \beta + \cos \delta \cos \beta)}{\sin \beta \sin \theta_0} \quad (D.15)$$

$$g_{H_2^+\bar{t}b}^R = -\frac{gm_b}{\sqrt{2}M_W} \frac{(-\sin \delta \cos \theta_0 \cos \beta - \cos \delta \sin \beta)}{\cos \beta \sin \theta_0}. \quad (D.16)$$

In the Type I model, the couplings are the same except for,

$$g_{H_1^+\bar{t}b}^L = \frac{gm_t}{\sqrt{2}M_W} \frac{(\cos \delta \cos \theta_0 \cos \beta - \sin \delta \sin \beta)}{\cos \beta \sin \theta_0} \quad (D.17)$$

$$g_{H_2^+\bar{t}b}^L = \frac{gm_t}{\sqrt{2}M_W} \frac{(-\sin \delta \cos \theta_0 \cos \beta - \cos \delta \sin \beta)}{\cos \beta \sin \theta_0}. \quad (D.18)$$

The Z-Higgs-Higgs couplings take the form,

$$ig_{ZH_iH_j}(p_i - p_j)_\mu, \quad (D.19)$$

where p_i (p_j) is the incoming momentum of H_i (H_j). The charged Higgs couplings to Z are,

$$g_{ZG^+(G^+)^*} = -\frac{e}{s_W c_W} \left[\frac{1}{2} - s_W^2 + \frac{1}{2} \cos^2 \theta_0 \right] \quad (D.20)$$

$$g_{ZG^+(H_1^+)^*} = \frac{e}{s_W c_W} \frac{1}{2} \sin \theta_0 \cos \theta_0 \cos \delta \quad (D.21)$$

$$g_{ZG^+(H_2^+)^*} = -\frac{e}{s_W c_W} \frac{1}{2} \sin \theta_0 \cos \theta_0 \sin \delta \quad (D.22)$$

$$g_{ZH_1^+(H_1^+)^*} = -\frac{e}{s_W c_W} \left[\frac{1}{2} - s_W^2 + \frac{1}{2} \sin^2 \theta_0 \cos^2 \delta \right] \quad (D.23)$$

$$g_{ZH_2^+(H_2^+)^*} = -\frac{e}{s_W c_W} \left[\frac{1}{2} - s_W^2 + \frac{1}{2} \sin^2 \theta_0 \sin^2 \delta \right] \quad (D.24)$$

$$g_{ZH_1^+(H_2^+)^*} = \frac{e}{s_W c_W} \frac{1}{2} \sin \delta \cos \delta \sin^2 \theta_0, \quad (D.25)$$

D.1 $Y = 0$ model

where s_W is the sine of the weak mixing angle.

The states and couplings can be simplified a great deal if we take the limit of large $\tan \theta_0$, as required by the measured value of the ρ parameter. As shown in section 6.2.1, the ρ parameter measurement requires $\tan \theta_0 > 18$. This corresponds to $\sin \theta_0 > 0.998$ and $\cos \theta_0 < 0.055$. We will make the approximation $\sin \theta_0 = 1$ and $\cos \theta_0 = 0$. Then the charged states are,

$$G^+ \simeq \cos \beta \phi_1^+ + \sin \beta \phi_2^+ \quad (\text{D.26})$$

$$H_1^{+'} \simeq -\xi^+ \quad (\text{D.27})$$

$$H_2^{+'} = -\sin \beta \phi_1^+ + \cos \beta \phi_2^+. \quad (\text{D.28})$$

Mixing $H_1^{+'}$ and $H_2^{+'}$ through the mixing angle δ , the physical mass eigenstates are,

$$H_1^+ \simeq \sin \delta (-\sin \beta \phi_1^+ + \cos \beta \phi_2^+) - \cos \delta \xi^+ \quad (\text{D.29})$$

$$H_2^+ \simeq \cos \delta (-\sin \beta \phi_1^+ + \cos \beta \phi_2^+) + \sin \delta \xi^+. \quad (\text{D.30})$$

In the Type II model, the charged Higgs couplings to $\bar{t}b$ simplify to,

$$g_{H_1^+ \bar{t}b}^L = \frac{gm_t}{\sqrt{2}M_W} \cot \beta \sin \delta \quad (\text{D.31})$$

$$g_{H_1^+ \bar{t}b}^R = +\frac{gm_b}{\sqrt{2}M_W} \tan \beta \sin \delta \quad (\text{D.32})$$

$$g_{H_2^+ \bar{t}b}^L = \frac{gm_t}{\sqrt{2}M_W} \cot \beta \cos \delta \quad (\text{D.33})$$

$$g_{H_2^+ \bar{t}b}^R = +\frac{gm_b}{\sqrt{2}M_W} \tan \beta \cos \delta. \quad (\text{D.34})$$

In the Type I model, $\cot \beta$ is replaced by $\tan \beta$ in the left-handed couplings.

The charged Higgs couplings to Z simplify to,

$$g_{ZG^+(G^+)^*} = -\frac{e}{s_W c_W} \left[\frac{1}{2} - s_W^2 \right] \quad (\text{D.35})$$

$$g_{ZG^+(H_1^+)^*} = 0 \quad (\text{D.36})$$

$$g_{ZG^+(H_2^+)^*} = 0 \quad (\text{D.37})$$

$$g_{ZH_1^+(H_1^+)^*} = -\frac{e}{s_W c_W} \left[\frac{1}{2} - s_W^2 + \frac{1}{2} \cos^2 \delta \right] \quad (\text{D.38})$$

$$g_{ZH_2^+(H_2^+)^*} = -\frac{e}{s_W c_W} \left[\frac{1}{2} - s_W^2 + \frac{1}{2} \sin^2 \delta \right] \quad (\text{D.39})$$

$$g_{ZH_1^+(H_2^+)^*} = \frac{e}{s_W c_W} \frac{1}{2} \sin \delta \cos \delta. \quad (\text{D.40})$$

Details of the models with two Higgs doublets and one triplet

Neutral Higgs bosons in the $Y = 0$ model

In the $Y = 0$ model there are three CP-even neutral degrees of freedom and only two CP-odd neutral degrees of freedom, because the real triplet contributes only a CP-even degree of freedom. These states mix to form three CP-even states, one CP-odd state, and the CP-odd neutral Goldstone boson.

The neutral Goldstone boson is,

$$G^0 = \cos \beta \phi_1^{0,i} + \sin \beta \phi_2^{0,i}, \quad (\text{D.41})$$

and the physical CP-odd neutral Higgs boson is the orthogonal state,

$$A^0 = -\sin \beta \phi_1^{0,i} + \cos \beta \phi_2^{0,i}. \quad (\text{D.42})$$

Note that G^0 and A^0 are the same as in the 2HDM.

We next define three orthogonal CP-even Higgs states. We allow the CP-even components of the two doublets to mix by an angle α , in analogy with the 2HDM. This gives two orthogonal states,

$$H^{0'} = \cos \alpha \phi_1^{0,r} + \sin \alpha \phi_2^{0,r} \quad (\text{D.43})$$

$$h^{0'} = -\sin \alpha \phi_1^{0,r} + \cos \alpha \phi_2^{0,r}. \quad (\text{D.44})$$

In general, both $H^{0'}$ and $h^{0'}$ mix with ξ^0 by angles determined by the details of the Higgs potential. However, for simplicity we will consider the case in which only $H^{0'}$ mixes with the triplet. We will parameterize this doublet-triplet mixing with the mixing angle γ . The resulting mass eigenstates are,

$$H_1^0 = \cos \gamma (\cos \alpha \phi_1^{0,r} + \sin \alpha \phi_2^{0,r}) + \sin \gamma \xi^0 \quad (\text{D.45})$$

$$H_2^0 = -\sin \gamma (\cos \alpha \phi_1^{0,r} + \sin \alpha \phi_2^{0,r}) + \cos \gamma \xi^0 \quad (\text{D.46})$$

$$H_3^0 = -\sin \alpha \phi_1^{0,r} + \cos \alpha \phi_2^{0,r}. \quad (\text{D.47})$$

The neutral Higgs couplings to quarks are,

$$g_{H_1^0 b\bar{b}}^V = -\frac{1}{\sqrt{2}} \left(\frac{gm_b}{\sqrt{2}M_W} \right) \frac{\cos \gamma \cos \alpha}{\cos \beta \sin \theta_0} \quad (\text{D.48})$$

$$g_{H_2^0 b\bar{b}}^V = -\frac{1}{\sqrt{2}} \left(\frac{gm_b}{\sqrt{2}M_W} \right) \frac{-\sin \gamma \cos \alpha}{\cos \beta \sin \theta_0} \quad (\text{D.49})$$

$$g_{H_3^0 b\bar{b}}^V = -\frac{1}{\sqrt{2}} \left(\frac{gm_b}{\sqrt{2}M_W} \right) \frac{-\sin \alpha}{\cos \beta \sin \theta_0} \quad (\text{D.50})$$

$$g_{G^0 b\bar{b}}^A = -\frac{i}{\sqrt{2}} \left(\frac{gm_b}{\sqrt{2}M_W} \right) \frac{1}{\sin \theta_0} \quad (\text{D.51})$$

$$g_{A^0 b\bar{b}}^A = -\frac{i}{\sqrt{2}} \left(\frac{gm_b}{\sqrt{2}M_W} \right) \frac{-\tan \beta}{\sin \theta_0}. \quad (\text{D.52})$$

D.2 $Y = 2$ model

The neutral Higgs couplings to Z are,

$$g_{ZH_1^0 G^0} = \frac{ie}{s_W c_W} \left[-\frac{1}{2} \cos \gamma \cos(\beta - \alpha) \right] \quad (\text{D.53})$$

$$g_{ZH_1^0 A^0} = \frac{ie}{s_W c_W} \left[\frac{1}{2} \cos \gamma \sin(\beta - \alpha) \right] \quad (\text{D.54})$$

$$g_{ZH_2^0 G^0} = \frac{ie}{s_W c_W} \left[\frac{1}{2} \sin \gamma \cos(\beta - \alpha) \right] \quad (\text{D.55})$$

$$g_{ZH_2^0 A^0} = \frac{ie}{s_W c_W} \left[-\frac{1}{2} \sin \gamma \sin(\beta - \alpha) \right] \quad (\text{D.56})$$

$$g_{ZH_3^0 G^0} = \frac{ie}{s_W c_W} \left[-\frac{1}{2} \sin(\beta - \alpha) \right] \quad (\text{D.57})$$

$$g_{ZH_3^0 A^0} = \frac{ie}{s_W c_W} \left[-\frac{1}{2} \cos(\beta - \alpha) \right]. \quad (\text{D.58})$$

The Higgs couplings to b quarks can be simplified if we take the limit of large $\tan \theta_0$, as required by the measured value of the ρ parameter. When we make the approximation $\sin \theta_0 \approx 1$, the neutral Higgs couplings to b quarks become,

$$g_{H_1^0 b \bar{b}}^V = -\frac{1}{\sqrt{2}} \left(\frac{gm_b}{\sqrt{2}M_W} \right) \frac{\cos \gamma \cos \alpha}{\cos \beta} \quad (\text{D.59})$$

$$g_{H_2^0 b \bar{b}}^V = -\frac{1}{\sqrt{2}} \left(\frac{gm_b}{\sqrt{2}M_W} \right) \frac{-\sin \gamma \cos \alpha}{\cos \beta} \quad (\text{D.60})$$

$$g_{H_3^0 b \bar{b}}^V = -\frac{1}{\sqrt{2}} \left(\frac{gm_b}{\sqrt{2}M_W} \right) \frac{-\sin \alpha}{\cos \beta} \quad (\text{D.61})$$

$$g_{G^0 b \bar{b}}^A = -\frac{i}{\sqrt{2}} \left(\frac{gm_b}{\sqrt{2}M_W} \right) \quad (\text{D.62})$$

$$g_{A^0 b \bar{b}}^A = -\frac{i}{\sqrt{2}} \left(\frac{gm_b}{\sqrt{2}M_W} \right) (-\tan \beta). \quad (\text{D.63})$$

D.2 $Y = 2$ model

We now consider the model with one doublet and one complex triplet field with $Y = 2$. The triplet field is $\chi = (\chi^{++}, \chi^+, \chi^0)$. We define the triplet vev as $\langle \chi^0 \rangle = v_\chi / \sqrt{2}$. The vevs are constrained by the W mass to satisfy,

$$v_{SM}^2 = v_1^2 + v_2^2 + 2v_\chi^2, \quad (\text{D.64})$$

where $v_{SM} = 246$ GeV. It is convenient to parameterize the ratio of the vevs by,

$$\tan \theta_2 = \frac{\sqrt{v_1^2 + v_2^2}}{\sqrt{2}v_\chi}. \quad (\text{D.65})$$

Details of the models with two Higgs doublets and one triplet

In this model, the tree-level ρ parameter is,

$$\rho = \frac{v_1^2 + v_2^2 + 2v_\chi^2}{v_1^2 + v_2^2 + 4v_\chi^2} = 1 - \frac{2v_\chi^2}{v_1^2 + v_2^2 + 4v_\chi^2} = 1 + \Delta\rho. \quad (\text{D.66})$$

Writing this in terms of $\tan\theta_2$, we find

$$\Delta\rho = -\frac{1}{\tan^2\theta_2 + 2}. \quad (\text{D.67})$$

We see that in order to have $\rho \approx 1$, the triplet vev must be very small, giving large $\tan\theta_2$.

This model contains three singly-charged states, one from each of the doublets and one from the triplet. The charged Higgs states mix to form the Goldstone boson,

$$G^+ = \sin\theta_2(\cos\beta\phi_1^+ + \sin\beta\phi_2^+) + \cos\theta_2\chi^+, \quad (\text{D.68})$$

and two orthogonal states which are the physical charged Higgs bosons. We define two orthogonal states,

$$H_1^{+'} = \cos\theta_2(\cos\beta\phi_1^+ + \sin\beta\phi_2^+) - \sin\theta_2\chi^+ \quad (\text{D.69})$$

$$H_2^{+'} = -\sin\beta\phi_1^+ + \cos\beta\phi_2^+, \quad (\text{D.70})$$

which will mix by an angle δ to form the mass eigenstates. The mixing angle δ depends on the details of the Higgs potential. The mass eigenstates then take the complicated form,

$$H_1^+ = (\cos\delta\cos\theta_2\cos\beta - \sin\delta\sin\beta)\phi_1^+ + (\cos\delta\cos\theta_2\sin\beta + \sin\delta\cos\beta)\phi_2^+ - \cos\delta\sin\theta_2\xi^+ \quad (\text{D.71})$$

$$H_2^+ = (-\sin\delta\cos\theta_2\cos\beta - \cos\delta\sin\beta)\phi_1^+ + (-\sin\delta\cos\theta_2\sin\beta + \cos\delta\cos\beta)\phi_2^+ + \sin\delta\sin\theta_2\xi^+. \quad (\text{D.72})$$

The Higgs couplings to quarks are of the form,

$$i(g_{H\bar{q}q}^L P_L + g_{H\bar{q}q}^R P_R) = i(g_{H\bar{q}q}^V + g_{H\bar{q}q}^A \gamma_5). \quad (\text{D.73})$$

In the Type II model, the charged Higgs couplings to $\bar{t}b$ are,

$$g_{G^+\bar{t}b}^L = \frac{gm_t}{\sqrt{2}M_W} \quad (\text{D.74})$$

$$g_{G^+\bar{t}b}^R = -\frac{gm_b}{\sqrt{2}M_W} \quad (\text{D.75})$$

$$g_{H_1^+\bar{t}b}^L = \frac{gm_t}{\sqrt{2}M_W} \frac{(\cos\delta\cos\theta_2\sin\beta + \sin\delta\cos\beta)}{\sin\beta\sin\theta_2} \quad (\text{D.76})$$

D.2 $Y = 2$ model

$$g_{H_1^+ \bar{t} b}^R = -\frac{gm_b}{\sqrt{2}M_W} \frac{(\cos \delta \cos \theta_2 \cos \beta - \sin \delta \sin \beta)}{\cos \beta \sin \theta_2} \quad (\text{D.77})$$

$$g_{H_2^+ \bar{t} b}^L = \frac{gm_t}{\sqrt{2}M_W} \frac{(-\sin \delta \cos \theta_2 \sin \beta + \cos \delta \cos \beta)}{\sin \beta \sin \theta_2} \quad (\text{D.78})$$

$$g_{H_2^+ \bar{t} b}^R = -\frac{gm_b}{\sqrt{2}M_W} \frac{(-\sin \delta \cos \theta_2 \cos \beta - \cos \delta \sin \beta)}{\cos \beta \sin \theta_2}. \quad (\text{D.79})$$

In the Type I model, the couplings are the same except for,

$$g_{H_1^+ \bar{t} b}^L = \frac{gm_t}{\sqrt{2}M_W} \frac{(\cos \delta \cos \theta_2 \cos \beta - \sin \delta \sin \beta)}{\cos \beta \sin \theta_2} \quad (\text{D.80})$$

$$g_{H_2^+ \bar{t} b}^L = \frac{gm_t}{\sqrt{2}M_W} \frac{(-\sin \delta \cos \theta_2 \cos \beta - \cos \delta \sin \beta)}{\cos \beta \sin \theta_2}. \quad (\text{D.81})$$

The Z -Higgs-Higgs couplings take the form,

$$ig_{ZH_i H_j}(p_i - p_j)_\mu, \quad (\text{D.82})$$

where p_i (p_j) is the incoming momentum of H_i (H_j). The charged Higgs couplings to Z are,

$$g_{ZG^+(G^+)^*} = -\frac{e}{s_W c_W} \left[\frac{1}{2} - s_W^2 - \frac{1}{2} \cos^2 \theta_2 \right] \quad (\text{D.83})$$

$$g_{ZG^+(H_1^+)^*} = -\frac{e}{s_W c_W} \frac{1}{2} \sin \theta_2 \cos \theta_2 \cos \delta \quad (\text{D.84})$$

$$g_{ZG^+(H_2^+)^*} = \frac{e}{s_W c_W} \frac{1}{2} \sin \theta_2 \cos \theta_2 \sin \delta \quad (\text{D.85})$$

$$g_{ZH_1^+(H_1^+)^*} = -\frac{e}{s_W c_W} \left[\frac{1}{2} - s_W^2 - \frac{1}{2} \sin^2 \theta_2 \cos^2 \delta \right] \quad (\text{D.86})$$

$$g_{ZH_2^+(H_2^+)^*} = -\frac{e}{s_W c_W} \left[\frac{1}{2} - s_W^2 - \frac{1}{2} \sin^2 \theta_2 \sin^2 \delta \right] \quad (\text{D.87})$$

$$g_{ZH_1^+(H_2^+)^*} = -\frac{e}{s_W c_W} \frac{1}{2} \sin \delta \cos \delta \sin^2 \theta_2, \quad (\text{D.88})$$

where s_W is the sine of the weak mixing angle.

The states and couplings can be simplified a great deal if we take the limit of large $\tan \theta_2$, as required by the measured value of the ρ parameter. As shown in section 6.2.1, the ρ parameter measurement requires $\tan \theta_2 > 15$. This corresponds to $\sin \theta_2 > 0.998$ and $\cos \theta_2 < 0.067$. We will make the approximation $\sin \theta_2 = 1$ and $\cos \theta_2 = 0$. Then the charged states are,

$$G^+ \simeq \cos \beta \phi_1^+ + \sin \beta \phi_2^+ \quad (\text{D.89})$$

$$H_1^{+'} \simeq -\chi^+ \quad (\text{D.90})$$

$$H_2^{+'} = -\sin \beta \phi_1^+ + \cos \beta \phi_2^+. \quad (\text{D.91})$$

Details of the models with two Higgs doublets and one triplet

Mixing $H_1^{+'}$ and $H_2^{+'}$ through the mixing angle δ , the physical mass eigenstates are,

$$H_1^+ \simeq \sin \delta (-\sin \beta \phi_1^+ + \cos \beta \phi_2^+) - \cos \delta \chi^+ \quad (\text{D.92})$$

$$H_2^+ \simeq \cos \delta (-\sin \beta \phi_1^+ + \cos \beta \phi_2^+) + \sin \delta \chi^+. \quad (\text{D.93})$$

In the Type II model, the charged Higgs couplings to $\bar{t}b$ simplify to,

$$g_{H_1^+ \bar{t}b}^L = \frac{gm_t}{\sqrt{2}M_W} \cot \beta \sin \delta \quad (\text{D.94})$$

$$g_{H_1^+ \bar{t}b}^R = + \frac{gm_b}{\sqrt{2}M_W} \tan \beta \sin \delta \quad (\text{D.95})$$

$$g_{H_2^+ \bar{t}b}^L = \frac{gm_t}{\sqrt{2}M_W} \cot \beta \cos \delta \quad (\text{D.96})$$

$$g_{H_2^+ \bar{t}b}^R = + \frac{gm_b}{\sqrt{2}M_W} \tan \beta \cos \delta. \quad (\text{D.97})$$

In the Type I model, $\cot \beta$ is replaced by $\tan \beta$ in the left-handed couplings.

The charged Higgs couplings to Z simplify to,

$$g_{ZG^+(G^+)^*} = -\frac{e}{s_W c_W} \left[\frac{1}{2} - s_W^2 \right] \quad (\text{D.98})$$

$$g_{ZG^+(H_1^+)^*} = 0 \quad (\text{D.99})$$

$$g_{ZG^+(H_2^+)^*} = 0 \quad (\text{D.100})$$

$$g_{ZH_1^+(H_1^+)^*} = -\frac{e}{s_W c_W} \left[\frac{1}{2} - s_W^2 - \frac{1}{2} \cos^2 \delta \right] \quad (\text{D.101})$$

$$g_{ZH_2^+(H_2^+)^*} = -\frac{e}{s_W c_W} \left[\frac{1}{2} - s_W^2 - \frac{1}{2} \sin^2 \delta \right] \quad (\text{D.102})$$

$$g_{ZH_1^+(H_2^+)^*} = -\frac{e}{s_W c_W} \frac{1}{2} \sin \delta \cos \delta. \quad (\text{D.103})$$

Neutral Higgs bosons in the $Y = 2$ model

In the $Y = 2$ model there are three CP-even neutral degrees of freedom and three CP-odd neutral degrees of freedom. These mix to form three CP-even states, two CP-odd states, and the CP-odd neutral Goldstone boson.

The neutral Goldstone boson is,

$$G^0 = \sin \theta_2 (\cos \beta \phi_1^{0,i} + \sin \beta \phi_2^{0,i}) + \cos \theta_2 \chi^{0,i}, \quad (\text{D.104})$$

and there are two orthogonal states which are the physical CP-odd neutral Higgs bosons. We define two orthogonal states,

$$A_1^{0'} = \cos \theta_2 (\cos \beta \phi_1^{0,i} + \sin \beta \phi_2^{0,i}) - \sin \theta_2 \chi^{0,i} \quad (\text{D.105})$$

$$A_2^{0'} = -\sin \beta \phi_1^{0,i} + \cos \beta \phi_2^{0,i}. \quad (\text{D.106})$$

D.2 $Y = 2$ model

Note that $A_2^{0'}$ corresponds to A^0 in the 2HDM. These states will mix by an angle ω to form the mass eigenstates. The mixing angle ω depends on the details of the Higgs potential. The mass eigenstates then take the complicated form,

$$\begin{aligned} A_1^0 &= (\cos \omega \cos \theta_2 \cos \beta - \sin \omega \sin \beta) \phi_1^{0,i} \\ &\quad + (\cos \omega \cos \theta_2 \sin \beta + \sin \omega \cos \beta) \phi_2^{0,i} - \cos \omega \sin \theta_2 \chi^{0,i} \end{aligned} \quad (\text{D.107})$$

$$\begin{aligned} A_2^0 &= (-\sin \omega \cos \theta_2 \cos \beta - \cos \omega \sin \beta) \phi_1^{0,i} \\ &\quad + (-\sin \omega \cos \theta_2 \sin \beta + \cos \omega \cos \beta) \phi_2^{0,i} + \sin \omega \sin \theta_2 \chi^{0,i}. \end{aligned} \quad (\text{D.108})$$

Similarly, we can define three orthogonal CP-even Higgs states. We allow the CP-even components of the two doublets to mix by an angle α , in analogy with the 2HDM. This gives two orthogonal states,

$$H^{0'} = \cos \alpha \phi_1^{0,r} + \sin \alpha \phi_2^{0,r} \quad (\text{D.109})$$

$$h^{0'} = -\sin \alpha \phi_1^{0,r} + \cos \alpha \phi_2^{0,r}. \quad (\text{D.110})$$

In general, both $H^{0'}$ and $h^{0'}$ mix with $\chi^{0,r}$ by angles determined by the details of the Higgs potential. However, for simplicity we will consider the case in which only $H^{0'}$ mixes with the triplet. We will parameterize this doublet-triplet mixing with the mixing angle γ . The resulting mass eigenstates are,

$$H_1^0 = \cos \gamma (\cos \alpha \phi_1^{0,r} + \sin \alpha \phi_2^{0,r}) + \sin \gamma \chi^{0,r} \quad (\text{D.111})$$

$$H_2^0 = -\sin \gamma (\cos \alpha \phi_1^{0,r} + \sin \alpha \phi_2^{0,r}) + \cos \gamma \chi^{0,r} \quad (\text{D.112})$$

$$H_3^0 = -\sin \alpha \phi_1^{0,r} + \cos \alpha \phi_2^{0,r}. \quad (\text{D.113})$$

The neutral Higgs couplings to quarks are,

$$g_{H_1^0 b \bar{b}}^V = -\frac{1}{\sqrt{2}} \left(\frac{gm_b}{\sqrt{2}M_W} \right) \frac{\cos \gamma \cos \alpha}{\cos \beta \sin \theta_2} \quad (\text{D.114})$$

$$g_{H_2^0 b \bar{b}}^V = -\frac{1}{\sqrt{2}} \left(\frac{gm_b}{\sqrt{2}M_W} \right) \frac{-\sin \gamma \cos \alpha}{\cos \beta \sin \theta_2} \quad (\text{D.115})$$

$$g_{H_3^0 b \bar{b}}^V = -\frac{1}{\sqrt{2}} \left(\frac{gm_b}{\sqrt{2}M_W} \right) \frac{-\sin \alpha}{\cos \beta \sin \theta_2} \quad (\text{D.116})$$

$$g_{G^0 b \bar{b}}^A = -\frac{i}{\sqrt{2}} \left(\frac{gm_b}{\sqrt{2}M_W} \right) \quad (\text{D.117})$$

$$g_{A_1^0 b \bar{b}}^A = -\frac{i}{\sqrt{2}} \left(\frac{gm_b}{\sqrt{2}M_W} \right) \frac{(\cos \omega \cos \theta_2 \cos \beta - \sin \omega \sin \beta)}{\cos \beta \sin \theta_2} \quad (\text{D.118})$$

$$g_{A_2^0 b \bar{b}}^A = -\frac{i}{\sqrt{2}} \left(\frac{gm_b}{\sqrt{2}M_W} \right) \frac{(-\sin \omega \cos \theta_2 \cos \beta - \cos \omega \sin \beta)}{\cos \beta \sin \theta_2}. \quad (\text{D.119})$$

Details of the models with two Higgs doublets and one triplet

The neutral Higgs couplings to Z are,

$$g_{ZH_1^0 G^0} = \frac{ie}{s_W c_W} \left[-\frac{1}{2} \cos \gamma \sin \theta_2 \cos(\beta - \alpha) - \sin \gamma \cos \theta_2 \right] \quad (D.120)$$

$$g_{ZH_1^0 A_1^0} = \frac{ie}{s_W c_W} \left[-\frac{1}{2} (\cos \gamma \cos \omega \cos \theta_2 \cos(\beta - \alpha) - \cos \gamma \sin \omega \sin(\beta - \alpha)) \right. \\ \left. + \sin \gamma \cos \omega \sin \theta_2 \right] \quad (D.121)$$

$$g_{ZH_1^0 A_2^0} = \frac{ie}{s_W c_W} \left[-\frac{1}{2} (-\cos \gamma \sin \omega \cos \theta_2 \cos(\beta - \alpha) - \cos \gamma \cos \omega \sin(\beta - \alpha)) \right. \\ \left. - \sin \gamma \sin \omega \sin \theta_2 \right] \quad (D.122)$$

$$g_{ZH_2^0 G^0} = \frac{ie}{s_W c_W} \left[\frac{1}{2} \sin \gamma \sin \theta_2 \cos(\beta - \alpha) - \cos \gamma \cos \theta_2 \right] \quad (D.123)$$

$$g_{ZH_2^0 A_1^0} = \frac{ie}{s_W c_W} \left[-\frac{1}{2} (-\sin \gamma \cos \omega \cos \theta_2 \cos(\beta - \alpha) + \sin \gamma \sin \omega \sin(\beta - \alpha)) \right. \\ \left. + \cos \gamma \cos \omega \sin \theta_2 \right] \quad (D.124)$$

$$g_{ZH_2^0 A_2^0} = \frac{ie}{s_W c_W} \left[-\frac{1}{2} (\sin \gamma \sin \omega \cos \theta_2 \cos(\beta - \alpha) + \sin \gamma \cos \omega \sin(\beta - \alpha)) \right. \\ \left. - \cos \gamma \sin \omega \sin \theta_2 \right] \quad (D.125)$$

$$g_{ZH_3^0 G^0} = \frac{ie}{s_W c_W} \left[-\frac{1}{2} \sin \theta_2 \sin(\beta - \alpha) \right] \quad (D.126)$$

$$g_{ZH_3^0 A_1^0} = \frac{ie}{s_W c_W} \left[-\frac{1}{2} (\cos \omega \cos \theta_2 \sin(\beta - \alpha) + \sin \omega \cos(\beta - \alpha)) \right] \quad (D.127)$$

$$g_{ZH_3^0 A_2^0} = \frac{ie}{s_W c_W} \left[-\frac{1}{2} (-\sin \omega \cos \theta_2 \sin(\beta - \alpha) + \cos \omega \cos(\beta - \alpha)) \right]. \quad (D.128)$$

The states and couplings can be simplified a great deal if we take the limit of large $\tan \theta_2$, as required by the measured value of the ρ parameter. We make the approximation, $\cos \theta_2 \approx 0$ and $\sin \theta_2 \approx 1$. Then the CP-odd neutral states simplify to,

$$G^0 \simeq \cos \beta \phi_1^{0,i} + \sin \beta \phi_2^{0,i} \quad (D.129)$$

$$A_1^0 \simeq -\sin \omega \sin \beta \phi_1^{0,i} + \sin \omega \cos \beta \phi_2^{0,i} - \cos \omega \chi^{0,i} \quad (D.130)$$

$$A_2^0 \simeq -\cos \omega \sin \beta \phi_1^{0,i} + \cos \omega \cos \beta \phi_2^{0,i} + \sin \omega \chi^{0,i}. \quad (D.131)$$

The couplings of A_1^0 and A_2^0 to quarks simplify to,

$$g_{A_1^0 b \bar{b}}^A \simeq +\frac{i}{\sqrt{2}} \left(\frac{gm_b}{\sqrt{2}M_W} \right) \tan \beta \sin \omega \quad (D.132)$$

$$g_{A_2^0 b \bar{b}}^A \simeq +\frac{i}{\sqrt{2}} \left(\frac{gm_b}{\sqrt{2}M_W} \right) \tan \beta \cos \omega. \quad (D.133)$$

D.2 $Y = 2$ model

Likewise, the neutral Higgs couplings to Z simplify to,

$$g_{ZH_1^0 G^0} \simeq \frac{ie}{s_W c_W} \left[-\frac{1}{2} \cos \gamma \cos(\beta - \alpha) \right] \quad (\text{D.134})$$

$$g_{ZH_1^0 A_1^0} \simeq \frac{ie}{s_W c_W} \left[\frac{1}{2} \cos \gamma \sin \omega \sin(\beta - \alpha) + \sin \gamma \cos \omega \right] \quad (\text{D.135})$$

$$g_{ZH_1^0 A_2^0} \simeq \frac{ie}{s_W c_W} \left[\frac{1}{2} \cos \gamma \cos \omega \sin(\beta - \alpha) - \sin \gamma \sin \omega \right] \quad (\text{D.136})$$

$$g_{ZH_2^0 G^0} \simeq \frac{ie}{s_W c_W} \left[\frac{1}{2} \sin \gamma \cos(\beta - \alpha) \right] \quad (\text{D.137})$$

$$g_{ZH_2^0 A_1^0} \simeq \frac{ie}{s_W c_W} \left[-\frac{1}{2} \sin \gamma \sin \omega \sin(\beta - \alpha) + \cos \gamma \cos \omega \right] \quad (\text{D.138})$$

$$g_{ZH_2^0 A_2^0} \simeq \frac{ie}{s_W c_W} \left[-\frac{1}{2} \sin \gamma \cos \omega \sin(\beta - \alpha) - \cos \gamma \sin \omega \right] \quad (\text{D.139})$$

$$g_{ZH_3^0 G^0} \simeq \frac{ie}{s_W c_W} \left[-\frac{1}{2} \sin(\beta - \alpha) \right] \quad (\text{D.140})$$

$$g_{ZH_3^0 A_1^0} \simeq \frac{ie}{s_W c_W} \left[-\frac{1}{2} \sin \omega \cos(\beta - \alpha) \right] \quad (\text{D.141})$$

$$g_{ZH_3^0 A_2^0} \simeq \frac{ie}{s_W c_W} \left[-\frac{1}{2} \cos \omega \cos(\beta - \alpha) \right]. \quad (\text{D.142})$$

Appendix E

Custodial $SU(2)$ symmetry and the Georgi–Machacek class of models

The Standard Model (SM) makes a number of successful predictions which arise naturally from the simple form of the SM; for example, the absence of tree-level flavor-changing neutral currents and the equality of the ρ parameter to one at tree-level. Many of these built-in successes are lost when the SM is extended, often requiring parameters of the extended models to be fine-tuned in order to agree with experimental results.

In particular, extended Higgs sectors which contain isospin multiplets larger than doublets will in general yield a value of the ρ parameter different from one. The ρ parameter parameterizes the relation between the W^\pm and Z boson masses and the electroweak mixing angle, as will be further described in section E.2. In such a model, certain parameters must be fine-tuned in order to agree with the measured value of ρ .

Fortunately, there is a class of extended Higgs sectors that automatically yield $\rho = 1$ at tree level, without fine-tuning of parameters. The Higgs doublet of the SM is a member of this class. These models preserve a symmetry, known as “custodial” $SU(2)$ symmetry, which ensures that $\rho = 1$ at tree level. The first extended model of this type was introduced by Georgi and Machacek [42], and contains isospin triplets in addition to the standard Higgs doublet. We will refer to this model as the Georgi–Machacek model. We have generalized the Georgi–Machacek model to include multiplets of arbitrary isospin, while still preserving the custodial symmetry that leads to $\rho = 1$ [63].

In section E.1 we introduce the $SU(2)_L \times SU(2)_R$ transformations and describe how the custodial symmetry is preserved after electroweak symmetry breaking. We also describe the Higgs doublet of the SM in this framework. In section E.2 we explain how models that preserve the custodial symmetry automatically lead to $\rho = 1$ at tree level. This

E.1 Symmetries, notation and conventions

is the motivation for considering models that preserve the custodial symmetry. In section E.3 we describe the Georgi–Machacek model with Higgs triplets and custodial symmetry, first described in reference [42]. In section E.4 we extend the Georgi–Machacek model to include Higgs multiplets of arbitrary size while still preserving the custodial symmetry and $\rho = 1$ at tree level. For the generalized models we derive certain Higgs couplings to fermions in section E.4.1, and to gauge bosons in section E.4.2. Finally in section E.5 we show that the generalized Georgi–Machacek model is not invariant under any accidental global U(1) symmetries, and thus does not contain a massless axion, as some extended Higgs sectors do.

E.1 Symmetries, notation and conventions

In the SM, the standard Higgs doublet can be written as a matrix,

$$\Phi = \begin{pmatrix} \phi^{0*} & \phi^+ \\ -\phi^{+*} & \phi^0 \end{pmatrix} \quad (\text{E.1})$$

which transforms under $\text{SU}(2)_L \times \text{SU}(2)_R$ as $\Phi \rightarrow U_L^\dagger \Phi U_R$. (The neutral states decompose into CP-even and CP-odd parts as $\phi^0 = (\phi^{0,r} + i\phi^{0,i})/\sqrt{2}$.) The transformation matrices are

$$U_{L,R} = \exp[-i\theta_{L,R} \hat{n}_{L,R} \cdot \vec{T}_{L,R}] \quad (\text{E.2})$$

where $\vec{T} = (T^1, T^2, T^3)$ are the generators of SU(2). Φ transforms as a $T_L = 1/2$ representation of $\text{SU}(2)_L$ and a $T_R = 1/2$ representation of $\text{SU}(2)_R$. We denote this by introducing the notation (T_L, T_R) for a multiplet transforming under $\text{SU}(2)_L \times \text{SU}(2)_R$; in this notation, $\Phi = (1/2, 1/2)$.

The $\text{SU}(2)_L \times \text{SU}(2)_R$ doublet Φ does not transform as a multiplet of the usual electroweak gauge symmetries $\text{SU}(2)_L \times \text{U}(1)_Y$, since the two columns of Φ have different values of hypercharge. In fact, hypercharge corresponds to the third component of $\text{SU}(2)_R$, $Y = -2T_R^3$. Because of this, a Higgs potential for Φ which is invariant under the full $\text{SU}(2)_L \times \text{SU}(2)_R$ is also invariant under $\text{SU}(2)_L \times \text{U}(1)_Y$. The SM Higgs potential can be written in a $\text{SU}(2)_L \times \text{SU}(2)_R$ symmetric form without loss of generality.

However, because the hypercharge operator corresponds to the T_3 of $\text{SU}(2)_R$, radiative corrections involving the interaction of the $\text{U}(1)_Y$ gauge boson B_μ with the Higgs sector break the $\text{SU}(2)_c$ symmetry. This violation of $\text{SU}(2)_c$ leads to one-loop corrections to ρ which are quadratically divergent. This problem was first noted in reference [43], and further elaborated in reference [45]. As pointed out in [45], fine-tuning is required to keep ρ near one in a grand-unification scheme in which the quadratic divergence is cut off by the grand-unification scale. However, this fine-tuning is no worse than the fine-tuning required in the SM to control the quadratically divergent one-loop corrections to the SM

Custodial SU(2) symmetry and the Georgi–Machacek class of models

Higgs mass. In what follows we will ignore the breaking of $SU(2)_c$ and the fine-tuning problem; these issues are addressed at length in reference [45].

Under the standard electroweak symmetry breaking, ϕ^0 acquires a vacuum expectation value (vev) $\langle\phi^0\rangle = v_{SM}/\sqrt{2}$, breaking $SU(2)_L \times U(1)_Y$ down to $U(1)_{EM}$. In the matrix notation the vev of Φ is

$$\langle\Phi\rangle = \frac{v_{SM}}{\sqrt{2}} \begin{pmatrix} 1 & 0 \\ 0 & 1 \end{pmatrix}. \quad (\text{E.3})$$

$SU(2)_L \times SU(2)_R$ is broken down to a “custodial” symmetry $SU(2)_c$, under which Φ transforms as $\Phi \rightarrow U_c^\dagger \Phi U_c$, with the transformation matrices

$$U_c = \exp[-i\theta_c \hat{n} \cdot \vec{T}]. \quad (\text{E.4})$$

This is the same as an $SU(2)_L \times SU(2)_R$ transformation with $\theta_L \hat{n}_L = \theta_R \hat{n}_R$. After electroweak symmetry breaking, Φ decomposes into a singlet and a triplet under $SU(2)_c$. The $SU(2)_c$ singlet is

$$H_1^0 = \phi^{0,r} \quad (\text{E.5})$$

and the $SU(2)_c$ triplet is

$$\Phi_3 = (\Phi_3^+, \Phi_3^0, \Phi_3^-) = (\phi^+, \phi^{0,i}, -\phi^{+*}). \quad (\text{E.6})$$

In the SM, the $SU(2)_c$ singlet is the physical Higgs boson and the states of the $SU(2)_c$ triplet are the Goldstone bosons. Electric charge corresponds to the third component of $SU(2)_c$, $Q = T_c^3$.

Let us now extend this notation to an arbitrary multiplet X that transforms as (T, T) under $SU(2)_L \times SU(2)_R$. X can be written as a $(2T+1)$ by $(2T+1)$ matrix. We will denote the vev of X by

$$\langle X \rangle = v_X \mathbf{I}, \quad (\text{E.7})$$

where \mathbf{I} is the identity matrix. In this notation, the vev of the SM doublet is $v_X = \sqrt{2}v_{SM}$.

When $SU(2)_L \times SU(2)_R$ is broken down to $SU(2)_c$, X decomposes as

$$(T, T) \rightarrow 2T \oplus 2T - 1 \oplus \cdots \oplus 1 \oplus 0. \quad (\text{E.8})$$

In this notation, the SM doublet decomposes as $(1/2, 1/2) \rightarrow 1 \oplus 0$, as described before.

Note that when the Higgs potential is invariant under $SU(2)_c$, all the states which transform in a single representation of $SU(2)_c$ must be degenerate in mass.

E.2 Motivation: the ρ parameter under custodial SU(2) symmetry

E.2 Motivation: the ρ parameter under custodial SU(2) symmetry

Perhaps the most important clue we have to the form of the Higgs sector is the relation between the W^\pm and Z masses and the electroweak mixing angle. This relation is parameterized by the ρ parameter,

$$\rho \equiv \frac{M_W^2}{M_Z^2 c_W^2} \quad (\text{E.9})$$

where M_W and M_Z are the W and Z masses and $c_W^2 = \cos^2 \theta_W$ is the cosine of the electroweak mixing angle. Experimentally, $\rho = 1$ to within one percent ([5], in which $\epsilon_1 = \rho - 1$). This follows if the electroweak symmetry breaking gives equal masses to W^\pm and W^3 . This is ensured in a model in which the symmetry breaking preserves $\text{SU}(2)_c$, giving $\langle X \rangle = v_X \mathbf{I}$, as we will now prove.

For simplicity, we will consider only one Higgs multiplet, $X = (T, T)$ under $\text{SU}(2)_L \times \text{SU}(2)_R$. Once we show that X gives equal masses to W^\pm and W^3 , the result is easily extended to a model consisting of an arbitrary set of multiplets X by noting that the resulting gauge boson mass-squared matrix is the sum of the mass-squared matrices coming from each X .

The electroweak gauge boson mass terms come from the covariant derivatives in the Lagrangian with the vev of X inserted. The covariant derivatives of X in the Lagrangian are

$$\mathcal{L} = \frac{1}{2} \text{Tr}[(\mathcal{D}_\mu X)^\dagger (\mathcal{D}^\mu X)] \quad (\text{E.10})$$

where the covariant derivative is

$$\mathcal{D}_\mu = \partial_\mu - ig W_\mu^a T^a - ig' \frac{Y}{2} B_\mu. \quad (\text{E.11})$$

T^a are the generators of $\text{SU}(2)_L$ and Y is the hypercharge. The hypercharge is related to the third component of the $\text{SU}(2)_R$ by,

$$\frac{Y}{2} X = -X T^3. \quad (\text{E.12})$$

The $\text{SU}(2)_c$ -symmetric vev of X is $\langle X \rangle = v_X \mathbf{I}$. Putting all this together, the relevant part of the Lagrangian becomes

$$\mathcal{L} = \frac{1}{2} \text{Tr} \left[\left(ig W_\mu^a v_X T^a - ig' B_\mu T^3 v_X \right) \left(-ig W^{b\mu} T^b v_X + ig' B^\mu v_X T^3 \right) \right] \quad (\text{E.13})$$

$$\begin{aligned} &= \frac{g^2}{2} v_X^2 W_\mu^a W^{b\mu} \text{Tr}[T^a T^b] - 2 \frac{gg'}{2} v_X^2 W_\mu^a B^\mu \text{Tr}[T^a T^3] \\ &\quad + \frac{g'^2}{2} v_X^2 B_\mu B^\mu \text{Tr}[T^3 T^3]. \end{aligned} \quad (\text{E.14})$$

Custodial SU(2) symmetry and the Georgi–Machacek class of models

The traces over the SU(2) generators of a representation r with isospin T are given by $\text{Tr}[T_r^a T_r^b] = C(r)\delta^{ab}$, where $C(r) = T(T+1)(2T+1)/3$ is a constant for each representation r . We find,

$$\mathcal{L} = \frac{T(T+1)(2T+1)}{3} \frac{v_X^2}{2} [g^2 W_\mu^a W^{a\mu} - 2gg' W_\mu^3 B^\mu + g'^2 B_\mu B^\mu]. \quad (\text{E.15})$$

The resulting mass-squared matrix for the gauge bosons is,

$$M^2 = \frac{T(T+1)(2T+1)}{3} v_X^2 \begin{pmatrix} g^2 & 0 & 0 & 0 \\ 0 & g^2 & 0 & 0 \\ 0 & 0 & g^2 & -gg' \\ 0 & 0 & -gg' & g'^2 \end{pmatrix} \quad (\text{E.16})$$

where the rows and columns correspond to W_μ^1 , W_μ^2 , W_μ^3 , and B_μ . Note that equal masses are given to all three W^a .

The gauge boson masses are as follows. W_μ^1 and W_μ^2 mix to form the charge eigenstates

$$W_\mu^\pm = \frac{1}{\sqrt{2}}(W_\mu^1 \mp W_\mu^2), \quad (\text{E.17})$$

with mass $M_W^2 = g^2 v_X^2 T(T+1)(2T+1)/3$. W_μ^3 and B_μ mix to form the Z_μ and the (massless) photon A_μ ,

$$Z_\mu = \frac{1}{\sqrt{g^2 + g'^2}}(gW_\mu^3 - g'B_\mu) \quad (\text{E.18})$$

$$= c_W W_\mu^3 - s_W B_\mu \quad (\text{E.19})$$

$$A_\mu = \frac{1}{\sqrt{g^2 + g'^2}}(g'W_\mu^3 + gB_\mu) \quad (\text{E.20})$$

$$= s_W W_\mu^3 + c_W B_\mu \quad (\text{E.21})$$

where $c_W = \cos \theta_W$, $s_W = \sin \theta_W$, and c_W is,

$$c_W = \frac{g}{\sqrt{g^2 + g'^2}}. \quad (\text{E.22})$$

Finally the Z mass is $M_Z^2 = (g^2 + g'^2)v_X^2 T(T+1)(2T+1)/3$.

Combining M_W , M_Z , and c_W , we find that the ρ parameter is

$$\rho = \frac{M_W^2}{M_Z^2 c_W^2} = 1 \quad (\text{E.23})$$

E.3 The Georgi–Machacek model with Higgs triplets

in this model, for any values of v_X and T . This result remains true for a Higgs sector consisting of any combination of multiplets X as long as $\langle X \rangle$ is invariant under $SU(2)_c$ for each X .

In the SM, $T = 1/2$ giving $C(r) = 1/2$. The resulting W and Z masses are, using $v_{SM} = \sqrt{2}v_X = 246$ GeV,

$$M_W^2 = \frac{g^2}{4} v_{SM}^2 \quad (\text{E.24})$$

$$M_Z^2 = \frac{g^2 + g'^2}{4} v_{SM}^2. \quad (\text{E.25})$$

E.3 The Georgi–Machacek model with Higgs triplets

In this section we review in detail a model with custodial $SU(2)$ symmetry and Higgs triplets. This model was first constructed by Georgi and Machacek [42]. It was considered in greater depth by Chanowitz and Golden [43], who showed that a Higgs potential for the model could be constructed that was invariant under the full $SU(2)_L \times SU(2)_R$. This ensured that radiative corrections from Higgs self-interactions preserved $SU(2)_c$. A more detailed study of the phenomenology of the model [44] and naturalness problems from one-loop effects [45] was made by Gunion, Vega, and Wudka. This model is also reviewed in [11].

Notation and conventions

This model contains a complex $Y = 1$ doublet $\Phi = (\phi^+, \phi^0)$, a real $Y = 0$ triplet $\xi = (\xi^+, \xi^0, \xi^-)$ (with $\xi^{0*} = \xi^0$ and $\xi^- = -\xi^{+*}$), and a complex $Y = 2$ triplet $\chi = (\chi^{++}, \chi^+, \chi^0)$. In the $SU(2)_L \times SU(2)_R$ notation, the Higgs fields take the form

$$\Phi = \begin{pmatrix} \phi^{0*} & \phi^+ \\ -\phi^{+*} & \phi^0 \end{pmatrix} \quad (\text{E.26})$$

$$\chi = \begin{pmatrix} \chi^{0*} & \xi^+ & \chi^{++} \\ -\chi^{+*} & \xi^0 & \chi^+ \\ \chi^{++*} & \xi^- & \chi^0 \end{pmatrix} \quad (\text{E.27})$$

which transform respectively as a $(1/2, 1/2)$ and $(1, 1)$ of $SU(2)_L \times SU(2)_R$. This definition differs slightly from that of references [42, 44, 45, 11], which use $\chi = (\chi^{++}, \chi^+, \chi^{0*})$, so that χ^{0*} appears in place of χ^0 . Otherwise the phase conventions here are the same. (References [42, 44, 45, 11] define the negative-charged states $\phi^- = -(\phi^+)^*$, $\chi^{--} = (\chi^{++})^*$, and $\chi^- = -(\chi^+)^*$. We avoid these definitions in order to avoid confusion when the Georgi–Machacek model is extended to larger representations of $SU(2)_L \times SU(2)_R$.)

Custodial SU(2) symmetry and the Georgi–Machacek class of models

The electroweak symmetry breaking preserves tree level custodial SU(2)_c when the vevs of the fields are diagonal,

$$\langle \Phi \rangle = \begin{pmatrix} v_\phi/\sqrt{2} & 0 \\ 0 & v_\phi/\sqrt{2} \end{pmatrix} \quad (\text{E.28})$$

$$\langle \chi \rangle = \begin{pmatrix} v_\chi & 0 & 0 \\ 0 & v_\chi & 0 \\ 0 & 0 & v_\chi \end{pmatrix} \quad (\text{E.29})$$

For the triplets, this means $\langle \chi^0 \rangle = \langle \xi^0 \rangle$. (In the notation of [42,44,45,11] the vevs are $v_\phi = a$, $v_\chi = b$.)

The W^\pm and Z masses fix a combination of the vevs. At tree level,

$$M_W^2 = M_Z^2 \cos^2 \theta_W = \frac{g^2}{4} v_{SM}^2 \quad (\text{E.30})$$

$$= \frac{g^2}{4} (v_\phi^2 + 8v_\chi^2). \quad (\text{E.31})$$

As in [42,44,45,11] we define the doublet–triplet mixing angle θ_H by

$$\tan \theta_H = \frac{2\sqrt{2}v_\chi}{v_\phi}, \quad (\text{E.32})$$

so that

$$c_H \equiv \cos \theta_H = \frac{v_\phi}{\sqrt{v_\phi^2 + 8v_\chi^2}} \quad (\text{E.33})$$

$$s_H \equiv \sin \theta_H = \sqrt{\frac{8v_\chi}{v_\phi^2 + 8v_\chi^2}}. \quad (\text{E.34})$$

We also define the charged states of χ transforming in the triplet and fiveplet representations of SU(2)_c,

$$\chi_3^+ = \frac{\chi^+ + \xi^+}{\sqrt{2}} \quad (\text{E.35})$$

$$\chi_5^+ = \frac{\chi^+ - \xi^+}{\sqrt{2}}, \quad (\text{E.36})$$

which obey the phase convention $\chi_3^- = -(\chi_3^+)^*$, $\chi_5^- = -(\chi_5^+)^*$. We use a slightly different notation from references [42,44,45,11]. This notation will make the analysis of the generalized Georgi–Machacek model in section E.4 more straightforward. In the notation of [42,44,45,11], $\chi_3^\pm = \psi^\pm$ and $\chi_5^\pm = \zeta^\pm$.

E.3 The Georgi–Machacek model with Higgs triplets

The W and Z are given mass by absorbing the Goldstone bosons,

$$G_3^0 = c_H \phi^{0,i} + s_H \chi^{0,i} \quad (\text{E.37})$$

$$G_3^+ = c_H \phi^+ + s_H \chi_3^+ \quad (\text{E.38})$$

which together form an $\text{SU}(2)_c$ triplet, with $G_3^- = -(G_3^+)^*$. The remaining physical states are classified according to their transformation properties under $\text{SU}(2)_c$. The model contains a five-plet $H_5^{++,+,0,-,--}$, a triplet $H_3^{+,0,-}$, and two singlets, H_1^0 and $H_1^{0'}$. In terms of the fields of Φ and χ , these states are,

$$H_5^{++} = \chi^{++} \quad (\text{E.39})$$

$$H_5^+ = \chi_5^+ \quad (\text{E.40})$$

$$H_5^0 = \frac{\sqrt{2}\xi^0 - \chi^{0,r}}{\sqrt{3}} \quad (\text{E.41})$$

$$H_3^+ = -s_H \phi^+ + c_H \chi_3^+ \quad (\text{E.42})$$

$$H_3^0 = -s_H \phi^{0,i} + c_H \chi^{0,i} \quad (\text{E.43})$$

$$H_1^0 = \phi^{0,r} \quad (\text{E.44})$$

$$H_1^{0'} = \frac{\sqrt{2}\chi^{0,r} + \xi^0}{\sqrt{3}}. \quad (\text{E.45})$$

According to our phase conventions, the charged states obey $H_5^{--} = (H_5^{++})^*$, $H_5^- = -(H_5^+)^*$, and $H_3^- = -(H_3^+)^*$. H_3^0 is CP-odd while all the other neutral states are CP-even.

Not all of these states need be mass eigenstates; in general they will mix with each other in a way determined by the details of the Higgs potential. H_5^{++} is always a mass eigenstate since there is no other doubly-charged Higgs state for it to mix with. If the Higgs potential is CP-invariant, then H_3^0 will be a mass eigenstate, since H_3^0 is CP-odd while all the other neutral Higgs states are CP-even. Finally, if the Higgs potential is invariant under the full $\text{SU}(2)_L \times \text{SU}(2)_R$ symmetry, the mixing is further constrained. After electroweak symmetry breaking, such a Higgs potential would remain invariant under $\text{SU}(2)_c$. Then states which transform under different representations of $\text{SU}(2)_c$ cannot mix with each other. Thus in this case only H_1^0 and $H_1^{0'}$ can mix; all the other states in equation E.45 are mass eigenstates.

Chanowitz and Golden [43] showed that a Higgs potential could be constructed which was invariant under $\text{SU}(2)_R \times \text{SU}(2)_L$, and therefore preserved $\text{SU}(2)_c$ after electroweak symmetry breaking. This potential has two benefits. First, the $\text{SU}(2)_c$ -preserving vevs of the Higgs multiplets are required by the symmetry of the potential. Second, when radiative corrections are included the $\text{SU}(2)_c$ symmetry is preserved to all orders in the Higgs self couplings. Then the radiative corrections to ρ from Higgs self-interactions are

Custodial SU(2) symmetry and the Georgi–Machacek class of models

zero. In addition, if the Higgs potential is invariant under $SU(2)_c$, then Higgs states which transform in a single representation of $SU(2)_c$ will be degenerate at tree level. This degeneracy will be preserved to all orders in the Higgs self couplings. In particular, H_3^0 and H_3^\pm will have the same mass, denoted M_{H_3} , and H_5^0 , H_5^\pm , and $H_5^{\pm\pm}$ will have the same mass, denoted M_{H_5} .

In the following sections we list the couplings for the Higgs states given in equation E.45.

Couplings to fermions

The fermion couplings in this model have been studied in [44,11]. Only $SU(2)_L$ doublets with $Y = \pm 1$ can have $SU(2)_L \times U(1)_Y$ invariant couplings to fermions without violating lepton number. We will only consider couplings of this type. In principle the $Y = 2$ triplet Higgs field can couple to the lepton–lepton channel, violating lepton number, but we will assume that this does not happen.

Since only the doublet field couples to fermions, the fermion couplings of Higgs mass eigenstates will arise from the overlap of the mass eigenstates with Φ . Under $SU(2)_c$ Φ contains a singlet (H_1^0) and a triplet. Therefore if the Higgs potential preserves the $SU(2)_c$ symmetry, only $SU(2)_c$ singlets and triplets can have an overlap with Φ . This is evident in the states of equation E.45. Only H_3^\pm , H_3^0 , and H_1^0 will have nonzero fermion–antifermion couplings. The couplings of the Higgs mass eigenstates to fermions in this model are of the form

$$i(g_{H\bar{f}f'}^L P_L + g_{H\bar{f}f'}^R P_R) = i(g_{H\bar{f}f'}^V + g_{H\bar{f}f'}^A \gamma_5) \quad (\text{E.46})$$

where $P_{R,L} = (1 \pm \gamma_5)/2$. Using third-generation notation,

$$g_{H_1^0 f \bar{f}}^V = -\frac{gm_f}{2M_W c_H} \quad (\text{E.47})$$

$$g_{H_3^0 t \bar{t}}^A = -\frac{igm_t s_H}{2M_W c_H} \quad (\text{E.48})$$

$$g_{H_3^0 b \bar{b}}^A = \frac{igm_b s_H}{2M_W c_H} \quad (\text{E.49})$$

$$g_{H_3^\pm t \bar{b}}^L = \frac{-gm_t s_H}{\sqrt{2}M_W c_H} \quad (\text{E.50})$$

$$g_{H_3^\pm t \bar{b}}^R = \frac{gm_b s_H}{\sqrt{2}M_W c_H}. \quad (\text{E.51})$$

Analogous expressions hold for the couplings to leptons. H_1^0 is CP-even so it has only vector couplings to fermions. G^0 and H_3^0 are CP-odd so they have only axial–vector

E.3 The Georgi–Machacek model with Higgs triplets

couplings to fermions. For completeness we also list the couplings of the Goldstone bosons to fermions,

$$g_{G^0 t \bar{t}}^A = \frac{igm_t}{2M_W} \quad (\text{E.52})$$

$$g_{G^0 b \bar{b}}^A = -\frac{igm_b}{2M_W} \quad (\text{E.53})$$

$$g_{G^+ \bar{t} b}^L = \frac{gm_t}{\sqrt{2}M_W} \quad (\text{E.54})$$

$$g_{G^+ \bar{t} b}^R = \frac{-gm_b}{\sqrt{2}M_W}. \quad (\text{E.55})$$

These couplings agree with those in reference [11] except for the H_3^0 couplings, which differ by a minus sign. This sign comes from the sign of $\langle H_3^0 | \phi^{0,i} \rangle = -s_H$, whereas in reference [11], $\langle H_3^0 | \phi^{0,i} \rangle = +s_H$. This difference is due ultimately to reference [11] defining the neutral state of the $Y = 2$ $\text{SU}(2)_L$ triplet to be χ^{0*} instead of χ^0 .

Couplings to gauge bosons

In this section we list the Higgs couplings to vector bosons. The Higgs–Vector–Vector (HVV) couplings in this model were first studied in [42], while the Higgs–Higgs–Vector (HHV) couplings were first studied in [44]. For completeness we list them here, using our phase conventions.

We list first the HVV couplings. The $HV_1 V_2$ vertex is $ig_{HV_1 V_2} g^{\mu\nu}$, where V_1 and V_2 are any two vector bosons. The couplings are,

$$g_{H_5^{++} W^- W^-} = \sqrt{2} g M_W s_H \quad (\text{E.56})$$

$$g_{H_5^+ W^- Z} = -\frac{g M_W s_H}{c_W} \quad (\text{E.57})$$

$$g_{H_5^+ W^- \gamma} = 0 \quad (\text{E.58})$$

$$g_{H_5^0 W^- W^+} = \frac{g M_W s_H}{\sqrt{3}} \quad (\text{E.59})$$

$$g_{H_5^0 Z Z} = -\frac{2g M_W s_H}{\sqrt{3} c_W^2} \quad (\text{E.60})$$

$$g_{H_1^0 W^- W^+} = g M_W c_H \quad (\text{E.61})$$

$$g_{H_1^0 Z Z} = \frac{g M_W c_H}{c_W^2} \quad (\text{E.62})$$

$$g_{H_1^{0'} W^- W^+} = \frac{2\sqrt{2}}{\sqrt{3}} g M_W s_H \quad (\text{E.63})$$

$$g_{H_1^{0'} ZZ} = \frac{2\sqrt{2}}{\sqrt{3}} \frac{gM_W s_H}{c_W^2}. \quad (\text{E.64})$$

The H_3^\pm, H_3^0 states do not couple to vector boson pairs.

In the limit of $s_H \rightarrow 0$, H_1^0 plays the role of the SM Higgs boson with SM couplings, while the HVV and Higgs–fermion couplings of the rest of the states go to zero. However we reemphasize that in this model with SU(2)_c, s_H is not required to be small.

There is a nonzero $H_5^+ W^- Z$ coupling in this model, which is absent in any model containing only Higgs doublets and singlets. This coupling raises the possibility of charged Higgs production via $Z \rightarrow H_5^+ W^-$ or $W^+ \rightarrow H_5^+ Z$, which are unmistakable indications of a Higgs sector containing multiplets larger than doublets.

Finally we note that the couplings of H_3 and H_5 are strikingly different. H_3 couples to fermion–antifermion pairs and not to gauge boson pairs, while H_5 couples to gauge boson pairs and not to fermion–antifermion pairs. Thus, disregarding HV and HH channels, the H_3 can only couple and decay to fermion–antifermion pairs while the H_5 can only couple and decay to gauge boson pairs.

We now list the HHV couplings. The $H_1 H_2 V$ vertex is $ig_{H_1 H_2 V}(p_1 - p_2)^\mu$, where p_1 (p_2) is the incoming momentum of H_1 (H_2). The couplings are,

$$g_{H_1^0(H_3^+)^*W^+} = +\frac{gs_H}{2} \quad (\text{E.65})$$

$$g_{H_1^0(H_5^+)^*W^+} = 0 \quad (\text{E.66})$$

$$g_{H_1^{0'}(H_3^+)^*W^+} = -\sqrt{\frac{2}{3}}g^{c_H} \quad (\text{E.67})$$

$$g_{H_1^{0'}(H_5^+)^*W^+} = 0 \quad (\text{E.68})$$

$$g_{H_5^0(H_3^+)^*W^+} = \frac{-g^{c_H}}{2\sqrt{3}} \quad (\text{E.69})$$

$$g_{H_5^0(H_5^+)^*W^+} = \frac{\sqrt{3}}{2}g \quad (\text{E.70})$$

$$g_{H_3^0(H_5^+)^*W^+} = -i\frac{g}{2}c_H \quad (\text{E.71})$$

$$g_{H_3^0(H_3^+)^*W^+} = -i\frac{g}{2} \quad (\text{E.72})$$

$$g_{H_5^+(H_5^{++})^*W^+} = \frac{-g}{\sqrt{2}} \quad (\text{E.73})$$

$$g_{H_3^+(H_5^{++})^*W^+} = \frac{-g^{c_H}}{\sqrt{2}} \quad (\text{E.74})$$

$$g_{H_3^0 H_1^0 Z} = \frac{-igs_H}{2c_W} \quad (\text{E.75})$$

E.4 The generalized Georgi–Machacek models

$$g_{H_3^0 H_1^{0'} Z} = \frac{\sqrt{2}igc_H}{\sqrt{3}c_W} \quad (\text{E.76})$$

$$g_{H_3^0 H_5^0 Z} = \frac{-igc_H}{\sqrt{3}c_W} \quad (\text{E.77})$$

$$g_{(H_5^+)^* H_3^+ Z} = \frac{-gc_H}{2c_W} \quad (\text{E.78})$$

$$g_{(H_3^+)^* H_3^+ Z} = \frac{g}{c_W} \left(\frac{1}{2} - s_W^2 \right) \quad (\text{E.79})$$

$$g_{(H_5^+)^* H_5^+ Z} = \frac{g}{c_W} \left(\frac{1}{2} - s_W^2 \right) \quad (\text{E.80})$$

$$g_{(H_5^{++})^* H_5^{++} Z} = \frac{g}{c_W} (1 - 2s_W^2). \quad (\text{E.81})$$

Couplings of a pair of charged Higgs bosons to the photon are diagonal and are determined solely by the charge,

$$g_{H_3^+ (H_3^+)^* \gamma} = g_{H_5^+ (H_5^+)^* \gamma} = -e \quad (\text{E.82})$$

$$g_{H_5^{++} (H_5^{++})^* \gamma} = -2e. \quad (\text{E.83})$$

E.4 The generalized Georgi–Machacek models

In this section we describe our generalization of the Georgi–Machacek model to include multiplets of arbitrary isospin, while still preserving $\text{SU}(2)_c$ [63].

We construct a generalized Georgi–Machacek model out of a set of multiplets $X = (T, T)$ of $\text{SU}(2)_L \times \text{SU}(2)_R$. The $\text{SU}(2)_L \times \text{U}(1)_Y$ content of some of these are listed in table E.1. The multiplets X acquire vevs proportional to the unit matrix, $\langle X \rangle = v_X \mathbf{I}$, in order to preserve $\text{SU}(2)_c$. We assume that the Higgs potential is symmetric under the full $\text{SU}(2)_L \times \text{SU}(2)_R$, so that after electroweak symmetry breaking the Higgs potential preserves $\text{SU}(2)_c$. This has three significant consequences. First, the vevs of the multiplets X automatically preserve $\text{SU}(2)_c$. Second, $\text{SU}(2)_c$ is not broken by radiative corrections in the Higgs sector, so $\rho = 1$ to all orders in the Higgs self couplings. Finally, the physical Higgs states can be classified by their transformation properties under $\text{SU}(2)_c$, and states in different representations of $\text{SU}(2)_c$ do not mix with each other.

Let us define the following notation for the states that transform under $\text{SU}(2)_c$. A Higgs doublet $\Phi = (1/2, 1/2)$ decomposes after electroweak symmetry breaking into a singlet and a triplet under $\text{SU}(2)_c$. We will denote the singlet by $\Phi_1 = H_1^0$ (in analogy to the triplet Georgi–Machacek model), and the triplet by $\Phi_3 = (\Phi_3^+, \Phi_3^0, \Phi_3^-)$. Similarly, a general multiplet $X = (T, T)$ decomposes into the $\text{SU}(2)_c$ multiplets $2T \oplus 2T - 1 \oplus \dots \oplus 1 \oplus 0$. We will denote these as $X_{4T+1}, X_{4T-1}, \dots, X_3, X_1$. We will also define $X_1 = H_1^{0'}$, in analogy to the triplet Georgi–Machacek model.

T	Y	(T_L, T_R)
1/2	1	(1/2, 1/2)
1	0	(1, 1)
1	2	
3/2	1	(3/2, 3/2)
3/2	3	
2	0	(2, 2)
2	2	
2	4	
5/2	1	(5/2, 5/2)
5/2	3	
5/2	5	
3	0	(3, 3)
3	2	
3	4	
3	6	
\vdots	\vdots	\vdots

Table E.1: Sets of multiplets of $SU(2)_L \times U(1)_Y$ which combine into a single multiplet of $SU(2)_L \times SU(2)_R$ in the generalized Georgi–Machacek models. Multiplets with $Y = 0$ are real; the rest are complex.

E.4 The generalized Georgi–Machacek models

For simplicity we consider a model which contains only two multiplets of fields, one doublet, $\Phi = (1/2, 1/2)$, and one larger multiplet, $X = (T, T)$. In general, the two $SU(2)_c$ singlets, Φ_1 and X_1 , will mix with each other to form mass eigenstates. The two $SU(2)_c$ triplets, Φ_3 and X_3 , will also mix with each other to form the triplet of Goldstone bosons and a physical triplet of Higgs states. The remaining $SU(2)_c$ multiplets of X will not mix and will be mass eigenstates.

In section E.4.1 we derive the fermion–antifermion couplings of all the Higgs states in a generalized Georgi–Machacek model. In section E.4.2 we derive some of the Higgs couplings to vector bosons. In particular, we find the $ZH_3^+H_3^-$ coupling, which appears in the loop corrections to the $Zb\bar{b}$ vertex, and the $H_1^0, H_1^{0'}$ couplings to vector boson pairs, which are relevant for Higgs boson production at LEP and the Tevatron.

E.4.1 Couplings to fermions

In this section we describe how the Higgs couplings to fermions arise in the generalized Georgi–Machacek models. For simplicity we consider a model containing two multiplets of fields, $\Phi = (1/2, 1/2)$ and $X = (T, T)$. Φ is the usual $SU(2)_L$ doublet with hypercharge 1. X is an exotic multiplet with isospin T under both $SU(2)_L$ and $SU(2)_R$.

Φ couples to fermions in the normal way, while X does not couple to fermions. The Yukawa coupling to a fermion f is

$$\lambda_f = \frac{\sqrt{2}m_f}{v_\phi} \quad (\text{E.84})$$

where $\langle\phi^0\rangle = v_\phi/\sqrt{2}$. This is a Type I model since a single Higgs doublet gives mass to all fermions.

The vevs are constrained by the W mass to obey the relation

$$\left(\frac{2M_W}{g}\right)^2 = v_{SM}^2 = \sum_k 2v_k^2(T_k(T_k + 1) - Y_k^2/4) + \sum_i 2v_i^2T_i(T_i + 1) \quad (\text{E.85})$$

where k runs over the complex representations of $SU(2)_L$, i runs over the real representations of $SU(2)_L$ with $Y_i = 0$, and the vevs are normalized according to $\langle\phi_k^0\rangle = v_k/\sqrt{2}$ and $\langle\eta_i^0\rangle = v_i$. Summing over Φ and the multiplets of X , and using $v_k = \sqrt{2}v_X$ for the complex representations in X , we obtain

$$\left(\frac{2M_W}{g}\right)^2 = v_{SM}^2 = v_\phi^2 + \frac{4}{3}T(T + 1)(2T + 1)v_X^2 \quad (\text{E.86})$$

for any T . Using this, we can write v_ϕ as

$$v_\phi = v_{SM} \cos \theta_H \quad (\text{E.87})$$

Custodial SU(2) symmetry and the Georgi–Machacek class of models

where we have defined a mixing angle θ_H in analogy with the triplet Georgi–Machacek model as

$$\tan \theta_H = \frac{\sqrt{\frac{4}{3}T(T+1)(2T+1)}v_X}{v_\phi}. \quad (\text{E.88})$$

This mixing angle also appears in the Goldstone bosons, as we will show below. In terms of θ_H the Yukawa coupling for fermion f is

$$\lambda_f = \frac{gm_f}{\sqrt{2}M_W \cos \theta_H}. \quad (\text{E.89})$$

Note that the Yukawa couplings increase as v_ϕ decreases.

The couplings of the Higgs mass eigenstates to fermions in this model are of the form

$$i(g_{H\bar{f}f'}^L P_L + g_{H\bar{f}f'}^R P_R) = i(g_{H\bar{f}f'}^V + g_{H\bar{f}f'}^A \gamma_5) \quad (\text{E.90})$$

where $P_{R,L} = (1 \pm \gamma_5)/2$ and using third-generation notation,

$$g_{H_i^0 f \bar{f}}^V = -\frac{1}{\sqrt{2}} \lambda_f \langle H_i^0 | \phi^{0,r} \rangle \quad (\text{E.91})$$

$$g_{A_i^0 t \bar{t}}^A = +\frac{i}{\sqrt{2}} \lambda_t \langle A_i^0 | \phi^{0,i} \rangle \quad (\text{E.92})$$

$$g_{A_i^0 b \bar{b}}^A = -\frac{i}{\sqrt{2}} \lambda_b \langle A_i^0 | \phi^{0,i} \rangle \quad (\text{E.93})$$

$$g_{H_i^+ t \bar{b}}^R = -\lambda_b \langle H_i^+ | \phi^+ \rangle \quad (\text{E.94})$$

$$g_{H_i^+ t \bar{b}}^L = +\lambda_t \langle H_i^+ | \phi^+ \rangle. \quad (\text{E.95})$$

Thus the Higgs–fermion couplings depend on the overlap of Higgs mass eigenstates with Φ . Since Φ contains only a singlet and a triplet of $\text{SU}(2)_c$, only singlets and triplets of $\text{SU}(2)_c$ can couple to fermions.

$\text{SU}(2)_c$ singlets

The fermion couplings of the $\text{SU}(2)_c$ singlets are straightforward to find. The two singlets are,

$$H_1^0 = \Phi_1 = \phi^{0,r} \quad (\text{E.96})$$

$$H_1^{0'} = X_1. \quad (\text{E.97})$$

An expression for X_1 is derived in section E.4.2. H_1^0 and $H_1^{0'}$ mix by an arbitrary angle to form the mass eigenstates. Their couplings to fermions are

$$g_{H_1^0 f \bar{f}}^V = -\frac{gm_f}{2M_W \cos \theta_H} \quad (\text{E.98})$$

E.4 The generalized Georgi–Machacek models

$$g_{H_1^{0'} f \bar{f}}^V = 0. \quad (\text{E.99})$$

Since H_1^0 and $H_1^{0'}$ are CP-even they have only vector couplings to fermions. Their axial-vector couplings g^A are zero. Note that in terms of θ_H , these couplings are the same as the corresponding couplings in the triplet Georgi–Machacek model. If H_1^0 and $H_1^{0'}$ mix by an angle α to form the mass eigenstates

$$H^0 = \cos \alpha H_1^0 + \sin \alpha H_1^{0'} = \cos \alpha \phi^{0,r} + \sin \alpha X_1 \quad (\text{E.100})$$

$$h^0 = -\sin \alpha H_1^0 + \cos \alpha H_1^{0'} = -\sin \alpha \phi^{0,r} + \cos \alpha X_1, \quad (\text{E.101})$$

then the couplings to fermions will be

$$g_{H^0 f \bar{f}}^V = -\frac{gm_f \cos \alpha}{2M_W \cos \theta_H} \quad (\text{E.102})$$

$$g_{h^0 f \bar{f}}^V = +\frac{gm_f \sin \alpha}{2M_W \cos \theta_H}. \quad (\text{E.103})$$

$\text{SU}(2)_c$ triplets

In order to find the fermion couplings of the $\text{SU}(2)_c$ triplets, we must first find the mass eigenstates. The $\text{SU}(2)_c$ triplets Φ_3 and X_3 mix to form a triplet of Goldstone bosons and a triplet of physical states. We will denote the triplet of Goldstone bosons by $G_3 = (G^+, G^0, G^-)$ and the triplet of physical states by $H_3 = (H_3^+, H_3^0, H_3^-)$.

The neutral Goldstone boson is given by

$$G^0 = \frac{\sum_k Y_k v_k \phi_k^{0,i}}{\sqrt{\sum_k Y_k^2 v_k^2}} \quad (\text{E.104})$$

where again k runs over the complex representations of $\text{SU}(2)_L$ and the vevs are normalized according to $\langle \phi_k^0 \rangle = v_k / \sqrt{2}$. X_3^0 is the combination of the multiplets of X that appears in G^0 , which can be obtained by setting $v_\phi = 0$,

$$X_3^0 = \frac{\sum_{k \in X} Y_k v_k \chi_k^{0,i}}{\sqrt{\sum_{k \in X} Y_k^2 v_k^2}}. \quad (\text{E.105})$$

Inserting this and the contribution from Φ into equation E.104 we obtain

$$G^0 = \frac{\sqrt{\sum_{k \in X} (Y_k^2 v_k^2)} X_3^0 + v_\phi \Phi_3^0}{\sqrt{\sum_{k \in X} (Y_k^2 v_k^2) + v_\phi^2}} \quad (\text{E.106})$$

Custodial SU(2) symmetry and the Georgi–Machacek class of models

where $\Phi_3^0 = \phi^{0,i}$. Summing over the multiplets of X , and using $v_k = \sqrt{2}v_X$ for the complex representations in X , we obtain

$$G^0 = \frac{v_X \sqrt{\frac{4}{3}T(T+1)(2T+1)}X_3^0 + v_\phi \Phi_3^0}{\sqrt{v_X^2 \frac{4}{3}T(T+1)(2T+1) + v_\phi^2}} \quad (\text{E.107})$$

$$= \sin \theta_H X_3^0 + \cos \theta_H \Phi_3^0 \quad (\text{E.108})$$

where θ_H is the mixing angle defined in equation E.88. The orthogonal state is the neutral member of the physical SU(2)_c triplet,

$$H_3^0 = \cos \theta_H X_3^0 - \sin \theta_H \Phi_3^0. \quad (\text{E.109})$$

We can now find the fermion couplings of the neutral members of the SU(2)_c triplets. They are, using third-generation notation,

$$g_{G^0 t\bar{t}}^A = \frac{igm_t}{2M_W} \quad (\text{E.110})$$

$$g_{G^0 b\bar{b}}^A = -\frac{igm_b}{2M_W} \quad (\text{E.111})$$

$$g_{H_3^0 t\bar{t}}^A = -\frac{igm_t \tan \theta_H}{2M_W} \quad (\text{E.112})$$

$$g_{H_3^0 b\bar{b}}^A = \frac{igm_b \tan \theta_H}{2M_W}. \quad (\text{E.113})$$

Since G^0 and H_3^0 are CP-odd they have only axial-vector couplings to fermions. Their vector couplings g^V are zero. Note that in terms of θ_H , these couplings are the same as the corresponding couplings in the triplet Georgi–Machacek model.

We now find the couplings for the charged states G^\pm and H_3^\pm . The charged Goldstone boson is given by

$$\begin{aligned} G^+ = & \left\{ \sum_k \left[[T_k(T_k+1) - Y_k(Y_k-2)/4]^{1/2} v_k \phi_k^+ \right. \right. \\ & \left. \left. - [T_k(T_k+1) - Y_k(Y_k+2)/4]^{1/2} v_k (\phi_k^-)^* \right] + \sum_i [2T_i(T_i+1)]^{1/2} v_i \eta_i^+ \right\} \\ & \times \left\{ \sum_k 2v_k^2 [T_k(T_k+1) - Y_k^2/4] + \sum_i 2v_i^2 T_i(T_i+1) \right\}^{-1/2} \end{aligned} \quad (\text{E.114})$$

where again k runs over the complex representations of SU(2)_L and the vevs are normalized according to $\langle \phi_k^0 \rangle = v_k/\sqrt{2}$. X_3^+ is the combination of the multiplets of X that appears in

E.4 The generalized Georgi–Machacek models

G^+ , which can be obtained by setting $v_\phi = 0$ in equation E.114,

$$\begin{aligned}
X_3^+ &= \left\{ \sum_{k \in X} \left[[T(T+1) - Y_k(Y_k - 2)/4]^{1/2} v_k \chi_k^+ \right. \right. \\
&\quad \left. \left. - [T(T+1) - Y_k(Y_k + 2)/4]^{1/2} v_k (\chi_k^-)^* \right] + \sum_{i \in X} [2T(T+1)]^{1/2} v_i \xi_i^+ \right\} \\
&\quad \times \left\{ \sum_{k \in X} 2v_k^2 [T(T+1) - Y_k^2/4] + \sum_{i \in X} 2v_i^2 T(T+1) \right\}^{-1/2}. \tag{E.115}
\end{aligned}$$

Inserting this and the contribution from Φ into equation E.114, we obtain

$$G^+ = \frac{\sqrt{\sum_{k \in X} 2v_k^2 (T(T+1) - Y_k^2/4) + \sum_{i \in X} 2v_i^2 T(T+1)} X_3^+ + v_\phi \Phi_3^+}{\sqrt{\sum_{k \in X} (2v_k^2 (T(T+1) - Y_k^2/4)) + \sum_{i \in X} (2v_i^2 T(T+1)) + v_\phi^2}} \tag{E.116}$$

where $\Phi_3^+ = \phi^+$. Summing over the multiplets of X , using $v_k = \sqrt{2}v_X$ for the complex representations in X , and remembering that X only contains a real representation if T is an integer (in which case $v_i = v_X$), we obtain for any T ,

$$G^+ = \frac{v_X \sqrt{\frac{4}{3}T(T+1)(2T+1)} X_3^+ + v_\phi \Phi_3^+}{\sqrt{v_X^2 \frac{4}{3}T(T+1)(2T+1) + v_\phi^2}} \tag{E.117}$$

$$= \sin \theta_H X_3^+ + \cos \theta_H \Phi_3^+ \tag{E.118}$$

where again θ_H is the mixing angle defined in equation E.88. The orthogonal state is the charged member of the physical $SU(2)_c$ triplet,

$$H_3^+ = \cos \theta_H X_3^+ - \sin \theta_H \Phi_3^+. \tag{E.119}$$

We can now find the fermion couplings of the charged members of the $SU(2)_c$ triplets. They are, using third-generation notation,

$$g_{G^+ \bar{t} b}^L = \frac{gm_t}{\sqrt{2}M_W} \tag{E.120}$$

$$g_{G^+ \bar{t} b}^R = \frac{-gm_b}{\sqrt{2}M_W} \tag{E.121}$$

$$g_{H_3^+ \bar{t} b}^L = \frac{-gm_t \tan \theta_H}{\sqrt{2}M_W} \tag{E.122}$$

$$g_{H_3^+ \bar{t} b}^R = \frac{gm_b \tan \theta_H}{\sqrt{2}M_W} \tag{E.123}$$

Note that in terms of θ_H , these couplings are the same as the corresponding couplings in the triplet Georgi–Machacek model.

E.4.2 Couplings to gauge bosons

In this section we derive some of the Higgs couplings to vector bosons in the generalized Georgi–Machacek models. In particular, we find the $ZH_3^+H_3^-$ coupling, which appears in the loop corrections to the $Zb\bar{b}$ vertex, and the H_1^0 , $H_1'^0$ couplings to vector boson pairs, which are relevant for Higgs boson production at LEP and the Tevatron.

$ZH_3^+H_3^-$ couplings

In general, all the charged Higgs bosons will couple to Z . However, since only singlets and triplets of $SU(2)_c$ can couple to fermions, only the $ZH_3^+H_3^-$, ZG^+G^- , and $ZH_3^+G^-$ couplings will affect the $Zb\bar{b}$ vertex.

The charged Higgs couplings to Z come from the covariant derivatives in the Lagrangian. The $\phi^+(\phi^+)^*Z$ vertex is $ig_{\phi^+(\phi^+)^*Z}(p_1 - p_2)^\mu$, where p_1 is the incoming momentum of ϕ^+ and p_2 is the incoming momentum of $(\phi^+)^*$. For a complex representation with hypercharge Y or a real representation with hypercharge $Y = 0$ the coupling is

$$g_{\phi^+(\phi^+)^*Z} = -\frac{e}{s_W c_W}(c_W^2 - Y/2). \quad (\text{E.124})$$

The electroweak eigenstates mix to form the mass eigenstates H_3^+ and G^+ . The couplings of these mass eigenstates are given by

$$g_{H_1H_2Z} = \sum_{\phi_i} \sum_{\phi_j} \langle H_1 | \phi_i \rangle \langle H_2 | \phi_j \rangle g_{\phi_i \phi_j Z}, \quad (\text{E.125})$$

or, for H_3^+ and G^+ ,

$$g_{H_3^+(H_3^+)^*Z} = \sum_{\phi_k} |\langle H_3^+ | \phi_k^+ \rangle|^2 g_{\phi_k^+(\phi_k^+)^*Z} \quad (\text{E.126})$$

$$g_{G^+(G^+)^*Z} = \sum_{\phi_k} |\langle G^+ | \phi_k^+ \rangle|^2 g_{\phi_k^+(\phi_k^+)^*Z} \quad (\text{E.127})$$

$$g_{H_3^+(G^+)^*Z} = \sum_{\phi_k} \langle H_3^+ | \phi_k^+ \rangle \langle \phi_k^+ | G^+ \rangle g_{\phi_k^+(\phi_k^+)^*Z}. \quad (\text{E.128})$$

We derive the couplings in two stages. We first derive the $\Phi_3^+(\Phi_3^+)^*Z$ and $X_3^+(X_3^+)^*Z$ couplings, then we take into account the mixing between Φ and X .

The Φ_3 coupling is simple to derive since Φ involves only one $SU(2)_L$ multiplet, the $Y = 1$ doublet. The Φ_3^+ coupling is, as in the SM,

$$g_{\Phi_3^+(\Phi_3^+)^*Z} = g_{\phi^+(\phi^+)^*Z} = -\frac{e}{s_W c_W} \left(\frac{1}{2} - s_W^2 \right). \quad (\text{E.129})$$

E.4 The generalized Georgi–Machacek models

In order to find the X_3^+ coupling, we must use equation E.125 to sum up the contributions of each of the $SU(2)_L$ multiplets in X . From equation E.115 we can find the overlap of X_3^+ with each of the $SU(2)_L$ multiplets of X . For the complex multiplets, using $v_k = \sqrt{2}v_X$ and evaluating the sums in the denominator,

$$\langle X_3^+ | \chi_k^+ \rangle^2 = \frac{2T(T+1) - Y_k(Y_k - 2)/2}{\frac{4}{3}T(T+1)(2T+1)} \quad (\text{E.130})$$

$$\langle X_3^+ | (\chi_k^-)^* \rangle^2 = \frac{2T(T+1) - Y_k(Y_k + 2)/2}{\frac{4}{3}T(T+1)(2T+1)}. \quad (\text{E.131})$$

If T is an integer there is also one real multiplet, with $Y = 0$ and $v_i = v_X$, which gives

$$\langle X_3^+ | \xi^+ \rangle^2 = \frac{2T(T+1)}{\frac{4}{3}T(T+1)(2T+1)}. \quad (\text{E.132})$$

The coupling of each of the $SU(2)_L$ multiplets is

$$g_{\chi_k^+(\chi_k^+)^*Z} = -\frac{e}{s_W c_W} (c_W^2 - Y_k/2) \quad (\text{E.133})$$

$$g_{(\chi_k^-)^* \chi_k^- Z} = +\frac{e}{s_W c_W} (-c_W^2 - Y_k/2) \quad (\text{E.134})$$

$$g_{\xi^+(\xi^+)^*Z} = -\frac{e}{s_W c_W} (c_W^2). \quad (\text{E.135})$$

Inserting these into equation E.125 and summing over the multiplets of X , we find, for any T ,

$$g_{X_3^+(X_3^+)^*Z} = -\frac{e}{s_W c_W} \left(\frac{1}{2} - s_W^2 \right), \quad (\text{E.136})$$

the same as for an $SU(2)_L$ doublet.

When Φ_3^+ and X_3^+ mix to form mass eigenstates, the couplings remain the same. They are,

$$g_{H_3^+(H_3^+)^*Z} = g_{G^+(G^+)^*Z} = -\frac{e}{s_W c_W} \left(\frac{1}{2} - s_W^2 \right) \quad (\text{E.137})$$

$$g_{H_3^+(G^+)^*Z} = 0. \quad (\text{E.138})$$

Note that the $H_3^+(H_3^+)^*Z$ coupling is the same as the H^+H^-Z coupling in the two Higgs doublet model, and there is no $H_3^+G^-Z$ coupling.

In general, for a model with $SU(2)_c$ containing any number of multiplets X , the couplings of the $SU(2)_c$ triplet mass eigenstates are

$$\begin{aligned} g_{H_3^+(H_3^+)^*Z} &= \sum_X g_{X_3^+(X_3^+)^*Z} \langle H_3^+ | X_3^+ \rangle \langle X_3^+ | H_3^+ \rangle \\ &= -\frac{e}{s_W c_W} \left(\frac{1}{2} - s_W^2 \right) \langle H_3^+ | H_3^+ \rangle. \end{aligned} \quad (\text{E.139})$$

$H_1^0, H_1^{0'}$ couplings to vector boson pairs

We now consider the couplings of the $SU(2)_c$ singlets to vector boson pairs. The neutral Higgs couplings to W^+W^- and ZZ come from the covariant derivatives in the Lagrangian. The $\phi^{0,r}V_1V_2$ vertex is $ig_{\phi^{0,r}V_1V_2}g^{\mu\nu}$, where V_1 and V_2 are any two vector bosons. Note that only CP–even states couple in this way to vector boson pairs. For a complex representation with hypercharge Y or a real representation with hypercharge $Y = 0$ the couplings are

$$g_{\phi^{0,r}W^+W^-} = g^2v \left(T(T+1) - Y^2/4 \right) \quad (\text{E.140})$$

$$g_{\phi^{0,r}ZZ} = \frac{g^2v}{c_W^2} \frac{Y^2}{2} \quad (\text{E.141})$$

where $\langle\phi^0\rangle = v/\sqrt{2}$ for a complex representation and $\langle\eta^0\rangle = v$ for a real representation.

The couplings of H_1^0 are easy to derive, because $H_1^0 = \phi^{0,r}$ involves only one $SU(2)_L$ multiplet, the $Y = 1$ doublet. The H_1^0 couplings are,

$$g_{H_1^0W^+W^-} = \frac{g^2v_\phi}{2} = gM_W \cos\theta_H \quad (\text{E.142})$$

$$g_{H_1^0ZZ} = \frac{g^2v_\phi}{2c_W^2} = \frac{gM_W \cos\theta_H}{c_W^2} \quad (\text{E.143})$$

where we have used $v_\phi/v_{SM} = \cos\theta_H$ and $v_{SM} = 2M_W/g$.

In order to find the couplings of $H_1^{0'}$, we must sum up the contribution of each electroweak eigenstate in $H_1^{0'}$ using

$$g_{H_1^{0'}V_1V_2} = \sum_{\phi_i} \langle H | \phi_i \rangle g_{\phi_i V_1 V_2}. \quad (\text{E.144})$$

We now need an expression for the composition of $H_1^{0'}$ in terms of electroweak eigenstates. $H_1^{0'}$ is the $SU(2)_c$ singlet of X ; that is, $H_1^{0'}$ is the state that remains invariant under simultaneous $SU(2)_L$ and $SU(2)_R$ rotations of X by the same angle. Clearly, $H_1^{0'}$ must be proportional to the unit matrix, just as $\langle X \rangle$ is. In terms of the electroweak eigenstates, for integer T ,

$$H_1^{0'} = \frac{\sum_{\text{complex}} (\chi_k^0 + (\chi_k^0)^*) + \xi^0}{\sqrt{2T+1}} = \frac{\sum_{k=1}^T \sqrt{2} \chi_k^{0,r} + \xi^0}{\sqrt{2T+1}}, \quad (\text{E.145})$$

and for half–odd–integer T ,

$$H_1^{0'} = \frac{\sum_{\text{complex}} (\chi_k^0 + (\chi_k^0)^*)}{\sqrt{2T+1}} = \frac{\sum_{k=1}^{T+1/2} \sqrt{2} \chi_k^{0,r}}{\sqrt{2T+1}}. \quad (\text{E.146})$$

E.5 Absence of a massless Goldstone boson in the generalized Georgi–Machacek models

We have denoted the $SU(2)_L$ components of X as follows. We denote the complex multiplets of $SU(2)_L$ as χ_k and, for integer T , the real multiplet as ξ . The couplings of each of the $SU(2)_L$ multiplets are

$$g_{\chi_k^{0,r} W^+ W^-} = \sqrt{2} g^2 v_X (T(T+1) - Y_k^2/4) \quad (\text{E.147})$$

$$g_{\xi^0 W^+ W^-} = g^2 v_X T(T+1) \quad (\text{E.148})$$

$$g_{\chi_k^{0,r} Z Z} = \frac{\sqrt{2} g^2 v_X Y_k^2}{c_W^2 2} \quad (\text{E.149})$$

$$g_{\xi^0 Z Z} = 0 \quad (\text{E.150})$$

where we have used $\langle \chi_k^0 \rangle = v_X$ and $\langle \xi^0 \rangle = v_X$. Inserting these into equation E.144 and summing over the multiplets of X , we find,

$$g_{H_1^{0'} W^+ W^-} = g M_W \sqrt{\frac{4}{3} T(T+1)} \sin \theta_H \quad (\text{E.151})$$

$$g_{H_1^{0'} Z Z} = \frac{g M_W}{c_W^2} \sqrt{\frac{4}{3} T(T+1)} \sin \theta_H \quad (\text{E.152})$$

where we have used $\sin \theta_H = \sqrt{\frac{4}{3} T(T+1)(2T+1)} v_X / v_{SM}$ and $v_{SM} = 2M_W/g$.

E.5 Absence of a massless Goldstone boson in the generalized Georgi–Machacek models

In a general extended Higgs sector which does not preserve $SU(2)_c$, the Higgs potential will sometimes have an accidental continuous global symmetry. For example, the Higgs potential may be invariant under a separate $U(1)$ rotation of each of the multiplets. This is the case, for example, in a model containing one doublet and one larger multiplet with $(T, Y) = (3, 4)$, which preserves $\rho = 1$. The Higgs potential for this model has the symmetries $SU(2)_L \times U(1)_Y \times U(1)$, where the second $U(1)$ is a rotation of the larger multiplet, leaving the doublet invariant. This second $U(1)$ is a global symmetry.

In general, the global symmetry is spontaneously broken when the multiplets larger than doublets get vevs, resulting in massless Goldstone bosons in the physical spectrum. As described in reference [41], the physical spectrum must also contain a light CP-even Higgs boson H^0 with mass on the order of the vev of the larger multiplet. This is required because the mass splitting between the massless Goldstone boson and H^0 is on the order of the vev that breaks the accidental global symmetry. Such a massless Goldstone boson is then ruled out by the experimental limits on $Z \rightarrow a^0 H^0$, where a^0 is the massless Goldstone boson [41].

Custodial SU(2) symmetry and the Georgi–Machacek class of models

In this section we will show that the generalized Georgi–Machacek models do not suffer from this massless Goldstone boson problem. The key feature of the Georgi–Machacek models that we will use is the fact that a multiplet X of $SU(2)_L \times SU(2)_R$ can be thought of as a real multiplet. X can be transformed into a Cartesian basis, in which all the components of X are real, through independent left- and right-handed unitary rotations. This is possible because an $n \times n$ matrix X contains n^2 degrees of freedom, so it can be written as an $n \times n$ real matrix. In contrast, a complex representation of $SU(2)_L \times U(1)_Y$ which is an n component vector has $2n$ degrees of freedom, and so cannot be rotated into a Cartesian basis.

In the Cartesian basis, the $SU(2)_L$ and $SU(2)_R$ generators $\vec{\tau}$ can be chosen to be imaginary and antisymmetric. Then the $SU(2)_L \times SU(2)_R$ transformation matrices have the property that,

$$U_{R,L}^T = \exp[-i\theta_{R,L} \hat{n}_{R,L} \cdot \vec{T}_{R,L}^T] = \exp[+i\theta_{R,L} \hat{n}_{R,L} \cdot \vec{T}_{R,L}] = U_{R,L}^\dagger \quad (\text{E.153})$$

$$U_{R,L}^* = \exp[+i\theta_{R,L} \hat{n}_{R,L} \cdot \vec{T}_{R,L}^*] = \exp[-i\theta_{R,L} \hat{n}_{R,L} \cdot \vec{T}_{R,L}] = U_{R,L}. \quad (\text{E.154})$$

Using these, we find that in the Cartesian basis, the term $\text{Tr}(X^T X)$ transforms as follows under $SU(2)_L \times SU(2)_R$,

$$\begin{aligned} \text{Tr}(X^T X) &\rightarrow \text{Tr}(U_R^T X^T U_L^* U_L^\dagger X U_R) \\ &= \text{Tr}(U_R^\dagger X^T U_L U_L^\dagger X U_R) \\ &= \text{Tr}(X^T X). \end{aligned} \quad (\text{E.155})$$

Thus in the Cartesian basis, the term $\text{Tr}(X^T X)$ is invariant under $SU(2)_L \times SU(2)_R$, and can appear in the Higgs potential. This term is not invariant under a global $U(1)$ transformation of X , under which $X \rightarrow e^{i\theta} X$. Instead, the term transforms as,

$$\begin{aligned} \text{Tr}(X^T X) &\rightarrow \text{Tr}(e^{i\theta} X^T e^{i\theta} X) \\ &= e^{2i\theta} \text{Tr}(X^T X) \neq \text{Tr}(X^T X). \end{aligned} \quad (\text{E.156})$$

Thus we conclude that the Higgs potential of a generalized Georgi–Machacek model is not invariant under any additional $U(1)$ rotations.

Appendix F

Calculation of one-loop integrals

In this section I describe the techniques used to calculate the integrals that arise in one-loop radiative corrections. The methods used here are based on the work of 't Hooft, Veltman and Passarino [64,65].

In section F.1 I introduce the one-loop integrals, following Hollik [66], and in section F.2 I provide details of their calculation. In section F.3 I list the derivatives of the one-loop integrals which appear in the calculation of wave-function renormalization. Finally, in section F.4 I list the symmetries of the one-loop integrals and in section F.5 I give expansions of some of the integrals in certain limits, following [67].

F.1 Notation for one-loop integrals

In this section I list the definitions of the one-loop integrals used. I use the metric $g_{\mu\nu} = \text{diag}(1, -1, -1, -1)$. This section follows the discussion of Hollik [66].

One-point integral:

This integral occurs in the calculation of tadpole diagrams, where the particle in the loop has mass m and k is the loop momentum.

$$\mu^{4-D} \int \frac{d^D k}{(2\pi)^D} \frac{1}{k^2 - m^2} = \frac{i}{16\pi^2} A(m^2). \quad (\text{F.1})$$

The integral will be evaluated in dimensional regularization (see section F.2) in D dimensions. The parameter μ is the renormalization scale with dimensions of mass.

Two-point integrals:

These integrals occur in the calculation of corrections to a particle propagator, with loop momentum k . The two particles in the loop have masses m_1 and m_2 . The external momentum is q .

$$\mu^{4-D} \int \frac{d^D k}{(2\pi)^D} \frac{1; k_\mu; k_\mu k_\nu}{[k^2 - m_1^2][(k+q)^2 - m_2^2]} = \frac{i}{16\pi^2} B_{0;\mu;\mu\nu}(q^2; m_1^2, m_2^2). \quad (\text{F.2})$$

The vector and tensor integrals B_μ and $B_{\mu\nu}$ can be expanded into scalar coefficients and Lorentz covariants as follows:

$$B_\mu = q_\mu B_1 \quad (\text{F.3})$$

$$B_{\mu\nu} = g_{\mu\nu} B_{22} + q_\mu q_\nu B_{21}. \quad (\text{F.4})$$

Note that the scalar coefficients depend only on the square of the external four-momentum q^2 .

Three-point integrals:

These integrals occur in the calculation of corrections to a three-particle vertex. The loop momentum is k and the three particles in the loop have masses m_1 , m_2 and m_3 . The external momenta are p_1 , p_2 , and $p = -(p_1 + p_2)$, where all momenta are defined to flow into the vertex.

$$\begin{aligned} \mu^{4-D} \int \frac{d^D k}{(2\pi)^D} \frac{1; k_\mu; k_\mu k_\nu}{[k^2 - m_1^2][(k+p_1)^2 - m_2^2][(k+p_1+p_2)^2 - m_3^2]} \\ = \frac{i}{16\pi^2} C_{0;\mu;\mu\nu}(p_1^2, p_2^2, p^2; m_1^2, m_2^2, m_3^2). \end{aligned} \quad (\text{F.5})$$

The vector and tensor integrals C_μ and $C_{\mu\nu}$ can again be expanded into scalar coefficients and Lorentz covariants:

$$C^\mu = p_1^\mu C_{11} + p_2^\mu C_{12} \quad (\text{F.6})$$

$$C^{\mu\nu} = g^{\mu\nu} C_{24} + p_1^\mu p_1^\nu C_{21} + p_2^\mu p_2^\nu C_{22} \quad (\text{F.7})$$

$$+ (p_1^\mu p_2^\nu + p_2^\mu p_1^\nu) C_{23}. \quad (\text{F.8})$$

Note that the scalar coefficients again depend only on the squares of the external four-momenta.

In reference [66] the three-point integrals are defined exactly as in equation F.5. Note, however, that reference [66] uses the notation $C_{0;\mu;\mu\nu}(p_1, p_2; m_1, m_2, m_3)$ for the three-point integrals.

F.2 Calculation of one-loop integrals

F.2 Calculation of one-loop integrals

The coefficients of the vector and tensor one-loop integrals can all be expressed algebraically in terms of the scalar integrals A , B_0 and C_0 . (For details of the calculation see [66].) We have, for the two-point integrals,

$$B_1(q^2; m_1^2, m_2^2) = \frac{1}{2q^2} \left[A(m_1^2) - A(m_2^2) + (m_2^2 - m_1^2 - q^2) B_0(q^2; m_1^2, m_2^2) \right] \quad (\text{F.9})$$

$$B_{22}(q^2; m_1^2, m_2^2) = \frac{1}{6} \left[A(m_2^2) + 2m_1^2 B_0(q^2; m_1^2, m_2^2) + (q^2 + m_1^2 - m_2^2) B_1(q^2; m_1^2, m_2^2) + m_1^2 + m_2^2 - \frac{q^2}{3} \right] \quad (\text{F.10})$$

$$B_{21}(q^2; m_1^2, m_2^2) = \frac{1}{3q^2} \left[A(m_2^2) - m_1^2 B_0(q^2; m_1^2, m_2^2) - 2(q^2 + m_1^2 - m_2^2) B_1(q^2; m_1^2, m_2^2) - \frac{m_1^2 + m_2^2}{2} + \frac{q^2}{6} \right]. \quad (\text{F.11})$$

Note that equation F.9 for B_1 differs from the expression in [66] in that m_1^2 and m_2^2 are interchanged in the coefficient of B_0 . This is necessary in order for B_1 to have the correct divergent piece, as discussed below.

The three-point integrals are listed below. The arguments of all the three-point integrals are assumed to be $(p_1^2, p_2^2, p^2; m_1^2, m_2^2, m_3^2)$, as in section F.1.

$$C_{11} = \frac{1}{\kappa} [p_2^2 R_1 - p_1 \cdot p_2 R_2] \quad (\text{F.12})$$

$$C_{12} = \frac{1}{\kappa} [-p_1 \cdot p_2 R_1 + p_1^2 R_2] \quad (\text{F.13})$$

$$C_{24} = \frac{1}{4} [B_0(p_2^2; m_2^2, m_3^2) + r_1 C_{11} + r_2 C_{12} + 2m_1^2 C_0 + 1] \quad (\text{F.14})$$

$$C_{21} = \frac{1}{\kappa} [p_2^2 R_3 - p_1 \cdot p_2 R_5] \quad (\text{F.15})$$

$$C_{23} = \frac{1}{\kappa} [-p_1 \cdot p_2 R_3 + p_1^2 R_5] = \frac{1}{\kappa} [p_2^2 R_4 - p_1 \cdot p_2 R_6] \quad (\text{F.16})$$

$$C_{22} = \frac{1}{\kappa} [-p_1 \cdot p_2 R_4 + p_1^2 R_6] \quad (\text{F.17})$$

where

$$\kappa = p_1^2 p_2^2 - (p_1 \cdot p_2)^2 \quad (\text{F.18})$$

$$r_1 = p_1^2 + m_1^2 - m_2^2 \quad (\text{F.19})$$

$$r_2 = p^2 - p_1^2 + m_2^2 - m_3^2 \quad (\text{F.20})$$

$$R_1 = \frac{1}{2}[B_0(p^2; m_1^2, m_3^2) - B_0(p_2^2; m_2^2, m_3^2) - (p_1^2 + m_1^2 - m_2^2)C_0] \quad (\text{F.21})$$

$$R_2 = \frac{1}{2}[B_0(p_1^2; m_1^2, m_2^2) - B_0(p^2; m_1^2, m_3^2) + (p_1^2 - p^2 - m_2^2 + m_3^2)C_0] \quad (\text{F.22})$$

$$R_3 = -C_{24} - \frac{1}{2}[r_1 C_{11} - B_1(p^2; m_1^2, m_3^2) - B_0(p_2^2; m_2^2, m_3^2)] \quad (\text{F.23})$$

$$R_4 = -\frac{1}{2}[r_1 C_{12} - B_1(p^2; m_1^2, m_3^2) + B_1(p_2^2; m_2^2, m_3^2)] \quad (\text{F.24})$$

$$R_5 = -\frac{1}{2}[r_2 C_{11} - B_1(p_1^2; m_1^2, m_2^2) + B_1(p^2; m_1^2, m_3^2)] \quad (\text{F.25})$$

$$R_6 = -C_{24} - \frac{1}{2}[r_2 C_{12} + B_1(p^2; m_1^2, m_3^2)]. \quad (\text{F.26})$$

Finally the integrals A , B_0 and C_0 are calculated using dimensional regularization [68,69,70] in D dimensions with $D = 4 - \epsilon$ and $\epsilon \rightarrow 0$ (for details see [66]). The one-point integral is

$$A(m^2) = m^2 \left(\Delta - \log \frac{m^2}{\mu^2} + 1 \right) + \mathcal{O}(\epsilon). \quad (\text{F.27})$$

The divergent part is

$$\Delta = \frac{2}{\epsilon} - \gamma + \log 4\pi, \quad (\text{F.28})$$

where $\gamma = 0.577 \dots$ is Euler's constant, and μ is the renormalization scale with dimensions of mass. Note that in computations of physical processes both Δ and μ must cancel out of the final result. This provides a useful check on computations. The divergent parts of all the one-loop integrals are listed at the end of this section. Note also that the divergent term can pick out the ϵ in $D = 4 - \epsilon$ yielding a finite additional term,

$$D \cdot \Delta = 4\Delta - 2 + \mathcal{O}(\epsilon). \quad (\text{F.29})$$

The two-point integral B_0 is

$$B_0(q^2; m_1^2, m_2^2) = \Delta - \int_0^1 dx \log \left(\frac{x^2 q^2 - x(q^2 + m_1^2 - m_2^2) + m_1^2 - i\varepsilon}{\mu^2} \right). \quad (\text{F.30})$$

The three-point integral $C_0(p_1^2, p_2^2, p^2; m_1^2, m_2^2, m_3^2)$ is

$$C_0 = - \int_0^1 dx \int_0^x dy \frac{1}{ax^2 + by^2 + cxy + dx + ey + f} \quad (\text{F.31})$$

F.3 Derivatives of two-point integrals

where

$$a = p^2 \quad (\text{F.32})$$

$$b = p_2^2 \quad (\text{F.33})$$

$$c = p_1^2 - p_2^2 - p^2 \quad (\text{F.34})$$

$$d = m_3^2 - m_1^2 - p^2 \quad (\text{F.35})$$

$$e = m_2^2 - m_3^2 + p^2 - p_1^2 \quad (\text{F.36})$$

$$f = m_1^2 - i\varepsilon. \quad (\text{F.37})$$

Note that there is a mistake in the expression for e in reference [66], in which m_3^2 is replaced with m_1^2 .

It is easy to find the divergent terms in the one-loop integrals. They are,

$$A(m^2) = m^2 \Delta + \text{finite} \quad (\text{F.38})$$

$$B_0 = \Delta + \text{finite} \quad (\text{F.39})$$

$$B_1 = -\frac{1}{2} \Delta + \text{finite} \quad (\text{F.40})$$

$$B_{22}(q^2; m_1^2, m_2^2) = \frac{1}{4} \left[m_1^2 + m_2^2 - \frac{q^2}{3} \right] \Delta + \text{finite} \quad (\text{F.41})$$

$$B_{21} = \frac{1}{3} \Delta + \text{finite} \quad (\text{F.42})$$

$$C_{24} = \frac{1}{4} \Delta + \text{finite}. \quad (\text{F.43})$$

The integrals C_0 , C_{11} , C_{12} , C_{21} , C_{22} , and C_{23} are all finite, as are the combinations R_1, \dots, R_6 . This list is useful because it allows one to easily check that the divergences cancel in the calculation of a physical process. The divergent terms are also relevant in the calculation of renormalization group equations.

F.3 Derivatives of two-point integrals

In this section I list the derivatives of the one-loop integrals B_0 , B_1 , B_{22} , and B_{21} with respect to the external momentum. These derivatives appear in calculations of corrections to a process from loop corrections to the external legs.

Let us define the shorthand notation

$$B'(M^2; m_1^2, m_2^2) \equiv \left[\frac{\partial}{\partial q^2} B(q^2; m_1^2, m_2^2) \right]_{q^2=M^2} \quad (\text{F.44})$$

for the type of derivative which typically appears in the wave-function renormalization. All of the derivatives of the two-point integrals can be expressed in terms of other two-point integrals and the derivative of B_0 .

$$B'_1(q^2; m_1^2, m_2^2) = -\frac{1}{q^2} \left[B_1 + \frac{1}{2}B_0 + \frac{1}{2}(q^2 + m_1^2 - m_2^2)B'_0 \right] \quad (\text{F.45})$$

$$B'_{22}(q^2; m_1^2, m_2^2) = \frac{1}{6} \left[B_1 - \frac{1}{3} + 2m_1^2 B'_0 + (q^2 + m_1^2 - m_2^2)B'_1 \right] \quad (\text{F.46})$$

$$B'_{21}(q^2; m_1^2, m_2^2) = -\frac{1}{3q^2} \left[3B_{21} + 2B_1 - \frac{1}{6} + m_1^2 B'_0 + 2(q^2 + m_1^2 - m_2^2)B'_1 \right]. \quad (\text{F.47})$$

Finally, B'_0 is given by

$$B'_0(q^2; m_1^2, m_2^2) = \int_0^1 dx \frac{x(1-x)}{x^2 q^2 - x(q^2 + m_1^2 - m_2^2) + m_1^2}. \quad (\text{F.48})$$

The integrals B'_0 , B'_1 , and B'_{21} are finite. The integral B'_{22} has a divergent term,

$$B'_{22} = -\frac{1}{12}\Delta + \text{finite}. \quad (\text{F.49})$$

F.4 Symmetries of the one-loop integrals under permutation of their arguments

In this section I list the symmetry properties of the one-loop integrals under interchange of their arguments.

The two-point integrals obey symmetry relations under the interchange of m_1 and m_2 . B_0 is symmetric under the exchange,

$$B_0(q^2; m_1^2, m_2^2) = B_0(q^2; m_2^2, m_1^2). \quad (\text{F.50})$$

The symmetry properties of the remaining two-point integrals are more complicated because they involve powers of the loop momentum in the numerator. B_1 obeys the following relation,

$$B_1(q^2; m_1^2, m_2^2) = -B_1(q^2; m_2^2, m_1^2) - B_0(q^2; m_2^2, m_1^2) \quad (\text{F.51})$$

or, using equation F.50 to symmetrize this,

$$\left[B_1 + \frac{1}{2}B_0 \right] (q^2; m_1^2, m_2^2) = - \left[B_1 + \frac{1}{2}B_0 \right] (q^2; m_2^2, m_1^2). \quad (\text{F.52})$$

F.4 Symmetries of the one-loop integrals under permutaion of their arguments

B_{22} and B_{21} obey the following relations,

$$B_{22}(q^2; m_1^2, m_2^2) = B_{22}(q^2; m_2^2, m_1^2) \quad (\text{F.53})$$

$$B_{21}(q^2; m_1^2, m_2^2) = [B_{21} + 2B_1 + B_0](q^2; m_2^2, m_1^2) \quad (\text{F.54})$$

or, using equation F.51 to symmetrize this,

$$[B_{21} + B_1](q^2; m_1^2, m_2^2) = [B_{21} + B_1](q^2; m_2^2, m_1^2). \quad (\text{F.55})$$

The three-point integrals can be represented by a triangle with the vertices labelled by the external momenta and the sides labelled by the masses of the particles in the loop. The symmetry properties of the three-point integrals under permutations of m_1 , m_2 and m_3 correspond to rotations and inversions of the triangle. C_0 obeys the following symmetries:

$$\begin{aligned} C_0(p_1^2, p_2^2, p^2; m_1^2, m_2^2, m_3^2) &= C_0(p_2^2, p_1^2, p^2; m_3^2, m_2^2, m_1^2) \\ &= C_0(p^2, p_1^2, p_2^2; m_3^2, m_1^2, m_2^2) = C_0(p_1^2, p^2, p_2^2; m_2^2, m_1^2, m_3^2) \\ &= C_0(p_2^2, p^2, p_1^2; m_2^2, m_3^2, m_1^2) = C_0(p^2, p_2^2, p_1^2; m_1^2, m_3^2, m_2^2). \end{aligned} \quad (\text{F.56})$$

The same symmetries are obeyed by C_{24} . The symmetries of the remaining three-point integrals are more complicated. They are as follows. The symmetries of C_{11} are,

$$C_{11}(p_1^2, p_2^2, p^2; m_1^2, m_2^2, m_3^2) = [-C_{12} - C_0](p_2^2, p_1^2, p^2; m_3^2, m_2^2, m_1^2) \quad (\text{F.57})$$

$$= [-C_{11} + C_{12} - C_0](p^2, p_1^2, p_2^2; m_3^2, m_1^2, m_2^2) \quad (\text{F.58})$$

$$= [-C_{11} + C_{12} - C_0](p_1^2, p^2, p_2^2; m_2^2, m_1^2, m_3^2) \quad (\text{F.59})$$

$$= [-C_{12} - C_0](p_2^2, p^2, p_1^2; m_2^2, m_3^2, m_1^2) \quad (\text{F.60})$$

$$= C_{11}(p^2, p_2^2, p_1^2; m_1^2, m_3^2, m_2^2). \quad (\text{F.61})$$

The symmetries of C_{12} are,

$$C_{12}(p_1^2, p_2^2, p^2; m_1^2, m_2^2, m_3^2) = [-C_{11} - C_0](p_2^2, p_1^2, p^2; m_3^2, m_2^2, m_1^2) \quad (\text{F.62})$$

$$= [-C_{11} - C_0](p^2, p_1^2, p_2^2; m_3^2, m_1^2, m_2^2) \quad (\text{F.63})$$

$$= C_{12}(p_1^2, p^2, p_2^2; m_2^2, m_1^2, m_3^2) \quad (\text{F.64})$$

$$= [C_{11} - C_{12}](p_2^2, p^2, p_1^2; m_2^2, m_3^2, m_1^2) \quad (\text{F.65})$$

$$= [C_{11} - C_{12}](p^2, p_2^2, p_1^2; m_1^2, m_3^2, m_2^2). \quad (\text{F.66})$$

The symmetries of C_{21} are,

$$C_{21}(p_1^2, p_2^2, p^2; m_1^2, m_2^2, m_3^2) = [C_{22} + 2C_{12} + C_0](p_2^2, p_1^2, p^2; m_3^2, m_2^2, m_1^2) \quad (\text{F.67})$$

$$= [C_{21} + C_{22} - 2C_{23} + 2C_{11} - 2C_{12} + C_0] (p^2, p_1^2, p_2^2; m_3^2, m_1^2, m_2^2) \quad (\text{F.68})$$

$$= [C_{21} + C_{22} - 2C_{23} + 2C_{11} - 2C_{12} + C_0] (p_1^2, p^2, p_2^2; m_2^2, m_1^2, m_3^2) \quad (\text{F.69})$$

$$= [C_{22} + 2C_{12} + C_0](p_2^2, p^2, p_1^2; m_2^2, m_3^2, m_1^2) \quad (\text{F.70})$$

$$= C_{21}(p^2, p_2^2, p_1^2; m_1^2, m_3^2, m_2^2). \quad (\text{F.71})$$

The symmetries of C_{22} are,

$$C_{22}(p_1^2, p_2^2, p^2; m_1^2, m_2^2, m_3^2) = [C_{21} + 2C_{11} + C_0](p_2^2, p_1^2, p^2; m_3^2, m_2^2, m_1^2) \quad (\text{F.72})$$

$$= [C_{21} + 2C_{11} + C_0](p^2, p_1^2, p_2^2; m_3^2, m_1^2, m_2^2) \quad (\text{F.73})$$

$$= C_{22}(p_1^2, p^2, p_2^2; m_2^2, m_1^2, m_3^2) \quad (\text{F.74})$$

$$= [C_{21} + C_{22} - 2C_{23}](p_2^2, p^2, p_1^2; m_2^2, m_3^2, m_1^2) \quad (\text{F.75})$$

$$= [C_{21} + C_{22} - 2C_{23}](p^2, p_2^2, p_1^2; m_1^2, m_3^2, m_2^2). \quad (\text{F.76})$$

Finally, the symmetries of C_{23} are,

$$C_{23}(p_1^2, p_2^2, p^2; m_1^2, m_2^2, m_3^2) = [C_{23} + C_{12} + C_{11} + C_0](p_2^2, p_1^2, p^2; m_3^2, m_2^2, m_1^2) \quad (\text{F.77})$$

$$= [C_{21} - C_{23} + 2C_{11} - C_{12} + C_0] (p^2, p_1^2, p_2^2; m_3^2, m_1^2, m_2^2) \quad (\text{F.78})$$

$$= [C_{22} - C_{23} - C_{12}](p_1^2, p^2, p_2^2; m_2^2, m_1^2, m_3^2) \quad (\text{F.79})$$

$$= [C_{22} - C_{23} - C_{11} + C_{12}](p_2^2, p^2, p_1^2; m_2^2, m_3^2, m_1^2) \quad (\text{F.80})$$

$$= [C_{21} - C_{23}](p^2, p_2^2, p_1^2; m_1^2, m_3^2, m_2^2). \quad (\text{F.81})$$

The symmetry relations of B_0 , B_1 , and all the C integrals agree with those in [71], except for equations F.70 and F.71 for C_{21} which are interchanged in [71], and equations F.78 and F.80 for C_{23} which are interchanged in [71]. Reference [71] does not list symmetry relations for B_{22} and B_{21} .

F.5 Approximations for the one-loop integrals in certain limits

Expansions for the one-loop integrals in certain limits have been given in [67]. For easy reference, I reproduce here the expansions which I have used in this thesis.

F.5 Approximations for the one-loop integrals in certain limits

F.5.1 $(m/M)^2 \equiv R \neq 0, \infty$

The results given below are valid for arbitrary R as long as $m^2, M^2 \gg p_1^2, p_2^2, p^2$. Note that for the corrections to the process $Z \rightarrow b\bar{b}$, the external momenta are $p_1^2 = p^2 = m_b^2$ and $p_2^2 = M_Z^2$. These results are relevant for the charged Higgs corrections to $Z \rightarrow b\bar{b}$, where $m = m_t$ and M is a charged Higgs mass.

$$B_1(p^2; m^2, M^2) = -\frac{1}{2} \left[\Delta - \log(M^2/\mu^2) + \frac{3}{2} + \frac{1}{R-1} - \frac{R^2 \log R}{(R-1)^2} \right] - \frac{p^2}{6M^2} \left[\frac{2}{R-1} + \frac{9}{(R-1)^2} + \frac{6}{(R-1)^3} - \frac{6R^2 \log R}{(R-1)^4} \right] \quad (\text{F.82})$$

$$C_0(p_1^2, p_2^2, p^2; M^2, m^2, m^2) = \frac{1}{M^2} \left[-\frac{1}{R-1} + \frac{\log R}{(R-1)^2} \right] \quad (\text{F.83})$$

$$C_{24}(p_1^2, p_2^2, p^2; M^2, m^2, m^2) = \frac{1}{4} \left[\Delta - \log(M^2/\mu^2) + \frac{1}{2} - \frac{1}{R-1} - \frac{R(R-2) \log R}{(R-1)^2} \right] + \frac{(p_1^2 + p^2)}{24M^2} \left[\frac{1}{R-1} - \frac{3}{(R-1)^2} - \frac{6}{(R-1)^3} + \frac{6R \log R}{(R-1)^4} \right] + \frac{p_2^2}{72M^2} \left[\frac{2}{R-1} - \frac{3}{(R-1)^2} + \frac{6}{(R-1)^3} - \frac{6 \log R}{(R-1)^4} \right]. \quad (\text{F.84})$$

There are also expansions of C_0 and C_{24} in the limit that all three particles in the loop are much heavier than the external particles,

$$C_0(0, 0, 0; m_1^2, m_2^2, m_3^2) = -\frac{[m_1^2 m_2^2 \log(m_1^2/m_2^2) + m_2^2 m_3^2 \log(m_2^2/m_3^2) + m_3^2 m_1^2 \log(m_3^2/m_1^2)]}{[m_1^2 - m_2^2][m_2^2 - m_3^2][m_1^2 - m_3^2]}, \quad (\text{F.85})$$

which is negative for any internal masses m_1 , m_2 , and m_3 . It is also symmetric under permutations of m_1 , m_2 , and m_3 . C_{24} is related to this by

$$C_{24}(0, 0, 0; m_1^2, m_2^2, m_3^2) = \frac{1}{4} \left[B_0(0; m_2^2, m_3^2) + m_1^2 C_0(0, 0, 0; m_1^2, m_2^2, m_3^2) + \frac{1}{2} \right] \quad (\text{F.86})$$

This equation is also symmetric under permutations of m_1 , m_2 , and m_3 . B_0 is given by,

$$B_0(0; m_2^2, m_3^2) = \Delta - \log(m_2^2/\mu^2) - \frac{m_3^2}{m_2^2 - m_3^2} \log(m_2^2/m_3^2) + 1. \quad (\text{F.87})$$

F.5.2 $m \simeq 0$ ($R \equiv (m/M)^2 \simeq 0$)

In expanding the two- and three-point integrals that appear in the neutral Higgs corrections to $Z \rightarrow b\bar{b}$, $m = m_b$ and M is a neutral Higgs mass. The external momenta are $p_1^2 = p^2 = m_b^2$ and $p_2^2 = M_Z^2$, as before. However, now one cannot use the expansions given above, because $m^2 \ll p_2^2$. The previous expansions were derived for $m^2 \gg p_2^2$. As pointed out in reference [67], one cannot simply take the limit $R \rightarrow 0$ in the formulas above, since some of the results will diverge. The divergences are cut off by p_2^2 . The results given below were derived in [67] for $M^2 \gg p_1^2, p_2^2, p^2 \gg m^2$. However, they are still valid for the case $p_1^2 = p^2 = m^2 = m_b^2$. In the formulas below we neglect m_b .

$$B_1(p_1^2; m^2, M^2) = -\frac{1}{2} \left[\Delta - \log(M^2/\mu^2) + \frac{1}{2} \right] + \mathcal{O}(p_1^2/M^2) \quad (\text{F.88})$$

$$\begin{aligned} C_0(p_1^2, p_2^2, p^2; M^2, m^2, m^2) &= -\frac{1}{M^2} [\log(-M^2/p_2^2) + 1] \\ &= -\frac{1}{M^2} [\log(M^2/p_2^2) + 1 + i\pi] \end{aligned} \quad (\text{F.89})$$

$$\begin{aligned} C_{24}(p_1^2, p_2^2, p^2; M^2, m^2, m^2) &= \frac{1}{4} \left[\Delta - \log(M^2/\mu^2) + \frac{3}{2} + \frac{p_2^2}{3M^2} \log(-M^2/p_2^2) + \frac{5p_2^2}{18M^2} \right] \\ &= \frac{1}{4} \left[\Delta - \log(M^2/\mu^2) + \frac{3}{2} + \frac{p_2^2}{3M^2} [\log(M^2/p_2^2) + i\pi] \right. \\ &\quad \left. + \frac{5p_2^2}{18M^2} \right] \end{aligned} \quad (\text{F.90})$$

$$\begin{aligned} [C_{22} - C_{23}](p_1^2, p_2^2, p^2; M^2, m^2, m^2) &= \frac{1}{6M^2} \left[\log(-M^2/p_2^2) - \frac{1}{6} \right] \\ &= \frac{1}{6M^2} \left[\log(M^2/p_2^2) + i\pi - \frac{1}{6} \right]. \end{aligned} \quad (\text{F.91})$$

Note the imaginary parts of the three-point functions above. These are a consequence of the fact that the internal b quark lines in the diagram of figure 5.1(b) can be cut, yielding the on-shell decay $Z \rightarrow b\bar{b}$.

Appendix G

Combining the LEP and SLD measurements of A_b

A_b is measured directly at SLD from the b quark left–right forward–backward asymmetry. This is possible because the electron and positron polarizations at SLD are nonzero and the polarizations are known. However, at LEP, the electron and positron beams are not polarized longitudinally. For this reason, A_b can only be measured indirectly at LEP, in the form of the b quark forward–backward asymmetry. The forward–backward asymmetry also depends on A_e . We assume lepton universality, so that $A_e = A_\mu = A_\tau \equiv A_l$.

In this appendix I describe the procedure used for combining the LEP and SLD determinations of A_b . The procedure is as follows. First the lepton asymmetry A_l is extracted from the LEP and SLD data. In particular, the LEP measurements of the electron forward–backward asymmetry and the tau polarization measurements are used. The SLD measurement of $\sin^2 \theta_{\text{eff}}^{\text{lept}}$ also yields a measurement of A_l . Second, the combined LEP and SLD value of A_l is used to extract A_b from the LEP measurement of the b quark forward–backward asymmetry. Finally, the value of A_b found indirectly from the LEP data in this way is combined with the direct measurement of A_b from SLD.

At LEP, A_l is measured in three different ways. First, it can be found from the lepton forward–backward asymmetry, $A_{FB}^{0,l}$,

$$A_{FB}^{0,l} = \frac{3}{4} A_l^2. \quad (\text{G.1})$$

Combining the LEP and SLD measurements of A_b

Solving this for A_l , we obtain the first LEP determination of A_l ,

$$A_l = \sqrt{\frac{4}{3}} A_{FB}^{0,l}. \quad (\text{G.2})$$

The second and third LEP measurements of A_l come from the τ polarization measurement. This allows a direct measurement of A_e and of A_τ . Assuming lepton universality, these are both equated to A_l .

At SLD, A_l is measured directly and the result is expressed in terms of $\sin^2 \theta_{\text{eff}}^{\text{lept}}$. Both A_l and $\sin^2 \theta_{\text{eff}}^{\text{lept}}$ are defined in terms of the vector and axial-vector couplings of leptons to Z , g_l^V and g_l^A . In particular,

$$\sin^2 \theta_{\text{eff}}^{\text{lept}} \equiv \frac{1}{4} \left(1 - \frac{g_l^V}{g_l^A} \right) \quad (\text{G.3})$$

$$A_l = \frac{2g_l^V g_l^A}{(g_l^V)^2 + (g_l^A)^2}. \quad (\text{G.4})$$

Solving these for A_l in terms of $\sin^2 \theta_{\text{eff}}^{\text{lept}}$, A_l is,

$$A_l = \frac{2(1 - 4 \sin^2 \theta_{\text{eff}}^{\text{lept}})}{1 + (1 - 4 \sin^2 \theta_{\text{eff}}^{\text{lept}})^2}. \quad (\text{G.5})$$

The three LEP values of A_l and the one SLD value are then combined.

The LEP value of A_b is extracted from the b quark forward-backward asymmetry, $A_{FB}^{0,b}$, using the combined LEP and SLD measurement of A_l . $A_{FB}^{0,b}$ is,

$$A_{FB}^{0,b} = \frac{3}{4} A_e A_b. \quad (\text{G.6})$$

Solving this for A_b , and again assuming lepton universality,

$$A_b = \frac{4}{3} \frac{A_{FB}^{0,b}}{A_l}. \quad (\text{G.7})$$

Then A_b is found by inserting the value of $A_{FB}^{0,b}$ measured at LEP and the combined value of A_l determined from LEP and SLD as described above.

At SLD, A_b is measured directly. To find the combined LEP and SLD value of A_b , the SLD measurement is combined with the LEP value determined above.

The current measurements of the input parameters and the combined value of A_b are summarized in table G.1.

$A_{FB}^{0,l}$ (LEP)	0.01683 ± 0.00096
A_e (LEP τ polarization)	0.1479 ± 0.0051
A_τ (LEP τ polarization)	0.1431 ± 0.0045
$\sin^2 \theta_{\text{eff}}^{\text{lept}}$ (SLD)	0.23109 ± 0.00029
A_l from LEP and SLD	0.1489 ± 0.0017
$A_{FB}^{0,b}$ (LEP)	0.0991 ± 0.0020
A_b from SLD	0.908 ± 0.027
A_b from LEP and SLD	0.895 ± 0.016

Table G.1: Input data and results for the combined LEP and SLD determination of A_b . Inputs are taken from reference [4].

Appendix H

SM parameters used in numerical calculations

In this appendix we list the SM parameters that have been used in our numerical calculations of R_b and A_b in extended Higgs sectors. The parameters are listed in table H.1.

For all the input parameters except m_b , we have used the values extracted from a fit of the precision electroweak data to the SM. As shown in table H.2, the difference between using the SM fit values and the measured values of the parameters is very small.

The largest fractional difference between the SM fit and measured value occurs for m_t . In order to show the effect of this difference on R_b , we calculate the correction to R_b from charged Goldstone boson exchange in the SM using both values for m_t . We obtain,

$$\Delta R_b(m_t^{\text{SM-fit}}) = -0.00174 \quad (\text{H.1})$$

$$\Delta R_b(m_t^{\text{measured}}) = -0.00180. \quad (\text{H.2})$$

The difference in R_b between the two choices of m_t is 0.00006. This is negligible compared to the experimental uncertainty in R_b , which is 0.00073. We thus ignore the uncertainty in m_t in our numerical calculations.

For the b quark mass, we use the $\overline{\text{MS}}$ running mass evaluated at M_Z , denoted $\bar{m}_b(M_Z)$. As discussed in reference [74], it is appropriate to use $\bar{m}_b(M_Z)$ in calculations involving b quarks at the scale M_Z , because the running mass takes into account the large QCD corrections to m_b which are enhanced by $\log(M_Z/m_b)$.

For the SM fit value of R_b , we have used $R_b^{SM} = 0.21587$, instead of the oft-quoted value, $R_b^{SM} = 0.2158$. The old SM prediction for R_b is no longer precise enough

Parameter	Value	Source	Reference
$\alpha^{-1}(M_Z)$	128.898	SM fit	[72]
$\sin^2 \theta_{eff}^{lept}$	0.23157	SM fit	[73]
M_W	80.371 GeV	SM fit	[73]
M_Z	91.1865 GeV	SM fit	[73]
m_b	3.0 GeV	$\bar{m}_b(M_Z)$ ($\overline{\text{MS}}$ mass)	[33]
m_t	171.8 GeV	SM fit	[4]
R_b^{SM}	0.21587	SM fit (from pull)	[4]
A_b^{SM}	0.935	SM fit	[4]

Table H.1: The SM parameters used in our numerical calculations.

Parameter	SM fit	Measured	Fractional difference (%)
$\alpha^{-1}(M_Z)$	128.898	128.878	0.02%
$\sin^2 \theta_{eff}^{lept}$	0.23157	0.2321	0.2%
M_W	80.371 GeV	80.448 GeV	0.1%
M_Z	91.1865 GeV	91.1867 GeV	0.0005%
m_t	171.8 GeV	174.3 GeV	1.4%

Table H.2: A comparison of the SM fit values of the SM parameters with their measured values, and the percent difference between the two. The SM fit values are the same as in table H.1, and the measured values are from reference [4].

SM parameters used in numerical calculations

	Measurement	Pull	SM value
R_b	0.21680 ± 0.00073	1.27	0.21587

Table H.3: The measured value of R_b , its pull from the SM fit, and the corresponding SM fit value. The pull is defined as the number of standard deviations by which the measured value differs from the SM fit value. The numbers are from reference [4].

Confidence level	Number of σ	R_b value
95%	1.96	0.21537
99%	2.58	0.21492
99.9%	3.3	0.21439

Table H.4: The values of R_b that correspond to the 95%, 99%, and 99.9% confidence levels below the measured value.

now that the measured value of R_b and its experimental error are quoted to five decimal places. Our value is extracted from reference [4], which quotes the measured value of R_b , the experimental error, and the pull, which is the number of standard deviations between the measured value and the SM fit. Although the SM fit value is not quoted in reference [4], we can deduce it from the pull. The numbers are summarized in table H.3. Note that a pull of 1.27 means that the measured value of R_b is 1.27 σ above the SM fit value.

Finally, in table H.4 we list the values of R_b that correspond to the 95%, 99%, and 99.9% confidence levels below the measured value. These confidence levels correspond to the contours in our exclusion plots in chapter 6.

Appendix I

Constraints from direct Higgs searches

In this appendix I describe the searches for Higgs boson production at LEP and the resulting limits on the masses of Higgs states.

I.1 Charged Higgs searches

The search for singly-charged Higgs bosons at LEP looks for charged Higgs boson pair production via $Z \rightarrow H^+ H^-$, followed by decays to $\tau \nu_\tau$ or $q \bar{q}'$. The best bound on the charged Higgs mass from the data at $\sqrt{s} = 189$ GeV comes from the OPAL collaboration, which excludes charged Higgs bosons up to a mass of 68.7 GeV at the 95% confidence level [54]. The bound is independent of the branching ratio $BR(H^\pm \rightarrow \tau \nu_\tau)$, assuming that $BR(H^\pm \rightarrow q \bar{q}') + BR(H^\pm \rightarrow \tau \nu_\tau) = 1$. This condition is true as long as the charged Higgs boson can only decay into quarks and leptons. In models with two or more singly-charged Higgs bosons, the heavier charged Higgs boson can decay into the lighter charged Higgs boson and a neutral Higgs boson, if the decay is kinematically allowed. However, we will be using the mass bound of reference [54] to constrain the mass of the lighter charged Higgs boson only, so this is not a concern. Finally, the charged Higgs boson decay into W^\pm and a neutral boson is not kinematically allowed.

The bound also depends on the production cross section of the charged Higgs boson pair. In the analysis of reference [54] it is assumed that the ZH^+H^- coupling is that in the 2HDM,

$$g_{ZH^+H^-} = -\frac{e}{s_W c_W} \left(\frac{1}{2} - s_W^2 \right). \quad (\text{I.1})$$

This coupling, and hence the production cross section, is the same in a model containing multiple doublets and singlets, and in the Georgi–Machacek models for H_3^\pm . The bound is

used for these models in figures 6.1 and 6.9. However, the coupling is not the same in the models containing doublets and triplets without $SU(2)_c$ symmetry. In the models with one or two doublets and one real, $Y = 0$ triplet, the coupling is larger than in the 2HDM, and hence the production cross section is larger. Therefore in these models, the charged Higgs mass bound from reference [54] is still valid, and is in fact a conservative bound. The bound is used in figure 6.7 for the model with two doublets and one $Y = 0$ triplet. In the models with one or two doublets and one complex, $Y = 2$ triplet, the coupling is smaller than in the 2HDM. Hence the charged Higgs boson production cross section is smaller, and the mass bound from reference [54] is no longer valid. This is the case in figure 6.8, for the model with two doublets and one $Y = 2$ triplet.

I.2 Neutral Higgs searches

The search for neutral Higgs bosons at LEP looks for neutral Higgs boson production in two ways. In the search for the standard model Higgs boson, LEP looks for the process $e^+e^- \rightarrow Z^* \rightarrow Zh^0$. In the search for the neutral Higgs bosons of the Minimal Supersymmetric Model (MSSM), LEP looks for the above process, in addition to the process $e^+e^- \rightarrow Z^* \rightarrow h^0 A^0$. The implications of these searches for the neutral Higgs bosons in the general 2HDM are discussed in the following sections.

I.2.1 SM Higgs search

In the SM, the dominant Higgs boson production mode at LEP energies is

$$e^+e^- \rightarrow Z^* \rightarrow Zh^0, \quad (\text{I.2})$$

where Z^* is an off-shell Z boson and the final Z and h^0 are on-shell.

From the LEP data taken at a center-of-mass energy of $\sqrt{s} = 189$ GeV, the lower limits on the SM Higgs mass from the four LEP experiments are summarized in table I.1 [56]. The best bound comes from the DELPHI and L3 experiments; they find $M_{h_{SM}^0} > 95.2$ GeV.

If we make some simplifying assumptions, we can extract from this measurement a lower bound on the mass of the CP-even neutral Higgs bosons in the 2HDM. In the 2HDM, the ZZh^0 coupling is reduced from its SM value by a factor of $\sin(\beta - \alpha)$. Thus the cross section for Zh^0 production is reduced by a factor of $\sin^2(\beta - \alpha)$. Also, for a fixed center-of-mass energy, the Zh^0 production cross section decreases with increasing Higgs mass.

If we assume that the background and the Zh^0 detection efficiency are fairly flat as a function of the Higgs mass, as suggested by figure 27 of reference [75], then we can take the LEP lower bound on the SM Higgs mass as an upper bound on the Zh^0 production

I.2 Neutral Higgs searches

	M_{h^0} (GeV)
ALEPH	90.2
DELPHI	95.2
L3	95.2
OPAL	91.0

Table I.1: The observed lower bounds on the SM Higgs mass from the four LEP experiments, from data taken at $\sqrt{s} = 189$ GeV. Data from reference [56].

cross section. We can then translate the LEP bound on the SM Higgs mass into a bound on $\sin^2(\beta - \alpha)$ as a function of the Higgs mass.

In the SM, the tree-level cross section for Zh^0 production in e^+e^- collisions is [11],

$$\sigma_{SM}(e^+e^- \rightarrow Zh^0) = \frac{\pi\alpha^2\lambda^{1/2}[\lambda + 12sM_Z^2][1 + (1 - 4s_W^2)^2]}{192s^2s_W^4c_W^4(s - M_Z^2)^2}, \quad (\text{I.3})$$

where s is the square of the center-of-mass energy, $s_W = \sin\theta_W$, $c_W = \cos\theta_W$, and λ is a kinematic factor,

$$\lambda = (s - M_{h^0}^2 - M_Z^2)^2 - 4M_{h^0}^2M_Z^2. \quad (\text{I.4})$$

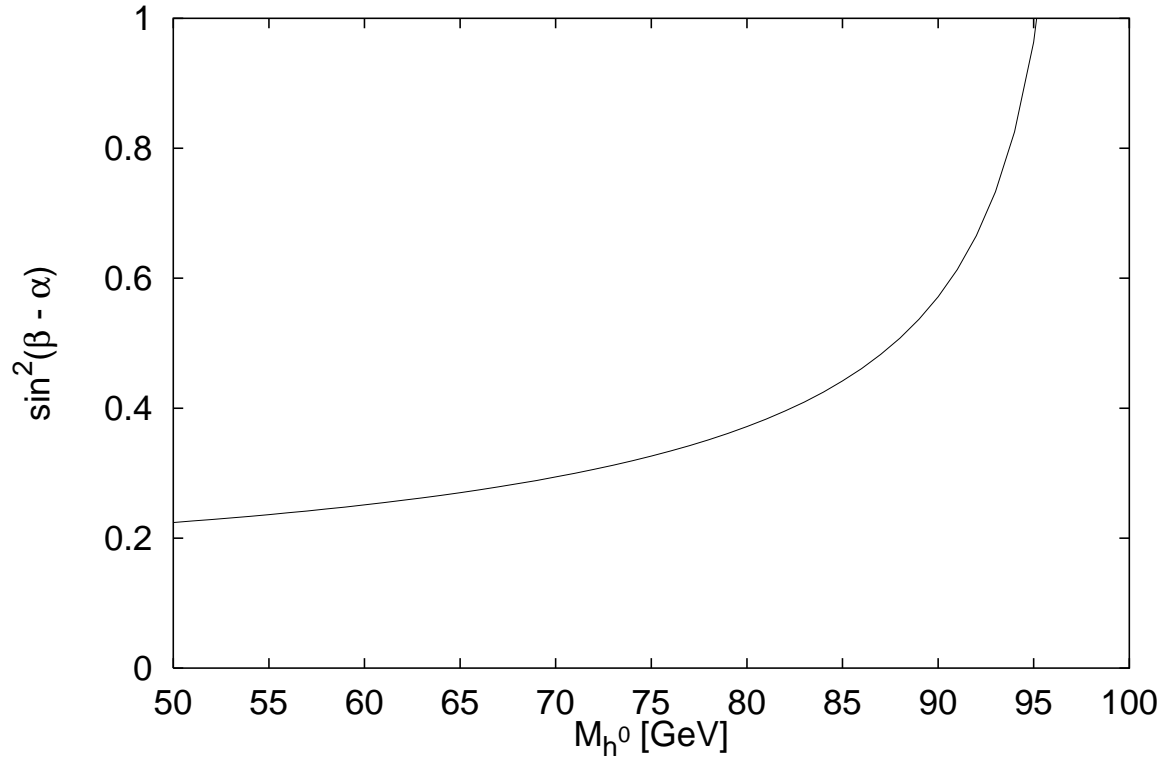
In the 2HDM, the cross section is multiplied by a factor of $\sin^2(\beta - \alpha)$,

$$\sigma(e^+e^- \rightarrow Zh^0) = \sigma_{SM}(e^+e^- \rightarrow Zh^0) \sin^2(\beta - \alpha). \quad (\text{I.5})$$

The LEP bound on M_{h^0} in the SM fixes $\sigma_{SM}(e^+e^- \rightarrow Zh^0)$. If we then vary M_{h^0} in the 2HDM cross section, we find a lower bound on the Higgs mass as a function of $\sin^2(\beta - \alpha)$. This bound is shown in figure I.1. A similar analysis was done by Sopczak in reference [76], using the LEP data taken at center-of-mass energies between 161 and 172 GeV.

For $\sin^2(\beta - \alpha) = 1$, the bound on M_{h^0} is the same as in the SM, $M_{h^0} > 95.2$ GeV. This bound is used in figure 6.6. For $\sin^2(\beta - \alpha) = 1/2$, the bound on M_{h^0} is $M_{h^0} > 87$ GeV. This bound is used in figures 6.2 and 6.3.

The decays of h^0 in the 2HDM differ from those of the SM Higgs boson in one important way. If the CP-odd state A^0 has less than half the mass of the h^0 , then the decay mode $h^0 \rightarrow A^0A^0$ becomes possible. Since the $h^0A^0A^0$ coupling is typically of order unity while the $h^0b\bar{b}$ coupling is suppressed by a factor of m_b/v_1 , $h^0 \rightarrow A^0A^0$ could be the dominant decay of h^0 . In this case, the final state will contain six b jets, since all three of the A^0 particles will decay dominantly to b quarks. This final state should be easy to detect in a dedicated search.

**Figure I.1:**

Constraint on $\sin^2(\beta - \alpha)$ as a function of M_{h^0} in the 2HDM. The area above the line is excluded. We have assumed that the Higgs boson detection efficiency and background are constant as a function of the Higgs mass.

I.2 Neutral Higgs searches

	M_{h^0} (GeV)	M_{A^0} (GeV)
ALEPH	80.8	81.2
DELPHI	83.5	84.5
L3	77.0	78.0
OPAL	74.8	76.5

Table I.2: The observed lower bounds on the masses of the MSSM Higgs bosons h^0 and A^0 from the four LEP experiments, from data taken at $\sqrt{s} = 189$ GeV. Data from reference [56].

I.2.2 2HDM Higgs search

The search for neutral Higgs bosons at LEP is sensitive to the neutral Higgs bosons of the 2HDM. However, the analysis of the LEP data is done in the context of the Higgs sector of the Minimal Supersymmetric Model (MSSM), in which the Higgs sector is constrained by supersymmetry relations. Fortunately, the Higgs mass bounds in the MSSM can be reinterpreted as constraints on a general 2HDM.

In the MSSM, the dominant Higgs boson production modes at LEP energies are,

$$e^+e^- \rightarrow Z^* \rightarrow Zh^0 \quad (\text{I.6})$$

and

$$e^+e^- \rightarrow Z^* \rightarrow h^0A^0, \quad (\text{I.7})$$

where again Z^* is an off-shell Z boson and the final-state particles are on-shell.

From the LEP data taken at a center-of-mass energy of $\sqrt{s} = 189$ GeV, the lower limits on the MSSM Higgs masses from the four LEP experiments are summarized in table I.2 [56]. The best bound comes from the DELPHI experiment, which finds $M_{h^0} > 83.5$ GeV and $M_{A^0} > 84.5$ GeV, for arbitrary $\tan\beta$.

As discussed in the previous section, the cross section for Zh^0 production is proportional to $\sin^2(\beta - \alpha)$ in a 2HDM. The Zh^0A^0 coupling is proportional to $\cos(\beta - \alpha)$, so the cross section for h^0A^0 production is proportional to $\cos^2(\beta - \alpha)$.

The limits on the MSSM Higgs masses observed by the LEP experiments actually depend on the value of $\tan\beta$. For both the h^0 and A^0 searches, the bounds are weakest at large $\tan\beta$; these are the values quoted in table I.2. In the MSSM, the parameters of the Higgs sector are correlated, so that at large $\tan\beta$, $\cos(\beta - \alpha)$ is very close to one. Thus the bounds quoted in table I.2 come from the search for h^0A^0 production.

As in the previous section, if we assume that the backgrounds and detection efficiency for h^0 and A^0 are independent of the Higgs masses, we can use the MSSM mass bounds to deduce bounds on the h^0 and A^0 masses in the general 2HDM.

In the 2HDM, the tree-level cross section for $h^0 A^0$ production in $e^+ e^-$ collisions is [11],

$$\sigma(e^+ e^- \rightarrow h^0 A^0) = \frac{g^2 f^2}{48\pi} \left(\frac{8s_W^4 - 4s_W^2 + 1}{c_W^2} \right) \frac{\kappa^3}{\sqrt{s}[(s - M_Z^2)^2 + \Gamma_Z^2 M_Z^2]} \quad (\text{I.8})$$

where Γ_Z is the Z decay width, κ is a kinematic factor,

$$\kappa = \frac{[(s - M_{h^0}^2 - M_{A^0}^2)^2 - 4M_{h^0}^2 M_{A^0}^2]^{1/2}}{2\sqrt{s}} \quad (\text{I.9})$$

and f is a coupling factor,

$$f = \frac{g}{2c_W} \cos(\beta - \alpha). \quad (\text{I.10})$$

We can now extend the MSSM Higgs boson search results to the general 2HDM. The LEP bound on M_{h^0} and M_{A^0} fixes the cross section with $\cos^2(\beta - \alpha) = 1$. With our assumptions, we can then vary M_{h^0} and $\cos^2(\beta - \alpha)$ and find lower bound on M_{A^0} . In our analysis, we fix $\cos^2(\beta - \alpha)$, then vary M_{h^0} and find a lower bound on M_{A^0} . We do this for two values of $\cos^2(\beta - \alpha)$.

For $\cos^2(\beta - \alpha) = 1$, we find the bound shown in figure I.2. As expected, this bound passes through the MSSM point with $M_{h^0} = 83.5$ GeV and $M_{A^0} = 84.5$ GeV. This bound is used in figures 6.4 and 6.5. Note also that for $\cos^2(\beta - \alpha) = 0$, the bound shown in figure I.2 is the bound on the A^0 mass as a function of the mass of the heavier CP-even neutral Higgs boson, H^0 . This bound is used in figure 6.6.

For $\cos^2(\beta - \alpha) = 1/2$, we find the bound shown in figure I.3. This bound is used in figures 6.2 and 6.3.

In making figures I.2 and I.3 we have assumed that the backgrounds and detection efficiencies for h^0 and A^0 are constant for all Higgs masses. This is not a good assumption for very light Higgs bosons (for example, below 10 GeV) because the Higgs branching ratio to b quarks will be suppressed by the non-negligible b quark mass. The LEP searches look for Higgs boson decays to b quarks in order to tag the events.

Also, as discussed before, if the A^0 has less than half the mass of the h^0 , the decay mode $h^0 \rightarrow A^0 A^0$ becomes possible. Since the $h^0 A^0 A^0$ coupling is typically of order unity while the $h^0 b \bar{b}$ coupling is suppressed by a factor of m_b/v_1 , $h^0 \rightarrow A^0 A^0$ could be the dominant decay of h^0 . In this case, the final state will contain six b jets, since all three of the A^0 particles will decay dominantly to b quarks. Again, one would think that this final state would be easy to detect.

In summary, the bounds presented in figures I.2 and I.3 are good for M_{h^0} and M_{A^0} near 80 GeV. However, for either M_{h^0} or M_{A^0} very small, the assumptions on which our derivation is based become less reliable.

I.2 Neutral Higgs searches

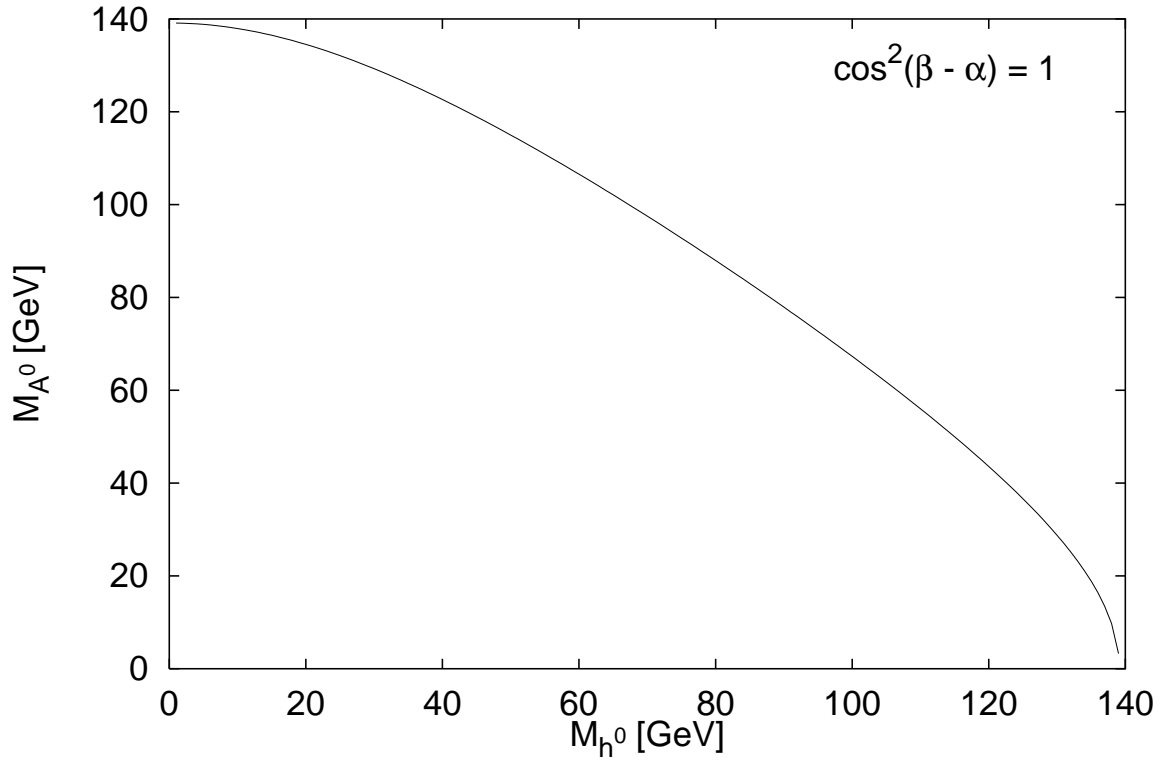


Figure I.2: Bounds on M_{h^0} and M_{A^0} in the 2HDM for $\cos^2(\beta - \alpha) = 1$. The area below the line is excluded. We have assumed that the Higgs boson detection efficiency and background are constant as a function of the Higgs masses.

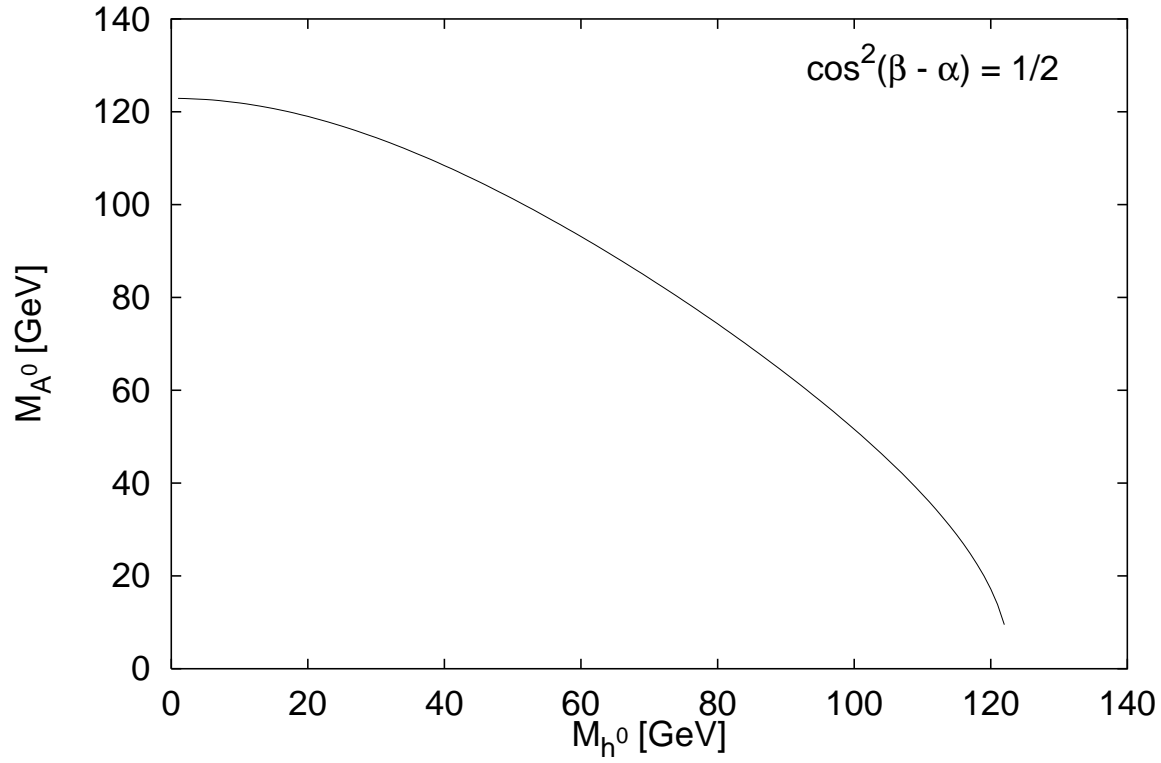


Figure I.3: Bounds on M_{h^0} and M_{A^0} in the 2HDM for $\cos^2(\beta - \alpha) = 1/2$. The area below the line is excluded. We have assumed that the Higgs boson detection efficiency and background are constant as a function of the Higgs masses.

Bibliography

- [1] S. L. Glashow, J. Iliopoulos, and L. Maiani, Phys. Rev. **D2**, 1285 (1970).
- [2] S. Weinberg, Phys. Rev. Lett. **19**, 1264 (1967).
- [3] A. Salam, in *Elementary Particle Theory*, edited by N. Svartholm (Almquist and Wiksells, Stockholm, 1968), p. 367.
- [4] R. Clare, talk presented at the American Physical Society Centennial Meeting, Atlanta, USA, March 20–26, 1999 (unpublished).
- [5] G. Altarelli, R. Barbieri, and F. Caravaglios, Int. J. Mod. Phys. **A13**, 1031 (1998).
- [6] P. Sikivie, L. Susskind, M. Voloshin, and V. Zakharov, Nucl. Phys. **B173**, 189 (1980).
- [7] H. E. Haber, in *Testing the Standard Model (TASI-90)*, edited by M. Cvetič and P. Langacker (World Scientific, Singapore, 1991).
- [8] P. W. Higgs, Phys. Lett. **12**, 132 (1964).
- [9] F. Englert and R. Brout, Phys. Rev. Lett. **13**, 321 (1964).
- [10] G. S. Guralnik, C. R. Hagen, and T. W. B. Kibble, Phys. Rev. Lett. **13**, 585 (1964).
- [11] J. F. Gunion, H. E. Haber, G. L. Kane, and S. Dawson, *The Higgs Hunters Guide* (Addison-Wesley, Redwood City, CA, 1990).
- [12] A. A. Akhundov, D. Y. Bardin, and T. Riemann, Nucl. Phys. **B276**, 1 (1986).
- [13] W. Beenakker and W. Hollik, Z. Phys. **C40**, 141 (1988).
- [14] J. Bernabeu, A. Pich, and A. Santamaria, Phys. Lett. **B200**, 569 (1988).

- [15] W. Hollik, Fortschr. Phys. **38**, 165 (1990).
- [16] B. W. Lynn and R. G. Stuart, Phys. Lett. **B252**, 676 (1990).
- [17] P. Antilogus *et al.* [ALEPH, DELPHI, L3, OPAL, and LEP Electroweak Working Group], in *Proceedings of the International Europhysics Conference on High-energy Physics : EPS-HEP '95 Brussels, Belgium ; 27 Jul - 2 Aug 1995*, edited by J. Lemonne, C. Vander Velde, and F. Verbeure (World Scientific, Singapore, 1996), CERN-PPE/95-172.
- [18] P. Bamert *et al.*, Phys. Rev. **D54**, 4275 (1996).
- [19] J. Field, Mod. Phys. Lett. **A13**, 1937 (1998).
- [20] M. Carena, H. E. Haber, and C. E. M. Wagner, Nucl. Phys. **B472**, 55 (1996).
- [21] A. K. Grant, Phys. Rev. **D51**, 207 (1995).
- [22] D. Comelli and J. P. Silva, Phys. Rev. **D54**, 1176 (1996).
- [23] M. Drees *et al.*, Phys. Rev. **D54**, 5598 (1996).
- [24] J. Cline, in *MRST '96: Current Ideas in Theoretical Physics*, edited by P. J. O'Donnell and B. H. Smith (World Scientific, Singapore, 1996), p. 41.
- [25] P. H. Chankowski and S. Pokorski, Nucl. Phys. **B475**, 3 (1996).
- [26] A. Kundu and B. Mukhopadhyaya, Int. J. Mod. Phys. **A11**, 5221 (1996).
- [27] A. Denner, R. J. Guth, W. Hollik, and J. H. Kuhn, Z. Phys. **C51**, 695 (1991).
- [28] A. Djouadi *et al.*, Nucl. Phys. **B349**, 48 (1991).
- [29] M. Boulware and D. Finnell, Phys. Rev. **D44**, 2054 (1991).
- [30] H. E. Haber, in *Properties of SUSY Particles*, edited by L. Cifarelli and V. Khoze (World Scientific, Singapore, 1993), p. 321, proceedings of the 23rd Workshop of the INFN Eloisatron Project, Erice, Italy, September 28–October 4, 1992.
- [31] A. Dobado, M. J. Herrero, and S. Penaranda, Eur. Phys. J. **C7**, 313 (1999).
- [32] A. Dobado, M. J. Herrero, and S. Penaranda, hep-ph/9903211 (unpublished).
- [33] H. Fusaoka and Y. Koide, Phys. Rev. **D57**, 3986 (1998).

BIBLIOGRAPHY

- [34] D. Abbaneo *et al.* [ALEPH, DELPHI, L3, OPAL, LEP Electroweak Working Group, and SLD Heavy Flavour Group], CERN-PPE/97-154 (unpublished).
- [35] M. E. Peskin and T. Takeuchi, Phys. Rev. **D46**, 381 (1992).
- [36] A. K. Grant and T. Takeuchi, hep-ph/9807413 (unpublished).
- [37] C. Caso *et al.*, European Physical Journal **C3**, 1 (1998).
- [38] B. W. Lee, in *Proceedings of the XVI International Conference on High Energy Physics*, edited by J. D. Jackson, A. Roberts, and R. Donaldson (University of Chicago and National Accelerator Laboratory, Batavia, IL, 1972), Vol. 4.
- [39] D. A. Ross and M. Veltman, Nucl. Phys. **B95**, 135 (1975).
- [40] H.-S. Tsao, in *Proceedings of the 1980 Guangzhou Conference on Theoretical Particle Physics*, edited by H. Ning and T. Hung-yuan (Science Press, Beijing, 1980), p. 1240.
- [41] M. Gonzalez-Garcia and Y. Nir, Phys. Lett. **232B**, 383 (1989).
- [42] H. Georgi and M. Machacek, Nucl. Phys. **B262**, 463 (1985).
- [43] M. S. Chanowitz and M. Golden, Phys. Lett. **165B**, 105 (1985).
- [44] J. F. Gunion, R. Vega, and J. Wudka, Phys. Rev. **D42**, 1673 (1990).
- [45] J. F. Gunion, R. Vega, and J. Wudka, Phys. Rev. **D43**, 2322 (1991).
- [46] D. Atwood, L. Reina, and A. Soni, Phys. Rev. **D55**, 3156 (1997).
- [47] S. L. Glashow and S. Weinberg, Phys. Rev. **D15**, 1958 (1977).
- [48] E. A. Paschos, Phys. Rev. **D15**, 1966 (1977).
- [49] W. Hollik, in *Precision Tests of the Standard Electroweak Model*, edited by P. Langacker (World Scientific, Singapore, 1995), p. 117.
- [50] H. E. Haber, in *Budapest Electroweak 1994*, edited by F. Csikor and G. Pocsik (World Scientific, Singapore, 1995), p. 1.
- [51] M. S. Alam *et al.* [CLEO Collaboration], CLEO CONF 98-17, Talk presented at the XXIX International Conference on High Energy Physics, Vancouver, B.C., Canada, 23-29 July 1998 (unpublished).
- [52] F. M. Borzumati and C. Greub, talk presented by C. Greub at the XXIX International Conference on High Energy Physics, Vancouver, B.C., Canada, 23-29 July 1998. hep-ph/9810240 (unpublished).

- [53] B. Abbott *et al.* [D0 Collaboration], hep-ex/9902028 (unpublished).
- [54] OPAL Collaboration, OPAL PN 99–373, OPAL contribution to the Winter 1999 conferences, available at <http://www.cern.ch/Opal/status-public.html> (unpublished).
- [55] H. E. Haber, in *Perspectives on Higgs Physics*, edited by G. L. Kane (World Scientific, Singapore, 1993), p. 79.
- [56] M. Felcini *et al.* [L3 Collaboration], talk presented at *XXXIVth Rencontres de Moriond, on Electroweak Interactions and Unified Theories*, Les Arcs, France, March 13–20, 1999 (unpublished).
- [57] B. Grinstein, R. Springer, and M. B. Wise, Nucl. Phys. **B339**, 269 (1990).
- [58] E. Gross *et al.* [ALEPH, OPAL, DELPHI, and L3 Collaborations], CERN-EP-98-094. To be published in the proceedings of 12th Les Rencontre de Physique de la Vallee d’Aoste: Results and Perspectives in Particle Physics, La Thuile, Aosta Valley, Italy, 1-7 Mar 1998. (unpublished).
- [59] J. Conway, talk presented at the Linear Collider Workshop, Sitges, Spain, April 30, 1999 (unpublished).
- [60] P. Krawczyk and S. Pokorski, Phys. Rev. Lett. **60**, 182 (1988).
- [61] J. Kalinowski, Phys. Lett. **B245**, 201 (1990).
- [62] Y. Grossman and Z. Ligeti, Phys. Lett. **B332**, 373 (1994).
- [63] J. F. Gunion, H. E. Haber, and H. E. Logan, in preparation (unpublished).
- [64] G. ‘t Hooft and M. Veltman, Nucl. Phys. **B153**, 365 (1979).
- [65] G. Passarino and M. Veltman, Nucl. Phys. **B160**, 151 (1979).
- [66] W. Hollik, in *Precision Tests of the Standard Electroweak Model*, edited by P. Langacker (World Scientific, Singapore, 1995), p. 37.
- [67] M. C. Peyranere, H. E. Haber, and P. Irulegui, Phys. Rev. **D44**, 191 (1991).
- [68] C. Bollini and J. Giambiagi, Nuovo Cim. **12B**, 20 (1972).
- [69] J. Ashmore, Nuovo Cim. Lett. **4**, 289 (1972).
- [70] G. ‘t Hooft and M. Veltman, Nucl. Phys. **B44**, 189 (1972).
- [71] P. Irulegui Gomes, Ph.D. thesis, University of California, Santa Cruz, 1991.

BIBLIOGRAPHY

- [72] S. Eidelmann and F. Jegerlehner, Z. Phys. **C67**, 585 (1995).
- [73] D. Karlen, talk presented at the XXIX International Conference on High Energy Physics, Vancouver, B.C., Canada, 23-29 July 1998 (unpublished).
- [74] J. Hisano, S. Kiyoura, and H. Murayama, Phys. Lett. **B399**, 156 (1997).
- [75] W. Adam *et al.* [DELPHI Collaboration], paper submitted to the XXIX International Conference on High Energy Physics, Vancouver, B.C., Canada, 23-29 July 1998 (unpublished).
- [76] A. Sopczak, Phys. Atom. Nucl. **61**, 938 (1998).